THE FACULTY OF ENGINEERING AND THE BUILT ENVIRONMENT

DEPARTMENT OF CIVIL ENGINEERING

Carbonation and Permeability Characteristics of Modern South African Concretes

Prepared by: Nabeel OMAR
Supervised by: Prof Hans BEUSHAUSEN
Date of submission: August 2018

A dissertation submitted to the Department of Civil Engineering, University of Cape Town in partial fulfilment of the requirements for the degree of Master of Science in Structural Engineering and Structural Materials Specialisation

Concrete Materials and Structural Integrity Research Unit

CoMSIRU

Plagiarism declaration:

I know the meaning of plagiarism and declare that all the work in the document, save for that which is properly acknowledged, is my own. This thesis/dissertation has been submitted to the Turnitin module (or equivalent similarity and originality checking software) and I confirm that my supervisor has seen my report and any concerns revealed by such have been resolved with my supervisor.

i) I know that plagiarism is wrong. Plagiarism is using another's work and to pretend that it is one's own.

ii) I have used the Harvard Convention for citation and referencing. Each significant contribution to, and quotation in, this report from the work, or works of other people has been attributed and has been cited and referenced

iii) This report is my own work.

iv) I have not allowed, and will not allow, anyone to copy my work with the intention of passing it off as his or her own work

v) I acknowledge that copying someone else's assignment or essay, or part of it, is wrong, and declare that this is our own work.

Student number: OMRNAB005
Surname: OMAR

Signature: Signed by candidate Date: August 2018

Dedication

In loving memory of Zainab Omar and Faieza Desai

Acknowledgements

The author would like to thank and acknowledge with gratitude the following persons, and companies who made significant contribution towards the completion of this dissertation:

- The supervisor, Professor Hans Beushausen, for his continuous support, encouragement, guidance and continual academic and technical assistance throughout the course of this dissertation.
- Emeritus Professor Mark Alexander, for providing advice over the duration of this study.
- Mr Nooredien Hassen, the civil engineering concrete laboratory manager, for his assistance and guidance with the laboratory-related experimentation.
- Mr Steve Croswell and Portland Pretoria Cement Ltd (PPC), for their advice and donations used in this research.
- Mr Tahir Mukkadam, senior technical officer, for his assistance with laboratory-related experimentation.
- Mr Charles Nicholas, the civil engineering workshop principal technical officer, for manufacturing the equipment required for the experimentation work.
- The departmental assistant Mr Leonard Adams, the civil engineering concrete laboratory staff, Mr Chris Caesar, Mr Elvino Witbooi and Mr Charlie May and the wastewater research laboratory assistant Mr Hector Mafungwa, for their help with experimental work when needed.
- The administration staff of the department of civil engineering for their assistance with administrative matters related to this research.
- The postgraduate students in civil engineering, especially Mr Zubair Lall Mahomed, for a priceless friendship and constant support throughout this journey.
- Family and friends for their continual support and love.

The author would also like to thank and acknowledge the financial support from CoMSIRU throughout the duration of the dissertation.

Abstract

The world's exponential growth in urbanisation has placed significant pressure on the construction industry to support development by expanding its provision of infrastructure. There is expected to be a rapid increase in the consumption of structural concrete to meet the associated requirements. This increase in concrete consumption has adverse effects on the environment. Firstly, the production of cement, one of the main components of concrete, is regarded as a system of energy-intensive processes. Secondly, the production of Portland cement (PC) releases a substantial amount of greenhouse gases (such as carbon dioxide), which in turn contributes to the global warming phenomenon.

In addition to the change in demand for concrete over time, its composition and mix proportions have indeed also undergone a significant evolution. Concrete is becoming more sophisticated and complex. The construction industry has introduced mineral admixtures as partial replacement of PC in the attempt to mitigate the negative environmental impact of cement production. The use of mineral admixtures has positive economic and environmental benefits. In the context of concrete durability, the use of mineral admixtures has the potential to improve the performance of concrete by mitigating the deterioration processes occurring in concrete structures, such as reinforcement corrosion.

Reinforcement corrosion is one of the most pervasive concerns within the construction industry. Carbonation is considered as of the main causes contributing to the corrosion phenomenon. The carbonation mechanism entails the reaction between atmospheric carbon dioxide and the cement paste and leads to an altered chemistry within concrete, which eventually causes the depassivation of steel reinforcement. The deterioration of the concrete caused by carbonation can be predicted using the oxygen permeability index (OPI) test results as an input parameter in the appropriate carbonation prediction model.

While South Africa has developed carbonation durability prediction models that can predict the performance of conventional concrete mixes (concrete containing 30% fly ash, 50% slag, 10% silica fume) relatively well, this formulation of the carbonation model was instituted approximately twenty years ago and is considered outdated. Therefore, this research seeks to investigate whether the previously established correlation between carbonation and oxygen permeability is still relevant for modern South African concretes. In this study, concrete constituting of different mineral admixtures at varying PC replacement levels or the use of chemical admixtures is defined as modern concrete.

The experimental work included investigating the permeability and carbonation performance of modern concretes made with modern binder types at varying binder replacement levels and binder combinations, including binary and ternary cement blends at two water:binder ratios of 0,50 and 0,65. This included addition of fly ash (FA) (20%-50% in 10% increments), blast furnace slag (BS) (20%-60% in 10% increments), Corex slag (CS) (20%-60% in 20% increments), and limestone (10% and 20%). For ternary blends, the concrete was limited to three mixes, that is, 5% SF with either 25% FA, 25% BS or 25% CS. Furthermore, two commercial blended cement products were tested namely CEM II A-L, and CEM Il B-M (L-S) 42,5N, referred to as A-L and B-M. A-L and B-M cement nominally contain 8% L, and 8% L coupled with 25% CS respectively.

The OPI test was conducted after 28-days of wet curing. The accelerated carbonation tests were conducted using a phenolphathein indicator solution at 6, 9 and 12 weeks of exposure. Prior the testing, the samples were wet cured for seven days and underwent a preconditioning regime in attempt to minimise the influence of the internal moisture of the concrete affecting the carbonation depth results. A statistical analysis was done on both OPI and the accelerated carbonation results to determine the significance in results with the increase in binder replacement percentage, different binders of the same binder replacement percentage and significance of using ternary mixes in comparison to binary mixes.

In conclusion it was found that, generally, mineral admixtures had a statistical insignificant influence on the permeability. This can be attributed to the fact that the control mixes already possessed a high permeability performance i.e. concretes exhibiting relatively low permeabilities. Therefore, the inclusion of a mineral admixture would result in a minor influence on the performance. Regarding carbonation depths, the inclusion of mineral admixtures resulted in a decrease in carbonation performance, as expected. This is attributed to the dilution effect and the pozzolanic effect to some degree, which decreased the amount of carbonatable material that is calcium hydroxide, subsequently decreasing the concrete's resistance to carbonation.

Finally, reasonable correlations were identified between carbonation depth and permeability when all concrete mixes were considered. The direction of the trend showed a positive and negative association when the carbonation coefficient was plotted against k-permeability and OPI respectively. Further investigation of the correlation between carbonation depth and a singular binder type regardless of the replacement level showed an increased in correlation strength between permeability and carbonation. It was concluded that using this approach may provide reasonable correlations for carbonation prediction modelling. However, more testing would be required to confirm the previous statement.

Abbreviations and symbols

A	Carbonation coefficient
A-L	CEM II A-L 52,5 N
B-M	CEM II B-M (L-S) 42,5 N
BS	Blast furnace slag
C_2S	Dicalcium silicate
C_3AH_{13}	Tricalcium aluminate
C_3S	Tricalcium silicate
C_4AF_{13}	Tetracalcium aluminoferrite
$CaCO_3$	Calcium carbonate
CH	Calcium hydroxide
CS	Corex slag
CSH	Calcium silica hydrate
d	Time (days)
DI	Durability Index
e	Electron
FA	Fly ash
Fe	Iron
H_2O	Water
ITZ	Interfacial transition zone
k	Coefficient of permeability
L	Limestone
O_2	Oxygen
OH^-	Hydroxide ion
OPI	Oxygen permeability Index
PC	Portland cement
pH	measure of acidity or alkalinity; scale: <7 (acidic), 7 (neutral), >7 (basic)
RH	Relative humidity
SCM	Supplementary cementitious materials
SF	Silica fume
SF BS	Concrete ternary mix with replacement level of 5% silica fume and 25% blast furnace slag
SF CS	Concrete ternary mix with replacement level of 5% silica fume and 25% Corex slag
SF FA	Concrete ternary mix with replacement level of 5% silica fume and 25% fly ash
SiO_2	Silica
w/b	Water to binder ratio
x	Carbonation depth (mm)

Table of contents

List of figures

List of tables

1 Introduction

1.1 Background and context

The world's exponential growth in urbanisation has placed significant pressure on the construction industry to support development by expanding its provision of infrastructure. There is expected to be a rapid increase in the consumption of structural concrete to meet the associated requirements (Wickens, 2013). However, if the degree of consumption continues to increase and if its supply persists in relying on outdated models of production or composition, this can lead to severe adverse environmental consequences.

Two consequences in particular are significant. Firstly, as concrete is commonly made up of cementitious materials, water, sand and stone. A large percentage of these concrete constituents is sourced from the world's precious natural resources, an increase in consumption may result in a global depletion (Ohanyere, 2013). Secondly, the production of concrete – especially for cement manufacturing – is regarded as one which involves a system of energy-intensive processes. Moreover, the production of Portland cement (PC) releases a substantial amount of greenhouse gases (such as carbon dioxide), which in turn contributes to the global warming phenomenon (Jin & Chen, 2013).

Concrete production's negative impact on the environment has driven the construction industry to orientate towards more sustainable production practices. Subsequently, this brings about a new paradigm within the construction industry. One which seeks a balance between the society's needs and the conservation of the world's natural reserves (Muigai & Alexander, 2010).

An example of this approach was observed in the Working Group Cement, which consists of many major multinational cement companies whose members have pledged to decrease their emissions (ACMP, 2007). They intend to do this either by improving their production through making it more efficient (with lower energy consumption) or by diluting the cement products they supply to the general market by using mineral admixtures (Grieve, 2009).

In addition to the change in demand for concrete over time, its composition and mix proportions have indeed also undergone a significant evolution. Concrete is becoming more sophisticated and complex, currently commonly containing mineral extenders which can improve its general properties. Furthermore, the inclusion of chemical admixtures continue to expand on efforts at altering the properties of concrete (Aitcïn, 2000). In this study, concrete constituting of different mineral admixtures at varying PC replacement levels or the use of chemical admixtures is defined as modern concrete.

Mineral admixtures are currently used to in an attempt to reduce the adverse impact on the environment caused by concrete consumption and production. In South Africa, these materials are mainly sourced from industry by-products (such as slag, fly ash, silica fume, etc.) or materials for which the production poses significantly fewer adverse effects to the environment, compared to PC production, e.g. ground limestone. These are partially substituted for PC. This is either in pre-mixed blended cements, or in cement substitution during batching on site (Grieve, 2009). Besides their economic and environmental benefits, these mineral admixtures have the potential to improve the concrete performance by mitigating the deterioration processes occurring in concrete structures. Usually such deterioration is primarily due to reinforcement corrosion, a phenomenon which poses significant challenges in concrete structures. This pervasive concern continuously challenges the

industry. One of the main causes of reinforcement corrosion is the concrete deterioration mechanism known as carbonation (Stanish, et al., 2008).

Carbonation initiates when carbon dioxide in the atmosphere reacts with alkaline compounds within the cement paste to produce carbonates like limestone. This in turn leads to the neutralisation and reduction of the concrete's alkalinity. Subsequently the concrete becomes more vulnerable to reinforcement corrosion. Given sufficient moisture and oxygen, the embedded steel is susceptible to corrosion, which might lead to cracking, and eventually to delamination and subsequently spalling (Bertolini, et al., 2013).

In numerous countries more money is spent on the rehabilitation of structures than is used for new construction. South Africa in particular devotes a significant portion of its Gross Domestic Product to the maintenance and rehabilitation of existing concrete structures. This kind of expenditure might better have been incurred for projects that contribute towards improving the overall development of the nation. Such (misplaced) emphases may largely be attributed to a lack of understanding of the concept of durability in relation to concrete structures (Ballim, et al., 1999; Alexander & Heiyantuduwa, 2009).

This shortfall has arisen due to engineers' reliance on construction codes in the absence of a proper understanding of the principles behind durability. Moreover, the knowledge upon which these codes and standards are based is often outdated and cannot always be applied to present day construction practices (Lobo, et al., 2005). It is therefore crucial that the fundamental aspects of the corrosion phenomenon be explicitly understood as this will help ensuring adequate construction practice (Richardson, 2002).

Within a structural context durability may be defined as the structure's capacity to perform its intended function over its specific design life (Ballim, et al., 2009). Durability design may be conceptualised through two distinct practical approaches: prescriptive- and performance-based approaches. Prescriptive approaches focus on material specifications and proportions based on input parameters such as environmental exposure class and design life-span. Limits and thresholds are set to various concrete properties and mix proportions for example, water:binder ratio, cement content, cover depth, etc, depending on the concrete structure's specified conditions. The durability of the concrete will therefore be designed and assessed on the basis of its correctly assumed environmental exposure class and its compliance with the limiting mix proportions and requirements, cover depth and curing regimes (Ballim, et al., 2009).

Many researchers and engineers claim that the durability of the material cannot simply be determined through simple mix design parameters (Mackechnie, et al., 2001; Simons, 2004; Hunkeler, 2005). They argue that durability is a material performance concept for a structure in a specific environment. The prescriptive approach fails to consider the performance of the various cement types and of the mineral components added to the cement, or to the concrete mix itself. Additionally, the influences of on-site practice during the construction process are often neglected (Ballim, et al., 2009).

By contrast, the performance-based approach offers a more rational method for concrete durability design. This approach entails certain performance requirements or parameters that the concrete must achieve regardless of its mix design. It constitutes an alternative approach as it relies on input parameters such as measured material parameters and exposure conditions, to predict and

define the structure's durability quantitatively. The material properties related to deterioration such as the permeability coefficient of the concrete, are determined by using appropriate performance tests. These properties are then compared with environmental effects of deterioration, taking into account the change in time. Thus, the estimated deterioration of the structure during its design life may be quantified by using appropriate service life models (Ballim, et al., 2009).

South Africa has adopted the performance-based approach known as the Durability Index (DI) Approach (Alexander, 2017). In the context of carbonation-induced corrosion this entails the assessment of permeability characteristics of the concrete. These are obtained from the Oxygen Permeability Index (OPI) test, which determines the permeation of oxygen through a concrete sample. The OPI result is used as an input parameter for carbonation deterioration in the appropriate service life model. The expected service life of a structure may thus be quantified, based on the concrete cover quality and quantity, as well as the environmental exposure (Ballim, et al., 2009). Over the years there has been a steady development of the DI approach in design, testing and specifications (Alexander & Heiyantuduwa, 2009). However, there is still room for improvement surrounding the DI Approach and the service life modelling of concrete in particular around carbonation and modern concretes.

1.2 Problem statement

While South Africa has developed carbonation durability prediction models that can predict the performance of conventional concrete mixes (concrete containing 30% fly ash, 50% slag, 10% silica fume) relatively well, this formulation of the carbonation model was instituted approximately twenty years ago (Ballim, et al., 1999) and is considered outdated. The concrete materials used at that time differ significantly from modern concretes utilised today. As mentioned previously, currently concretes tend to combine different types and percentages of mineral admixtures i.e. modern concretes making these cement/binder systems more sophisticated and complex. As a result, long-term carbonation prediction performance data for these concretes is not yet available. Also, due to the current lack of research on durability predictions for modern concretes, the performance of modern concretes with respect to carbonation cannot be adequately determined.

This study seeks to improve the carbonation prediction for modern concretes. Additionally, it seeks to investigate whether the use of permeability and carbonation parameters of modern concretes still hold true in an existing South African carbonation model, and to determine whether adjustments are required. Currently carbonation prediction is based on the correlation between the oxygen permeability index (OPI) and carbonation. Since the OPI test is based on permeation – a transport mechanism related with deterioration, it was thought that the results obtained with this test could be used for carbonation predictions (Mackechnie & Alexander, 2002). This prediction now requires updating in relation to the various levels of mineral admixtures so that the existing model might be improved. Additionally, to get a better understanding of the correlation between the permeability and the carbonation coefficient, the effects of the various levels of mineral admixtures on the concretes permeability and carbonation performance ought to be individually investigated.

1.3 Hypothesis

This study proposes that the varying the percentage levels and types of mineral admixtures has an influence on the carbonation rate and permeability coefficient of concrete as the physical and chemical properties of the mineral admixtures modify the characteristics of the concrete pore

structure. Furthermore, it is proposed that a linear correlation exists between the permeability of concrete and carbonation coefficient as both are influenced by the interconnectedness of the concrete pore structure.

1.4 Research aim and objectives

The underlying aim of this research is to assist in further developing and refining the carbonation prediction model used in South Africa by investigating one of the aspects used in the model that is the correlation between permeability and carbonation for modern concretes. Hence the main objectives of this research are to:

- determine the correlation between the oxygen permeability and carbonation depths for modern concretes using the appropriate carbonation prediction models;
- assess the performance of binary and ternary mixes containing different mineral admixtures (slag, fly ash, silica fume and limestone) at varying replacement percentages, with regard to oxygen permeability; and to
- assess the performance of binary and ternary mixes containing different mineral admixtures at varying replacement percentages, with regard to carbonation.

1.5 Scope and limitations

Only a certain range of percentage replacement levels at varying increments for each mineral admixture were investigated. This research tested the addition of fly ash (FA) (20%-50% in 10% increments), blast furnace slag (BS) (20%-60% in 10% increments), Corex slag (CS) (20%-60% in 20% increments), and limestone (10% and 20%). For ternary blends, the concrete was limited to three mixes, that is, SF 5% with either 25% FA, 25 BS or 25% CS. Furthermore, the experimental scope was limited to two water:binder ratios (0,5 and 0,65) and one curing method (28-days wet curing).

1.6 Research significance

This research could potentially further improve the service life models of concrete by providing additional information and specifically by making the models more relevant to present day construction in South Africa. Consequently, this research may improve the fundamental understanding of concrete durability, specifically for carbonation-induced reinforcement corrosion. The construction industry is generally reluctant to venture into new technologies and innovations and instead tends to rely on existing building codes and standards. This reluctance is mainly related to a lack of knowledge of the performance of new materials. Potentially this research might inspire more confidence in the practice of using non-conventional concrete mixes (with varying amounts of cement extenders or supplementary cementitious materials) in concrete structures.

1.7 Thesis outline

The points that follow outline the manner in which this thesis has been set out.

- Chapter 1 provides an introduction and background to the dissertation.
- Chapter 2 presents the literature review together with the theoretical background to this research.

- Chapter 3 describes the experimental methods used in this study. It gives a detailed account of the work that was carried out in the laboratory as well as the statistical tools used to analyse the results.
- Chapter 4 presents the results and discussion where they are analysed and discussed.
- Chapter 5 consists of the conclusions and recommendations. Conclusions are drawn, and recommendations are made with regard to further work that may be beneficial in the field.
- Appendices are provided comprising of an ethic form, concrete material information with detailed concrete mix specifications, detailed experimental results and worked examples of the statistical results used in this study.

2 Literature review

This chapter provides a review of literature on reinforcement corrosion, concrete permeability, carbonation and mineral additives. It begins with Section 2.1, whereby a discussion on reinforcement corrosion and the effects of corrosion on the concrete structure, with an explanation of the mechanics involved. Thereafter in Section 2.2, the transport mechanisms involved in carbonation are investigated with a focus on the factors that affect concrete permeability. The discussion unfolds as a comparison of the various test methods used to determine the permeability characteristic.

Thus, the chapter explores carbonation in Section 2.4, its mechanisms and the methods used to measure and predict its severity. This chapter includes a discussion on the correlation between permeability and carbonation. In particular, Section 2.5 focuses on the composition of concrete through an examination of how its performance is affected by the most common types of mineral additives used in industry. Finally, Section 2.6 provides a summary of the literature review presented in this chapter.

2.1 Reinforcement corrosion

Reinforcement corrosion is one of the greatest causes of deterioration within reinforced concrete structures today (Hunkeler, 2005; Broomfield, 2008; Bertolini, et al., 2013). The rise of this phenomenon came about because of engineers and contractor's reliance on outdated codes that did not have the proper understanding of reinforcement corrosion (Richardson, 2002). It is, therefore, vital that the fundamental aspects of corrosion are properly understood.

Reinforcement corrosion produces rust and consequently results in a loss to the cross-sectional area of the steel. Rust is less dense than the parent steel and therefore occupies more volume (approximately 2 -5 times that of the parent steel). The complication which arises is that not only is there a loss in the cross-sectional area of the steel, but concrete must accommodate for the expansion caused by this reaction. If the concrete cannot accommodate this expansion, internal tensile pressures will ensue (Richardson, 2002).

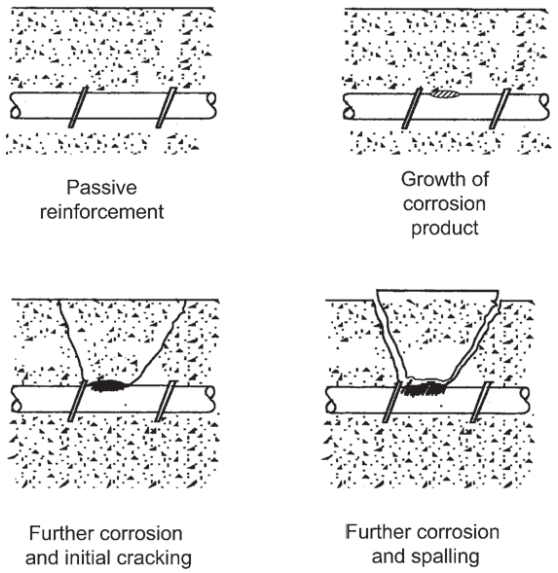

Figure 2-1: Stages of corrosion-induced damage in concrete (Richardson, 2002)

Due to the relatively low tensile strength of the concrete, its resistance to the expansion is limited. If the induced tensile stresses are greater than the tensile strength threshold of the concrete, cracking within the concrete will commence. Further development may result in delamination and eventually spalling (Ballim, et al., 2009). This phenomenon is more explicit in in concrete with low cover depths (Newman & Choo, 2003).

Reinforcement corrosion can be induced by carbonation, corrosive contaminants such as chlorides, or stray currents (Raupach & Büttner, 2014). However, the two main causes of reinforcement corrosion are chloride attack and carbonation (Papadakis, 2000; Broomfield, 2008; Ballim, et al., 2009) and will be the focus for the rest of this section. Tuutti (1982) proposed that reinforcement corrosion can be subdivided into two phases, namely: initiation and propagation phases (Refer to Figure 2-2). The initiation phase is defined as the time required to depassivate the embedded steel. Minimal to no corrosion damage is anticipated during this phase.

Carbonation and chloride attack occur within this phase as these mechanisms deal mainly with the depassivation of the concrete. The total time duration of this phase is governed by the concrete quality, cover depth, environmental class, and the threshold concentration needed to commence corrosion (Hunkeler, 2005; Ballim, et al., 2009; Raupach & Büttner, 2014). The propagation phase translates to the corrosion of steel on the condition that there is adequate water and oxygen on the surface of the steel. This is accompanied by the development of cracking, delamination and the eventual spalling of the concrete, contributing to the concrete structure's deterioration (Ballim, et al., 2009). The corrosion rate in the propagation phase will depend on temperature, moisture content, oxygen availability, pH of the water and resistivity of concrete (Hunkeler, 2005).

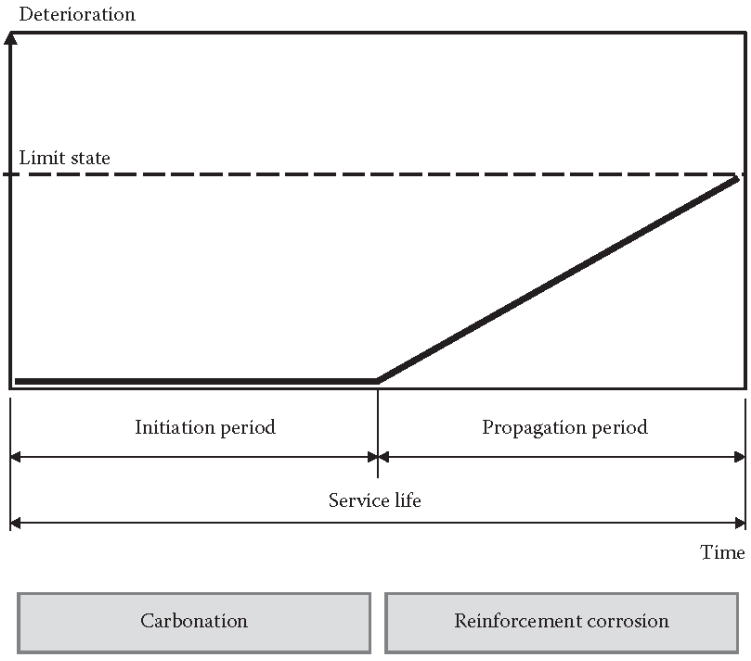

Figure 2-2: Stages of corrosion-induced damage in concrete (Richardson, 2002)

2.1.1 Mechanism of corrosion

The corrosion of steel is an electrochemical process as depicted in Figure 2-3 controlled by the formation of cathodic and anodic sites which exist on various locations of the surface of the steel. The formation of these sites is due to the chemical and physical imbalance on the homogeneous steel surfaces (Ballim, et al., 2009). In reinforced concrete the alkaline pore solution serves as the

electrolyte, and the embedded steel allows for the electrons to travel between the anodic and cathodic sites present on the steel's surface (Richardson, 2002; Broomfield, 2008). The reaction that occurs at the anode is shown in Equation 2.1:

$$Fe \rightarrow Fe^{2+}+2e^{-} \quad (2\text{-}1)$$

$$2H_2O+ O_2+4e^{-} \rightarrow 4OH^{-} \quad (2\text{-}2)$$

A loss of electrons takes place in anodic areas. The steel oxidises whereby the iron (Fe) atoms are converted into iron ions (Fe^{2+}) dissolving into the pore solution surrounding the embedded steel. The electrons (e^{-}) are now released and begin to flow towards the cathodic sites. The electrons needs to be consumed via a chemical reaction at another site on the surface of the steel to preserve electrical neutrality (Broomfield, 2008). Subsequently, electrical current is induced through the steel. Once the electrons reach the cathodic area, it reacts with water (H_2O) and oxygen (O_2) to form hydroxide ions (OH^{-}). The reaction which occurs at the cathode is shown in Equation 2.2. Using the pore solution as an electrolyte, the Fe^{2+} ions and the OH^{-} react to form ferric hydroxide, commonly known as rust in practice (Richardson, 2002).

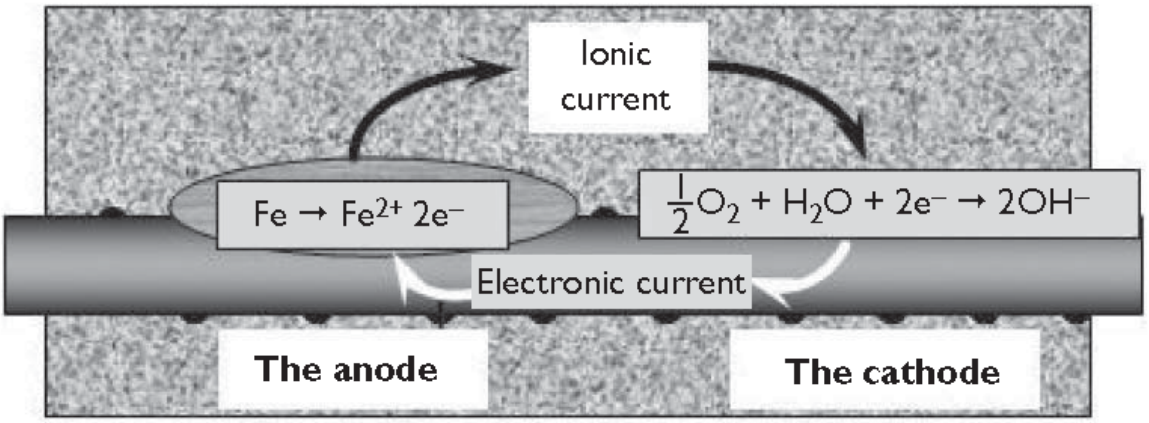

Figure 2-3: Reinforcement corrosion reactions (Broomfield, 2008)

Two concrete attributes allow for the protection of the embedded steel against corrosion. The first is concrete cover which serves as a barrier, thus hindering the ingress of aggressive corrosive agents upon the steel. The steel in concrete is commonly depassivated by the ingress of aggressive agents such as chloride ions, or in a reduction in alkalinity through carbonation. Once the steel is depassivated it becomes vulnerable to corrosion. Additionally, any cracks existing within the cover accelerate the migration of aggressive ions towards the steel, increasing the rate of corrosion (Bertolini, et al., 2013). This is why concrete cover at adequate depth and of high quality, that is, low permeability and with low susceptibility to cracking, is recommended for adequate resistance to corrosion (Alexander & Beushausen, 2009).

The second feature is that a high alkalinity naturally exists within the concrete. This develops a protective film known as gamma ferric oxide (Ballim, et al., 2009). It is characterised as a dense, impenetrable film which surrounds the embedded steel. If fully established and maintained it will passivate the steel preventing contact with oxygen and water to initiate corrosion (Broomfield, 2008). One method whereby the susceptibility of steel to corrosion can be estimated is the use of the Poubaix diagram shown in Figure 2-4. It is a potential-pH diagram which represents the stability of a metal as a function of potential and pH. The diagram assesses the metal's immunity that is, whether it

is thermodynamically stable or immune to corrosion. Additionally, it determines passivity that is, whether compounds of the metal are thermodynamically stable via passive film surrounding and protecting the metal against corrosion. Based on the diagram, for a pH of less than 9 the protection layer will be lost, and the metal will be in a corrosive state. While this diagram is useful for identifying the metal's potential corrosive state, it cannot be used to determine the rate of corrosion (Markeset & Myrdal, 2008; Roberge, 2008).

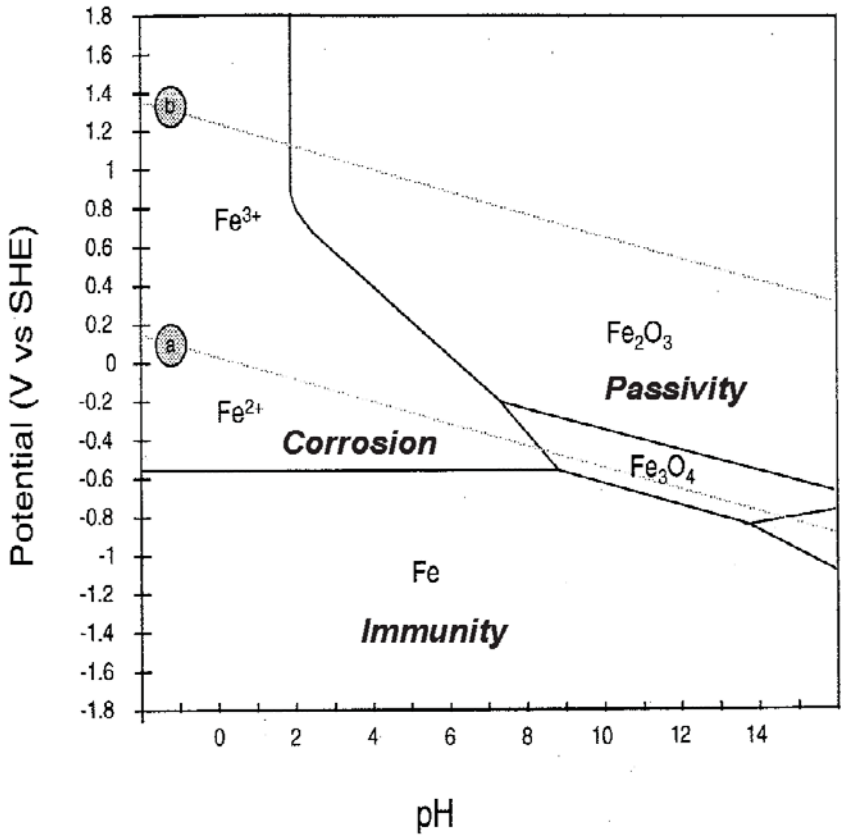

Figure 2-4: Simplified Pourbaix diagram for iron in water showing the most stable products at a given pH and potential (Markeset & Myrdal, 2008)

2.2 Transport mechanisms

Transport properties of concrete are essential for predicting its durability as the severity of all deterioration mechanisms (that is, carbonation, chloride ingress, etc.) correlates with penetrability - the resistance to which a fluid or ion can migrate through the concrete's microstructure. Transport parameters, which relate to this concept, include permeation, sorption, diffusion and migration (Ballim, et al., 2009). However, this section will mainly focus on the transport mechanisms governing the degree of carbonation.

2.2.1 Permeation

Permeation is described as the flow of liquids and gases through a porous medium caused by a pressure. Permeation (also referred to as permeability) is described as the flow of liquids and gases through a porous medium caused by a pressure head (Ballim, et al., 2009). The movement of the permeating liquid or gas through the concrete, described as capillary flow can be described as either laminar or turbulent. The type of capillary flow is dependent on the following factors: such as the pore structure of the material and the viscosity of the flowing media. For gases, if it is assumed that laminar flow exists within the concrete medium, the Hagen-Poiseuille law applies. Additionally, taking

into account that the compressibility as well as the viscosity of the gas is considered, Equation 2-3 can be used to determine the coefficient of permeability (Kropp & Hilsdorf, 1995):

$$K_g = \eta \frac{Ql}{tA} \frac{2p}{(p_1 - p_2)(p_1 + p_2)} \quad (2\text{-}3)$$

Where
- K_g = Coefficient of permeability (m^2)
- η = Viscosity of the gas (Ns/m^2)
- Q = Volume of gas flowing (m^3)
- l = Thickness of penetrated section (m)
- A = Penetrated area (m^2)
- p = Pressure at which volume is measured (N/m^2)
- p_1 = Pressure at entry of gas (N/m^2)
- p_2 = Pressure at exit of gas (N/m^2)
- t = Time (s)

2.2.2 Diffusion

Diffusion is defined as the movement of liquid, gas or ions through a partially or fully saturated porous material under a concentration gradient. The concentration gradient within the concrete is developed through the adsorption of salts, creating a high concentration at the surface. This causes the salts to migrate to the material's interior where a low concentration region exists. The rate of diffusion is dependent on temperature, internal humidity of the material, type of diffusant and the inherent diffusability of the material (Ballim, et al., 2009).

For steady state diffusion (not dependent on time), Fick's first law of diffusion can be used to model gaseous and ionic diffusion within uniformly permeable concrete. It is presented in Equation 2-4 (Note, the negative sign is due to diffusion occurring in the opposite direction to that of the increasing direction) (Ballim, et al., 2009):

$$J = -D \frac{\delta C}{\delta x} \quad (2\text{-}4)$$

Where:
- J = Mass transport rate (change in concentration over time) (g/m^2s)
- $-D$ = Effective diffusion coefficient (m^2/s)
- C = Concentration (g/m^3)
- x = Distance (m)
- $\frac{\delta C}{\delta x}$ = Concentration gradient ($g/m^3/m$)

2.2.3 Relationship between permeation and diffusion

Despite permeation and diffusion being two different processes driven by two different mechanisms – the pressure and concentration gradient respectively – a relationship can still be established as they occur within the pore network (Salvoldi, 2010). A theoretical relationship was presented by (Nilsson & Luping, 1995) which assumes Hagen-Poiseuille's law is applied especially in small pores, and thus that laminar flow in pores occurs. Factoring in the permeability of a small pore embedded in a medium of

cross-sectional area A, the relationship was determined in the following manner is shown in Equation 2-5 (Lobo, et al., 2005).

$$K = \frac{\pi r_{eff}^4}{8A} \quad (2\text{-}5)$$

Where K = Permeability (m^2)

A = Cross-sectional area of medium (m^2)

r_{eff} = Single straight pore radius (m)

The diffusion coefficient for the same pore can be expressed as follows where a_{eff} is the area fraction of effective pores and D_0 is the diffusion coefficient in a bulk fluid:

$$D = D_0 a_{eff} = D_0 \frac{\pi r_{eff}^2}{A} \quad (2\text{-}6)$$

As stated at the beginning of this section, permeability and diffusion occur in the same pore network. As such the radius from Eq 2.5 and Eq 2.6 can be from the same pore and thus, substituting Eq 2.5 into Eq 2.6 the following relationship is established:

$$K = \frac{r_{eff}^2}{8D_0} = \frac{A}{8\pi D_0^2} D^2 = \text{constant} \times D^2 \quad (2\text{-}7)$$

A power relationship can be observed between the two mechanisms. The effective radius for the pores is affected by the transport of different flow mechanisms, fluids, substances and cracks. One example of this is where the air permeability in a matrix that is partly saturated allows diffusion to occur in both a gaseous and a liquid medium. To consider this situation, the exponent of the equation can be altered to become Equation 2-8. The exponent b in this equation will depend on the condition of both permeation and diffusion. Table 2-1 displays the various b values that were attained experimentally:

$$K = \text{constant} \times D^b \quad (2\text{-}8)$$

As shown in Table 2-1, the relationship depends significantly on the moisture content of the pore system. The movement of gas within the system would be blocked by the existence of moisture within the pore structure. Additionally, diffusing and permeating species can react or interact with the pores, which can also significantly affect the flow for example, the ingress of carbon dioxide (CO_2) reacting with calcium hydroxide (CH). These factors can indicate limitations to the equation. However, despite these Equation 2-8 is still able to relate the transport mechanisms that can reasonably be established experimentally if required (Kropp & Hilsdorf, 1995).

Table 2-1:Experimental b values (Kropp & Hilsdorf, 1995)

Substance in Permeation	Diffusion	b
Water	Water Vapour	1.8
Gas	Gas	1.0
Water	Ions	1.5

2.3 Concrete permeability

Concrete cover properties govern the service life of a concrete structure. Insufficient depth or poor quality of cover concrete are two key reasons for premature deterioration (Alexander & Beushausen, 2009). According to Frenzer and Torrent (1995), permeability of concrete cover is considered as a crucial quality that determines the potential resistance of the concrete structure to deterioration such as carbonation-induced corrosion.

It is therefore necessary to investigate factors that affect permeability. Whether it increases the permeability performance i.e. lowers the permeability or vice versa. Moreover, a reliable method of doing so is required if one is to be able to determine the concrete permeability performance especially on site. To examine these factors more closely this section discusses and compares common permeability test methods used in practice. This is followed by an evaluation of intrinsic and extrinsic factors that affect concrete permeability.

2.3.1 Permeability tests

Concrete permeability tests can be divided into two types: destructive and non-destructive. The OPI test and the Cembureau permeability test are both destructive tests. The Torrent permeability test and Autoclam permeability test are double and single chamber non-destructive tests respectively.

2.3.1.1 South African oxygen permeability index test

The Oxygen Permeability Index (OPI) test measures the pressure decay of oxygen passed through a concrete sample. This test assesses the overall micro- and macro-structure of the outer surface of cast concrete. Moreover, it is known to be significantly sensitive to the presence of any macro-voids or cracks. This allows for factors such as the state of compaction, the presence of bleed voids and channels, and the degree of interconnectedness in the pore structure to be evaluated (Ballim, et al., 2009).

The test entails placing concrete specimens (30 mm thick and 70 mm in diameter) in a permeameter (See Figure 2-5). These concrete specimens are destructively obtained either from core in-situ in the element under inspection, or from concrete cubes during mix design. In accordance with SANS 3001 C03-11 (2015), samples are preconditioned by being dried in the oven at 50°C for seven days prior to testing. The oxygen passing through the sample is subjected to an initial pressure of 100 ± 5 kPa. The test ends once the pressure reaches a pressure of 50 kPa, or after six hours have elapsed, whichever comes first. The rate of pressure decay is incrementally measured and thereafter the permeability coefficient can be calculated (Ballim, et al., 2009).

OPI values are expressed as the negative log of the coefficient of permeability which is evaluated in accordance with D'Arcys law (units being m/s), with typical values ranging from 8-11. A higher OPI value indicates a lower permeability characteristic. It is important to note that as these values are measured on the log scale, variation between OPI values can be significant. For example, a permeability value of 10.5 is twenty times more permeable than a value of 8.5 (Ballim, et al., 2009). Table 2-2 provides suggested ranges for OPI durability classifications, based on site and laboratory data.

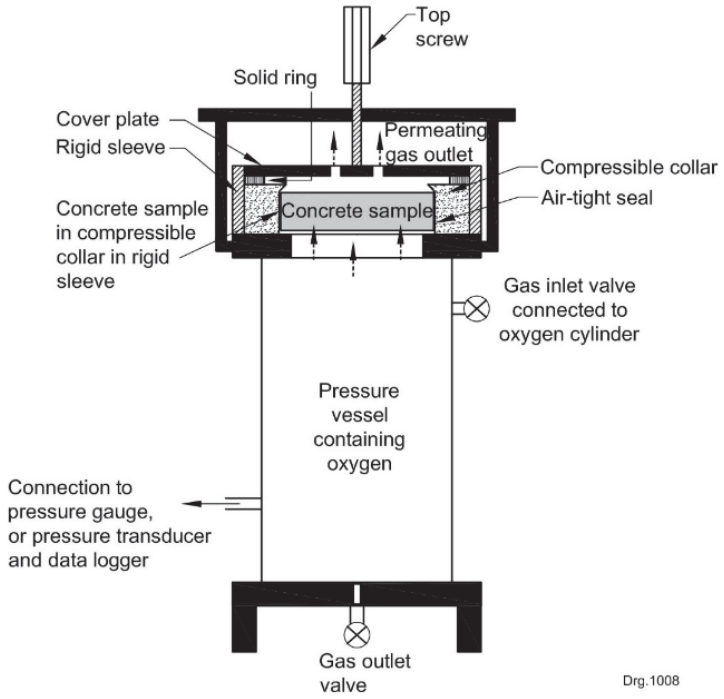

Figure 2-5: Permeability cell arrangement (Alexander, 2017)

In terms of the variability of the OPI test methods, repeatability and reproducibility were investigated to determine whether it was robust and practical for industry. Repeatability is defined as the variance in results from a single operator. Reproducibility is the variance in results amongst the laboratories, in this case a series of round robin tests between various laboratories in South Africa. After each round, the results and variability were inspected, and adjustments were made to the test methods, refining them to make them more accurate and/or simpler to use. The coefficient of variation (CoV) for the repeatability and reproducibility of this test were high, with values of 32,2% and 36,6% respectively. The relatively high results are generally accepted as being due to the inherent flaws within the concrete which influence its permeability (Stanish, et al., 2006). From. The Durability Index Testing Procedure Manual (2017) has provided typical CoV ranges for the repeatability and reproducibility of this test. The CoV for repeatability for laboratory data and site data is 30-40% and 40-50% respectively. The CoV for reproducibility is 30 - 50% (Alexander, 2017).

Table 2-2: Suggested ranges for durability classification using OPI values (Ballim, et al., 1999)

Durability class	OPI (log scale)
Excellent	>10
Good	9,5-10
Poor	9,0 – 9,5
Very Poor	<9,0

2.3.1.2 The Cembureau permeability test

The Cembureau permeability test is a destructive test in which a cored or cast concrete specimen (150 mm diameter; 50 mm thickness) is subjected to a unidirectional oxygen gas flow produced by a constant pressure gradient between the two flat surfaces of the specimen. The coefficient of permeability is based on the Hagen-Poiseulle principle (Kollek, 1989). The gas flow is dependent on the pressure difference, testing environment, testing area, specimen thickness, and the viscosity of

the test gas (Beushausen & Alexander, 2008). The advantage of this test is that it allows for a variety of preparation regimes which affect the internal moisture and hence the permeability measurement.

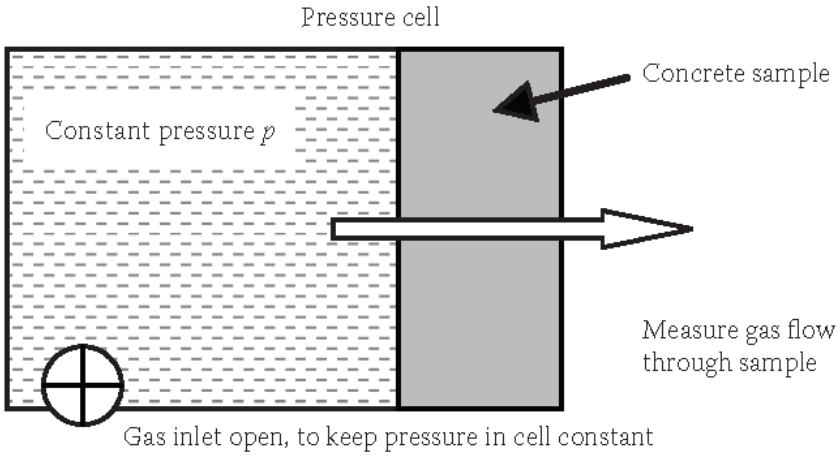

Figure 2-6: Schematic of the Cembureau permeameter (Beushausen & Alexander, 2008)

2.3.1.3 The Torrent permeability test

The torrent permeability test (TPT) is a non-destructive test (NDT) that can be applied to a flat concrete surface. This test is commonly used in several European countries. The distinctive characteristic features of this method include the use of a two-chamber vacuum cell attached to a regulator that balances the pressure between the inner and outer chambers (refer to Figure 2-7) (Ballim, et al., 2009).

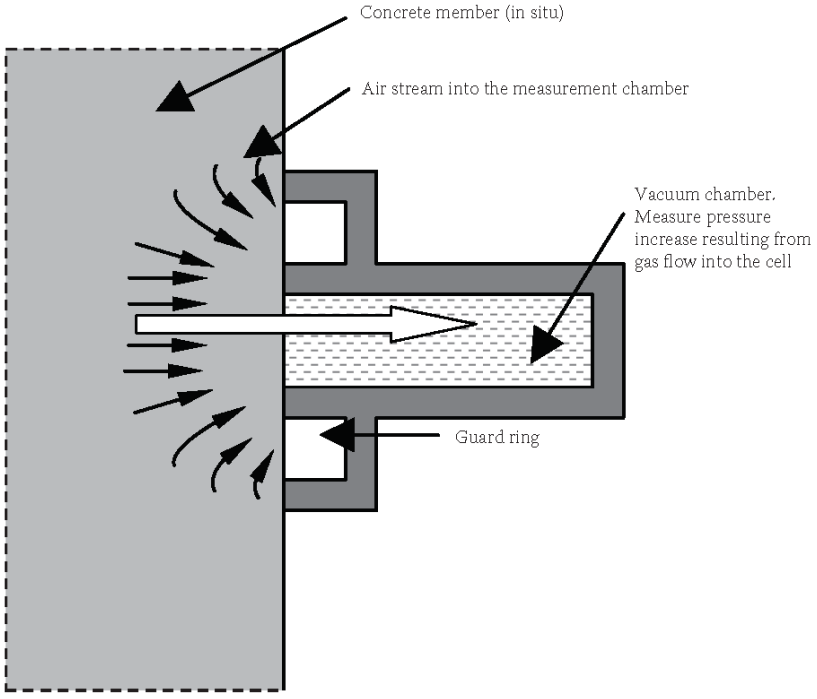

Figure 2-7: Detail of air-flow into the vacuum cell of the Torrent Permeability Tester (Beushausen & Alexander, 2008)

The test entails placing the device on the concrete surface where a vacuum pressure is produced in both chambers, using a pump. The outer chamber (the guard ring) prevents any surrounding air from entering the inner (measuring) chamber. Together with the regulator balancing the pressures in both chambers, this set-up allows for a controlled, unidirectional flow to enter the inner chamber from the

underlying surface. The inner chamber is then closed causing the pressure inside to increase. The rate of the increasing pressure is associated with the permeability coefficient of the concrete surface (Frenzer & Torrent, 1995).

The advantages of this method include its being relatively quick (1,5-12 min), and its rendition of readings with low variability. The benefit of this feature is that only one reading per position is needed. Moreover, the method allows for the adjustment of the permeability measurement based on the concrete's internal relative humidity which is indicated by the concrete obtained from resistivity readings. Lastly, due to the test being non-destructive, it is also appropriate for both laboratory and site conditions (Fernández Luco & Torrent, 2007).

2.3.1.4 The Autoclam air permeability test

The Autoclam air permeability test is a non-destructive test. It entails sealing a base ring plate with an internal diameter of 50 mm to a concrete surface, isolating an area. Sealing is performed either by adhesive bonding or by bolting the plate to the surface. Thereafter the pressure chamber may be attached to the base ring and pressure applied. The concrete permeability is determined by monitoring and measuring the decay of pressure over time (every 15 minutes) into the surface of the concrete until the pressure reaches a value of zero (Bjegovic, et al., 2016).

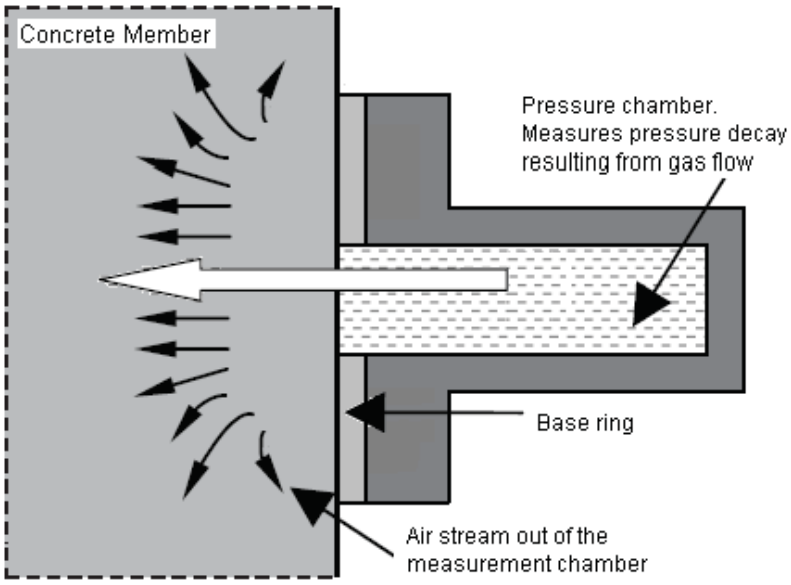

Figure 2-8: Schematic of the Autoclam permeameter (Salvoldi, 2010)

This test can measure both water and air permeability of the concrete surface. Additionally, it can determine the water absorption rate of concrete or sorptivity. Repeatability variability is low hence one measurement per position will suffice. However, significant variability is observed when testing is conducted on different locations (Bjegovic, et al., 2016). ‘

2.3.1.5 Discussion of the permeability test

As stated at the beginning of this section, the permeability tests are discussed under two categories: destructive and non-destructive tests (henceforth referred to as DTs and NDTs). NDT tests discussed in this study can also be considered as surface methods as they are applied directly on the structure of the concrete's surface during testing.

The permeability testing methods differ in relation to how the permeability of the concrete is obtained. The process is based on either assumption made or upon the way permeating gas is applied and measured. Different assumptions are made (D'Arcy's Law or The Hagen-Poiseuille relationship for laminar flow) based on the permeating gas for the calculation of permeability resulting in different units of measurement. Furthermore, depending on the test method, permeability can be obtained by either measuring the pressure decay, pressure increase or gas flow while the sample is under constant pressure, using either oxygen or ambient air.

The versatility of the various permeability methods ranges widely; with some tests being suitable for use in the laboratory and on site. This characteristic was observed in the NDTs, specifically in the Torrent and Autoclam permeability tests. This characteristic was most notable in the Autoclam permeability test as it can measure the air or water permeability as well as the sorptivity. By contrast, destructive tests such as the Cembureau and OPI tests are limited to a laboratory environment due to the sample preparations these require.

The internal moisture of the concrete condition plays a vital role in the permeability characteristic and variability. The preconditioning regime required for the two destructive tests minimises the variability of test. The purpose of the preconditioning regime is to control the internal humidity of the control to minimise the effect it has on the results Conversely; NDT results are highly affected by internal humidity due to their non-reliance on a preconditioning regime. The Torrent air permeability test complements its results with resistivity readings to account for concrete surface's moisture state. The Autoclam air permeability test, however, does not account for the internal moisture state and therefore caution needs to be taken when interpreting the results.

A study conducted by Alexander and Beushausen (2008) investigated a comparison between the South African OPI test and other internationally accepted permeability test methods namely, the Torrent and the Cembureau methods. The results showed that all test methods could distinguish between different mix parameters (w/b ratios and cementitious materials, curing regimes). Furthermore, near good linear correlations were shown (Refer to Figure 2-9 and Figure 2-10) and in the oxygen permeation results between OPI and the other permeability test methods. This indicates that these test methods have similar merit in assessing concrete cover quality.

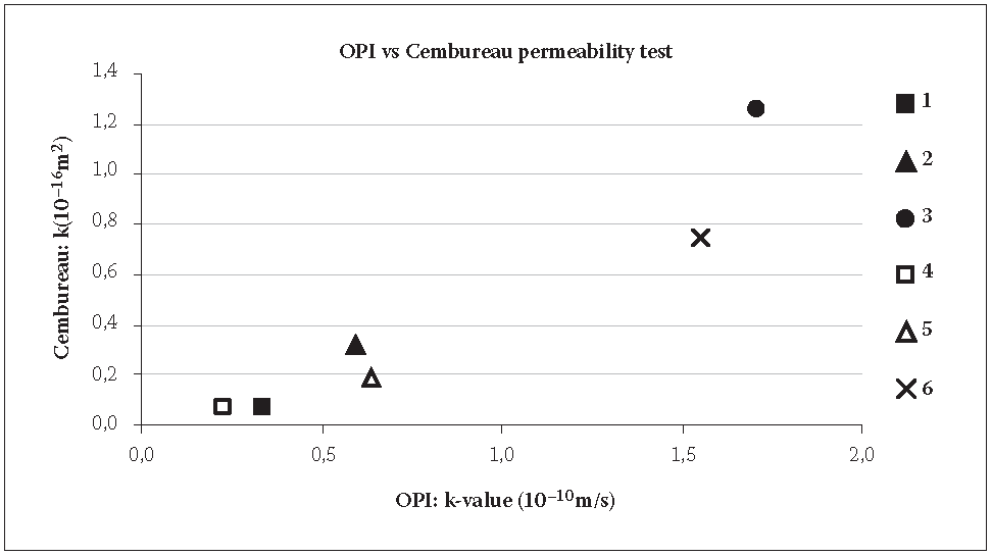

Figure 2-9: Correlation between test results obtained using the OPI method and the Cembureau method (Beushausen & Alexander, 2008)

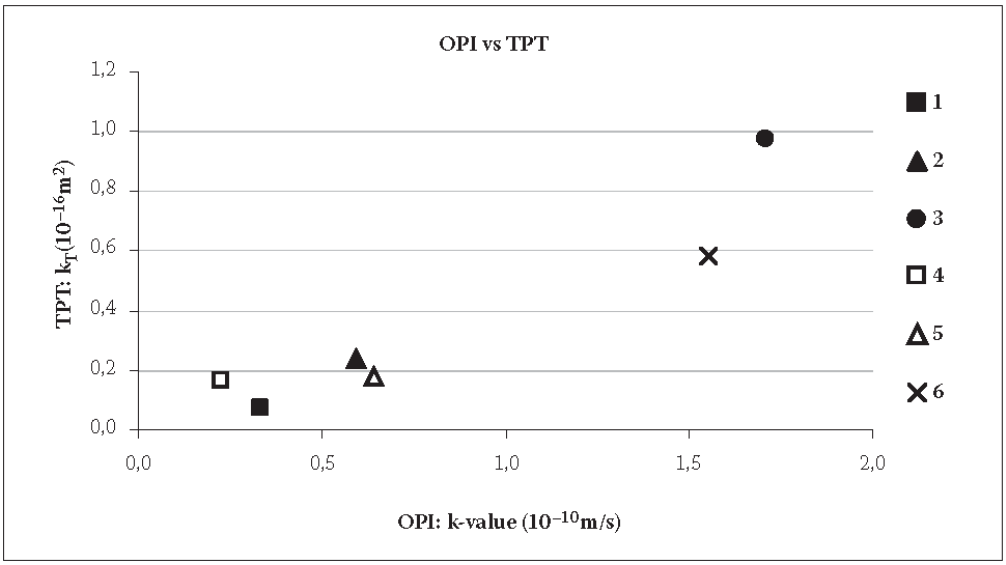

Figure 2-10: Correlation between test results obtained using the OPI method and the torrent permeability tester, TPT (Beushausen & Alexander, 2008).

2.3.2 Factors affecting permeability

2.3.2.1 Mineral admixture type

Both the physical and chemical attributes of mineral additives contributed to the influence in permeability performance. Commonly, particle sizes of the mineral admixtures are smaller than those of Portland cement (especially silica fume). Consequently, this makes mineral admixtures an effective fine filler. Additionally, mineral additives serve as nucleation sites, which aid in enhancing the cement hydration reaction. Its chemical effects such the pozzolanic reactions, forms additional cementing-like compounds in the presence of calcium hydroxide (CH) (Bertolini, et al., 2013). More information regarding mineral additives is shown in Section 2.4.4 of this chapter.

The area between the cement paste and the aggregate, referred to as the ITZ (refer to Figure 2-11), is considered as the main area of weakness in terms of its resistance to the penetration of aggressive ions. This is due to its having a higher w/b ratio relative to the rest of the concrete as fewer cement particles are located in that area. Due the pozzolanic reactions, calcium hydroxide (CH) present at the ITZ can react with mineral admixtures to form cementing-like compounds. This leads to the refinement of the ITZ and subsequently to the densification of the overall pore structure (Bertolini, et al., 2013).

It is important to note that the use of mineral admixtures may not result in the decrease of permeability. This is possibly due to the weak reactivity of the mineral admixtures, inadequate replacement levels or inadequate curing time. However, the likelihood of beneficial results in terms of permeability with the use of SCMs increases with time (Pacheco-Torgal, et al., 2013).

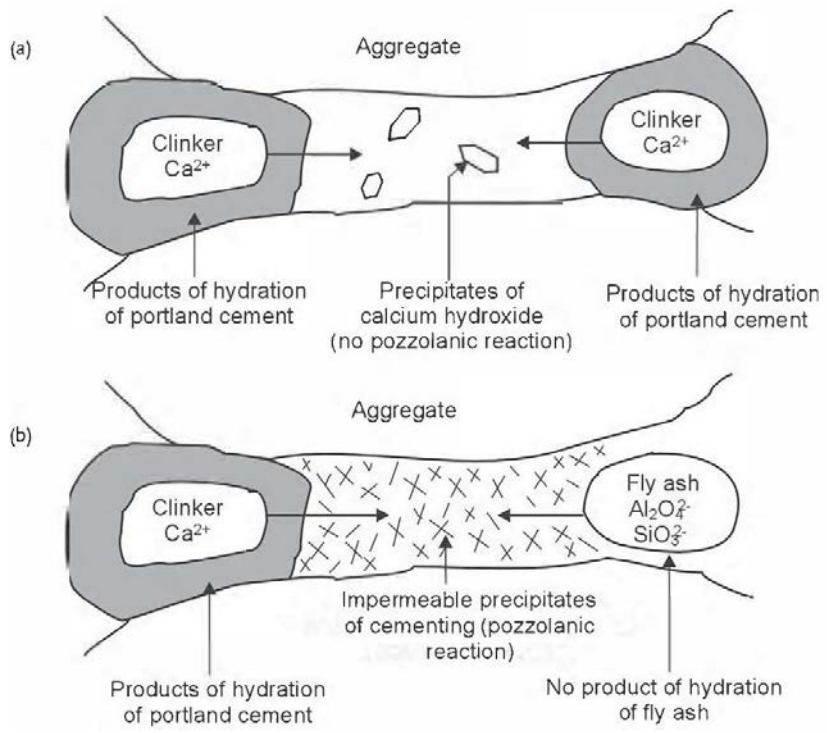

Figure 2-11: Reactions present at the ITZ, hydration of PC (a), and PC with the addition of a mineral admixture (fly ash) (b) (Bertolini, et al., 2013)

2.3.2.2 Curing regime

Curing is described as the maintenance of adequate moisture and temperature for the onset of hydrations and/or pozzolanic reactions. Cementitious compounds in cement can only be formed in water-filled spaces. These cementing compounds bind to each other and to the aggregate, leading to a dense micro-structure. The hydration reaction will cease if the concrete dries out. Adequate curing is, therefore, essential to promote mechanical strength development; but most importantly for the improvement of the permeability, particularly near the concrete surface. This is crucial for the durability potential of the structure (Newman & Choo, 2003). Figure 2-14 depicts the influence of curing on the permeability of concrete.

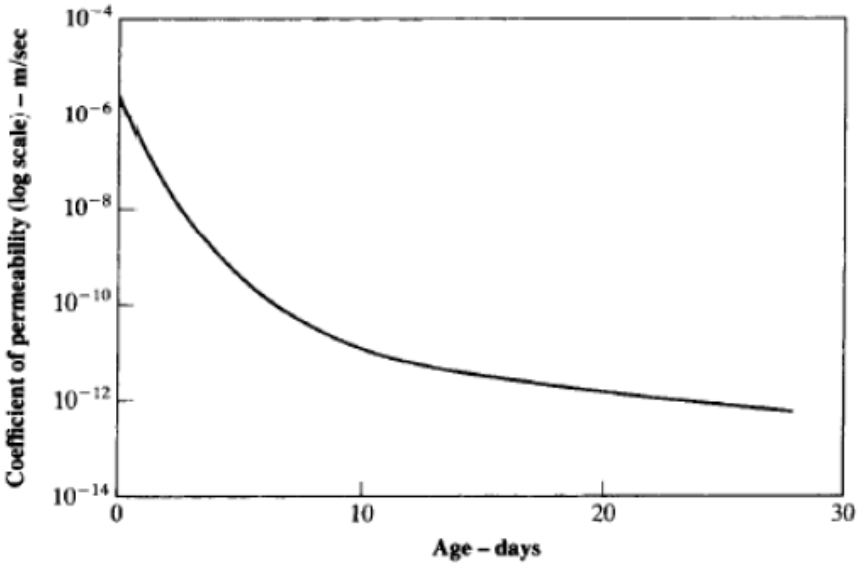

Figure 2-12: Effect of curing on concrete permeability (Powers, et al., 1959)

2.3.2.3 Water:binder ratio

The gross volume of the concrete mixture does not practically change during the hydration reaction – that is, the volume of the combined water and cement is equal to the hardened concrete (Bertolini, et al., 2013). It can thus be said that the hydration reaction plays a role in permeability performance (Powers, et al., 1959).

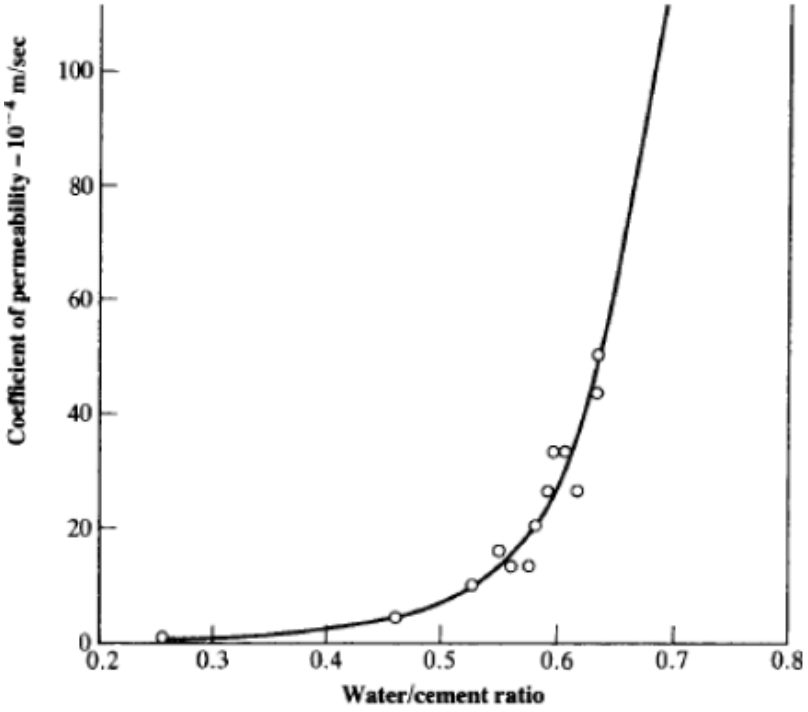

Figure 2-13: Effect of w/c ratio on permeability for mature cement paste (Powers, et al., 1954)

The hydration products, predominantly tricalcium and dicalcium silicates, interlock and form both physical and chemical bonds developing a particulate network with interstitial spaces. This phenomenon can be defined as the interlocking effect. These interstitial spaces consist of gel pores and capillary pores, where the latter is significantly the larger of the two. Capillary pores in concrete are defined as spaces originally occupied by water. During the hydration reaction, the products fill the spaces previously occupied by the water i.e. the capillary pores thus reduce the overall pore volume and thereafter, the interconnectedness of the pores (Bertolini, et al., 2013). For this reason, altering the w/b ratio alters the permeability performance. This is due its influence on degree of the hydration reaction as well as the initial spacing between cement particles. These factors govern the magnitude of the interlocking effect (Grieve, 2009).

2.4 Carbonation

Carbonation is a chemical reaction whereby carbon dioxide (CO_2) in the atmosphere reacts mainly with calcium hydroxide (CH) to form calcium carbonate ($CaCO_3$). The conversion of CH into ($CaCO_3$) decreases the pH of the pore solution of the concrete increasing the vulnerability of the reinforcement to corrosion in the presence of adequate oxygen and water. The corrosive products that develop on the surface of the reinforcement induce internal tensile stresses. Once the induced tensile stresses reaches the threshold tensile value of the concrete, it may result in cracks or eventually in the spalling of the concrete cover, compromising the structure's robustness (Raupach & Büttner, 2014).

Structures that are severely damaged due to corrosion require high cost repair and rehabilitation strategies (Alexander et al., 2007). The section that follows thus provides further insight into the deterioration process known as carbonation, its mechanism, influences and test methods. One sub-section briefly addresses the common carbonation models used while investigating the correlation between permeability and carbonation.

2.4.1 Carbonation mechanism

Of all the constituents of the atmosphere, carbon dioxide (CO_2) constitutes a minor component (approximately 0,03%) (Mays, 1992). Nevertheless, it plays a significant role in the initiation of reinforcement corrosion. Atmospheric CO_2 reacts with water in the concrete pore solution to form carbonic acid (H_2CO_3). Thereafter, in the concrete pores the carbonic acid reacts with calcium hydroxide (CH) to produce calcium carbonate ($CaCO_3$) (Papadakis, et al., 1991a; Papadakis, et al., 1991b). The simplified carbonation reaction is shown in Equation 2-9 (Mays, 1992; Papadakis, 2000; Bertolini, et al., 2013).

$$CO_2+Ca(OH)_2 \rightarrow CaCO_3+H_2O \quad (2\text{-}9)$$

Other gaseous compounds such as sulphur dioxide (SO_2) can mimic the carbonation process; however, their significance is considered negligible. Furthermore, within the concrete CO_2 may react with other alkaline constituents such as sodium and potassium hydroxides or even hydration products such as calcium silica hydrates (CSH). However, CO_2 is more inclined to react with the CH (Mays, 1992).

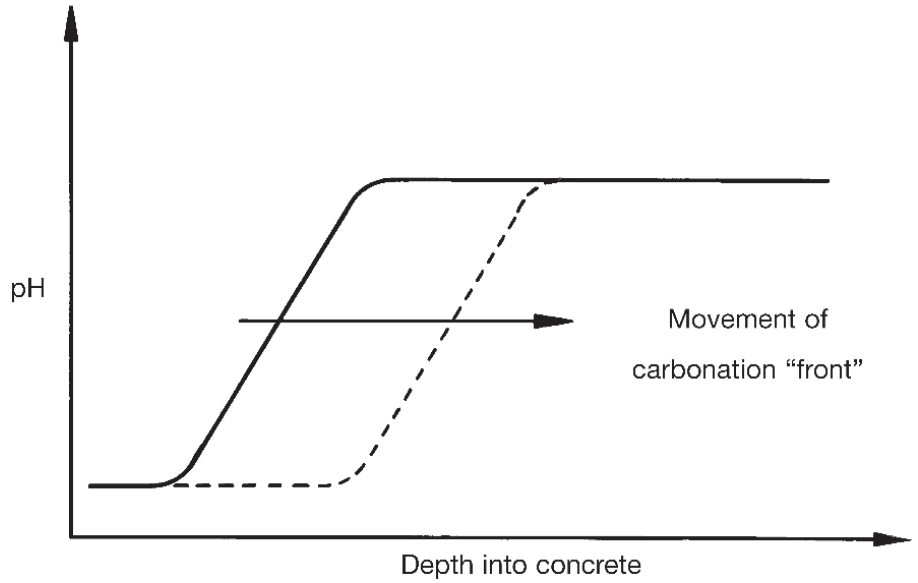

Figure 2-14: The pH reduction front behaviour due to carbonation (Ballim, et al., 2009)

As this reaction progresses, the pH of the concrete pores reduces. The carbonation process normally moves as a 'front' from the concrete surface. This front will progress beyond a specific point once all the CH has been converted into $CaCO_3$ (Ballim, et al., 2009). The carbonation front can be made visible by applying an indicator solution such the phenolphathein solution to the surface of the concrete. After application, a linear like boundary between the carbonated concrete and the unaffected area can be observed. This boundary separates the carbonated from the uncarbonated concrete (Raupach & Büttner, 2014). Due to the presence of coarse aggregates and material

inhomogeneity, the carbonation front is not always a straight line (Yam, 2004). More information regarding the carbonation depth is shown in Section 2.4.3.

2.4.2 Factors affecting carbonation

The rate of carbonation is dependent on extrinsic factors such as environmental exposure conditions (humidity, temperature, concentration of CO_2), and intrinsic factors such as the concrete's composition and cover depth.

2.4.2.1 Humidity levels

Varying levels of humidity can influence the rate of carbonation. The diffusion of CO_2 is generally facilitated through the unsaturated or air-filled pores in the concrete. However, saturated or relatively near saturated pores would hinder the diffusion. Therefore, at relatively high humidity levels (greater than 75%), the rate of carbonation is low: the diffusion is restricted, making it more difficult for the CO_2 to penetrate the concrete. Conversely, an absence of water within the concrete results in the cessation of the carbonation reaction. Therefore, with humidity levels relatively low, the rate of carbonation is hindered until the concrete reaches adequate humidity levels (Mays, 1992).

Figure 2-15 shows the relationship between humidity and the rate of carbonation. The humidity range for the highest rates of carbonation varies within literature. However, based on literature, the highest rate of carbonation may lie anywhere within the humidity range of 40% - 75% (Richardson, 2002; ACI Committee 201, 2003; Ballim, et al., 2009; Bertolini, et al., 2013). For high humidity levels (greater than 75%), the water-filled pores hinder the diffusion rate and the reaction is mainly dependent on the rate in which the CO_2 can diffuse and penetrate; thus, making diffusion the dominant factor for the rate of carbonation. Conversely, for low humidity levels, the reaction rate of CO_2 dominates the rate of carbonation and as the diffusion may be high, only a portion of the gas can dissolve and react within the water. (Salvoldi, 2010).

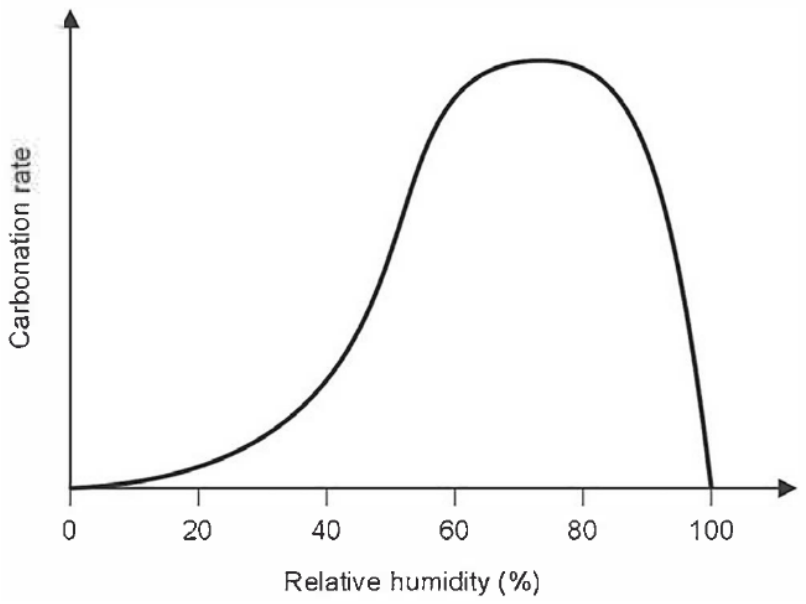

Figure 2-15: The rate of carbonation of concrete as a function of the relative humidity of the environment, under equilibrium condition (Bertolini, et al., 2013).

2.4.2.2 Temperature and CO_2 concentration

Generally, an increase in ambient temperature would result in an increased rate of carbonation as heat commonly accelerates most chemical reactions (Saetta, et al., 1993). A similar trend exists for

the effects of CO_2 concentration on the rate of carbonation (Bertolini, et al., 2013). CO_2 concentration may vary from 0.03% (300ppm by volume) in rural areas to greater than 0.1% in urban areas where air pollution is greater in comparison. Notable high CO_2 concentrations are experienced in motor vehicle tunnels (Bertolini, et al., 2013). Figure 2-16 shows the effect of environments with varying CO_2 concentration on the carbonation rate. Note that for coastal environments, its relatively high humidity also influences the rate of carbonation subsequently decreasing it (Richardson, 2002).

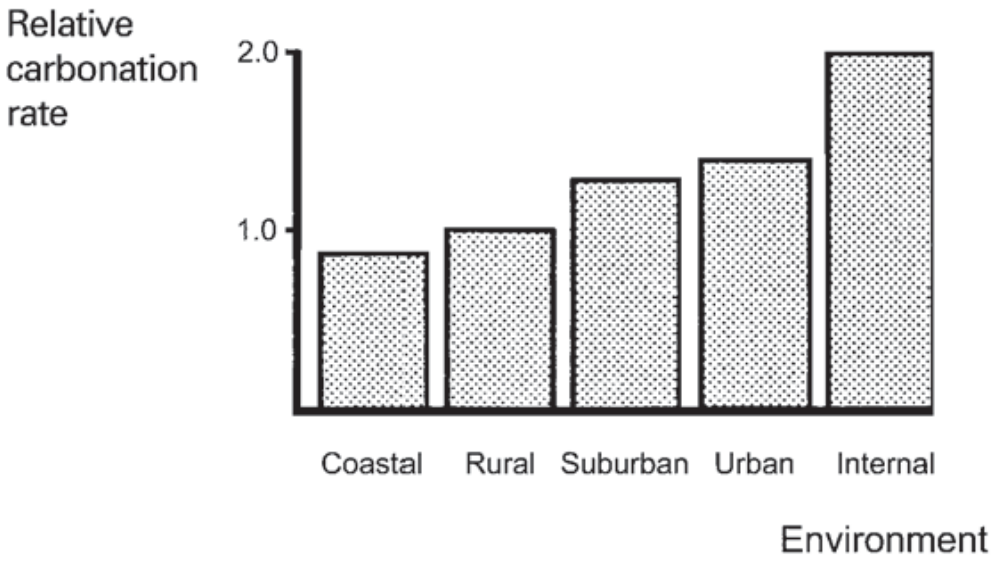

Figure 2-16: Influence of environment on the rate of carbonation

2.4.2.3 Concrete composition

As observed earlier the advancement of the carbonation front can be correlated with the amount of calcium hydroxide (CH) present. CH is present in concrete as it is a product of cement hydration. The quantity of CH produced is inversely proportional to the w/b ratio. Not only does CH provide a rich alkaline environment to form a passivating film surrounding the embedded steel, but it also acts as a sacrificial defence system. As noted in Section 2.1, CH is one of the reactants involved in the carbonation reaction. Hence the amount of CH is proportional to the concrete's resistance to carbonation.

The type of mineral admixture used influences the rate of carbonation. As illustrated in Section 2.3.2.1, the pore structure of concrete can be modified using mineral admixture due to its physical and chemical features which can potentially increase the carbonation resistance. However, its inclusion leads to the dilution effect, reducing the degree of hydration products due to the partial exclusion of cement. Moreover, binders which have pozzolanic attributes e.g. fly ash, slag and silicas can increase the rate of carbonation as these binders consume CH to produce cementing compounds. Section 2.4.4 provides more information regarding the physical and chemical effects of mineral admixtures.

2.4.3 Measuring carbonation depth

There are several methods by which the carbonation front may be identified within the concrete. Carbonation results in the depassivation of the steel due to the decrease in alkalinity and the formation of calcium carbonate ($CaCO_3$). Therefore, its progression or depth may be determined by

measuring either the change in pH or the concentration or amount of species present within the concrete (Salvoldi, 2010).

This section discusses and compares the various methods by which carbonation depth may be measured. These tests are divided into two types: qualitative and quantitative. Qualitative tests include the phenolphthalein indicator test, a scanning electron microscope (SEM), X-ray diffraction (XRD) and infrared (IR) spectrometry. Quantitative tests include Thermogravimetric analysis (TGA), chemical analysis (CA) and gammadensimetry (Villian, et al., 2007).

2.4.3.1 Phenolphthalein indicator test

The most commonly used test for determining the carbonation depth is a colourmetric method based on phenolphthalein spraying. Phenolphthalein is an acid-base indicator which changes to a pink shade depending on the pH of the environment during application. When the solution is sprayed onto a concrete surface the carbonated section will remain colourless. Conversely, the uncarbonated concrete will turn pink as its pH is greater than 9, though technically this only means that the carbonation in that zone has not progressed far enough to lower the pH sufficiently (Raupach & Büttner, 2014).

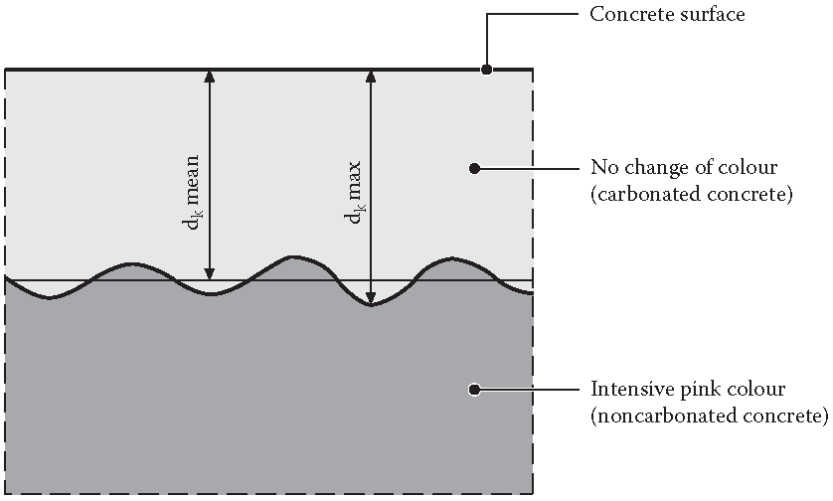

Figure 2-17: Measuring carbonation depth using phenolphthalein solution (Raupach & Büttner, 2014)

This method is quick, easy and reproducible. As such, it has become the most commonly used test within various carbonation models. Related results indicate that the carbonation front is steep. However, several studies show that the carbonation front is in fact gradual. When pH indicators are used, these define a boundary which is generally difficult to situate accurately within a gradual carbonation front (Villian, et al., 2007).

2.4.3.2 X-ray diffraction

X-Ray diffraction (hereafter referred to as XRD) is an analytical technique used for characterising crystalline materials. It can both quantify and identify the crystalline phases of a compound. X-ray beams are shot or directed at a sample at a specific angle of incidence. The deflection or diffraction and the intensity of the diffracted x-rays which are measured will vary depending on the sample's composition (Jumate & Manea, 2011).The results are presented on a diffractogram shown in Figure 2-18 – a graph showing a small number of diffraction peaks at their respective reflected angles on the abscissa, angle 2θ. The peak shapes and intensities measured can be used to determine the percentage of crystallinity and crystalline size. In a concrete composition context, it is known to have

the capacity to detect CH (also referred to as portlandite) and amphoras cementitious products and to distinguish types of calcium carbonates. Testing requires samples to be in powdered form for the analysis thus making it a destructive method (Jumate & Manea, 2011).

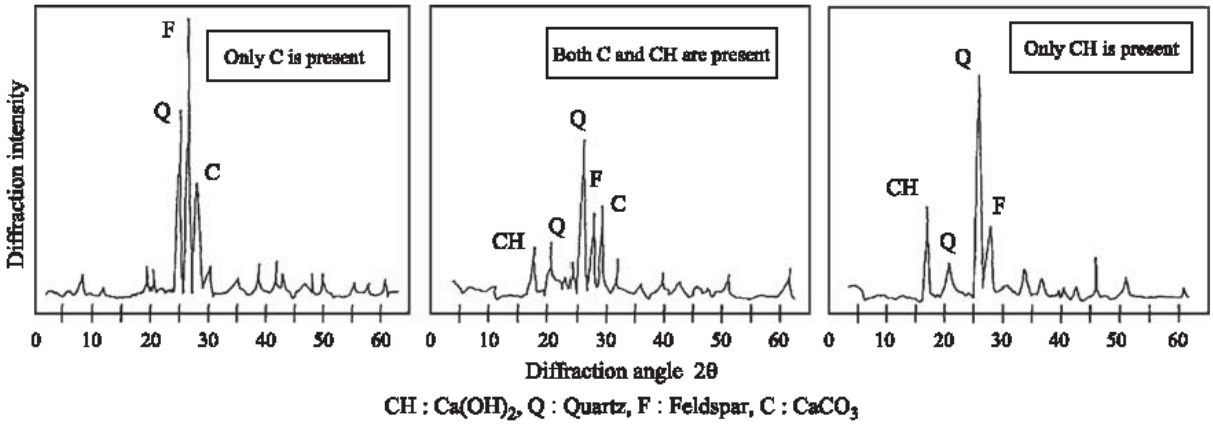

Figure 2-18: XRD carbonation depth analysis (Chang & Chen, 2006)

2.4.3.3 Scanning electron microscope (SEM)

SEM involves scanning a focused beam of electrons across a specimen. Thereafter a grey-scale image is created using the measured signals from the electron beam interaction with the specimen. The specimen preparation includes splitting a surface that was perpendicular to the carbonation front. The sample is then either dried or epoxy is applied before testing (Stutzman, 2000).

Two types of SEM methods are generally used, namely, secondary election and backscattered electron imaging. Secondary election uses a low-energy approach to get the image of the surface topography thus allowing the different shapes and forms of the concrete composition to be identified, as shown in Figure 2-19. Backscattered electron imaging uses high energy beam electrons in which a composition of the specimen is observed by the differential brightness in the image, as shown in Figure 2-20 (Stutzman, 2000).

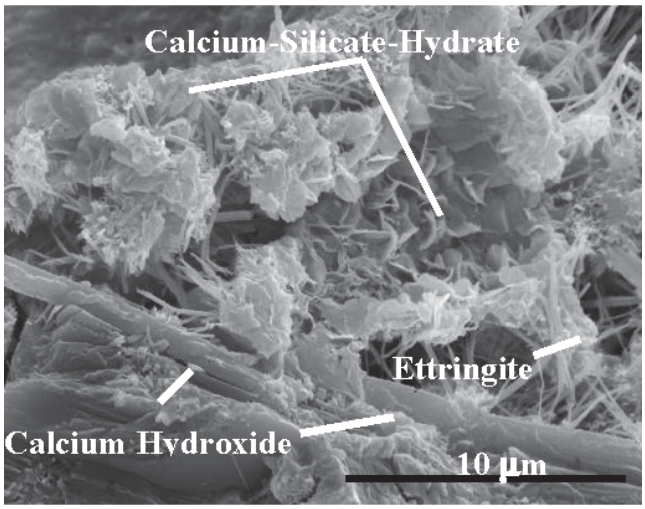

Figure 2-19: Secondary election SEM concrete of a concrete surfaceB (Stutzman, 2000)

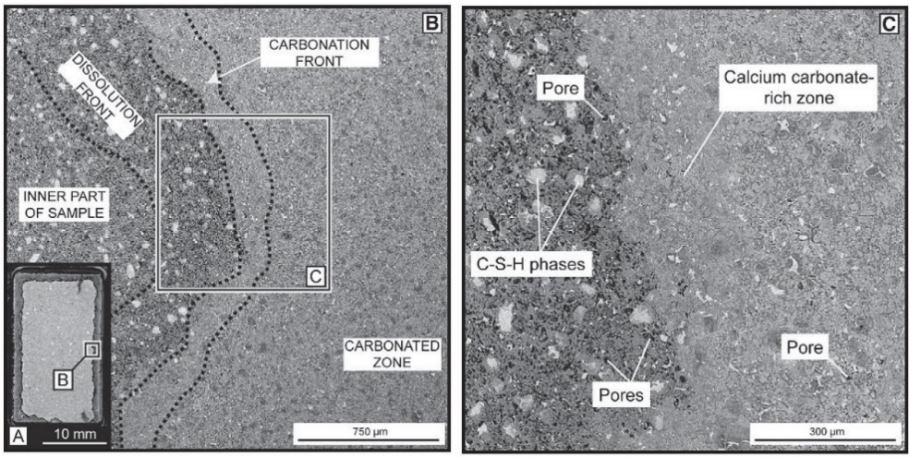

Figure 2-20: Backscattered SEM image of a carbonated concrete surface (Stutzman, 2000)

2.4.3.4 Infrared spectrometry

IR spectroscopy, also referred to as the Fourier transformation infrared spectroscopy (FTIR), is a method which can be used to determine the functional groups - group of atoms that make up a compound. When a specimen is subjected to infrared light, each functional group resonates with a unique absorption frequency characteristic. The intensity of IR light decreases due to the absorption of the functional group, which can be seen as 'peaks' on the TR electromagnetic spectrum or transmittance graph (Refer to Figure 2-22) (Lo & Lee, 2002).

In concrete subjected to carbonation-induced corrosion, the carbonation front represents the transformation of C=O bonds to C-O bonds (single and double bonds between the carbon and oxygen. This indicates the formation of calcium carbonate ($CaCO_3$), the product of carbonation. All peaks that have surpassed the baseline transmittance signify that carbonation has taken place (refer to Figure 2-21). Preparation of the sample includes taking powdered samples from the concrete at different depths and mixing these with Potassium Bromide (KBr) to aid measuring (Lo & Lee, 2002).

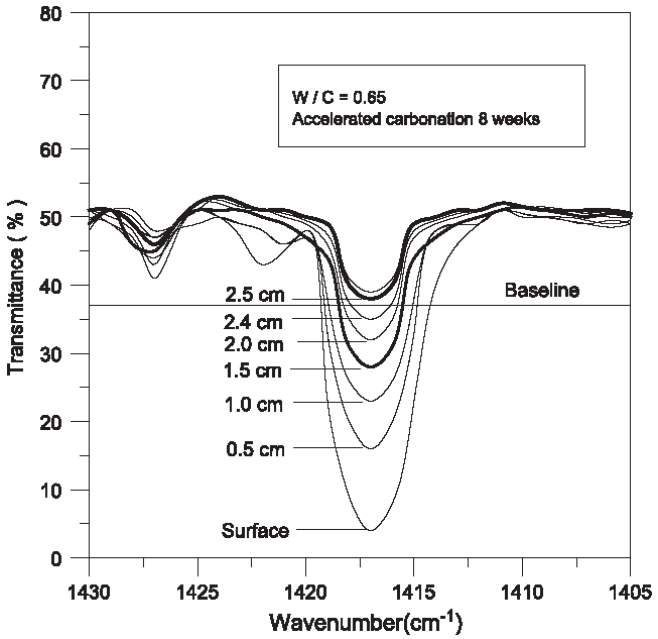

Figure 2-21: Carbonation depth profile using FTIR (Chang & Chen, 2006)

2.4.3.5 Thermogravimetric analysis

Thermogravimetric analysis (TGA) is a method that measures the change in mass of a sample as a function of temperature or time in a controlled environment. Measurements are used primarily to determine the composition of materials. The technique can characterize materials that exhibit weight change due to decomposition, oxidation, or dehydration. These can be observed at the inflection points from the differential thermogravimetric curve (DTG) (Refer to Figure 2-22). This curve is formed from the first derivation of a TGA curve. Each species will combust at a specific temperature, resulting in a weight change. In this way the amount for each species can be obtained (Villian, et al., 2007).

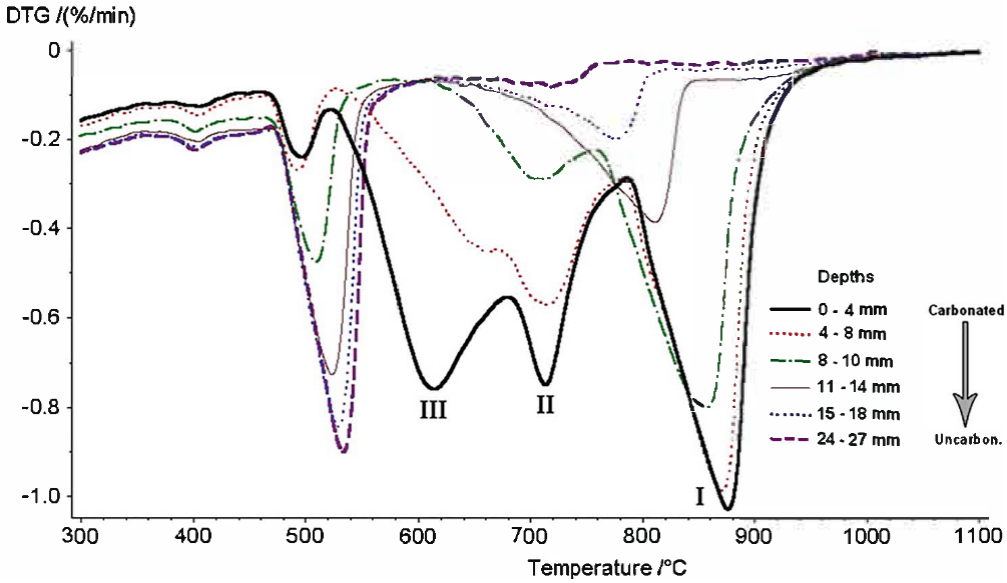

Figure 2-22: TGA results of concrete paste samples at different depths (Villain, et al., 2007)

A concern regarding this test is that the temperature ranges of decomposition of calcium carbonates might be confused with another species due to overlapping peaks. Hence a chemical analysis test should be conducted to supplement the TGA results, to produce a more precise result. For testing, small slices of a sample are converted into powder as required for conducting tests. Thereafter the carbonation front can be determined based on the results of the pulverized slices (Villian, et al., 2007).

2.4.3.6 Chemical analysis

Chemical analysis tests consist of analysing samples which are incrementally pulverised. Thereafter they are separated, identified and quantified based on their chemical components. The mineralogical phases of carbonated or uncarbonated concrete may then be determined (Villian, et al., 2007).

2.4.3.7 Gammadensimetry

Gammadensimetry is a non-destructive test method that requires no sample preparation. It can be used for both carbonation and moisture profiles in concrete. This test is conducted by analysing the concrete density over depth or time to detect the segregation of the different materials. The method of the test makes it possible to carry these out in the absence of both a hydric state and the chemical reactions of a concrete specimen (Villian, et al., 2007).

The test involves the adsorption of gamma-released by a radioactive source. If the mass adsorption coefficient of the material is known, it is possible to measure concrete's density over depth as depicted in Figure 2-24. Provided no drying occurs during carbonation, the density variation may be interpreted as being due to CO_2 fixation only. A carbonation profile may then be obtained because carbonation increases the density of the concrete and carbonation products have higher molar volumes (Villian, et al., 2007).

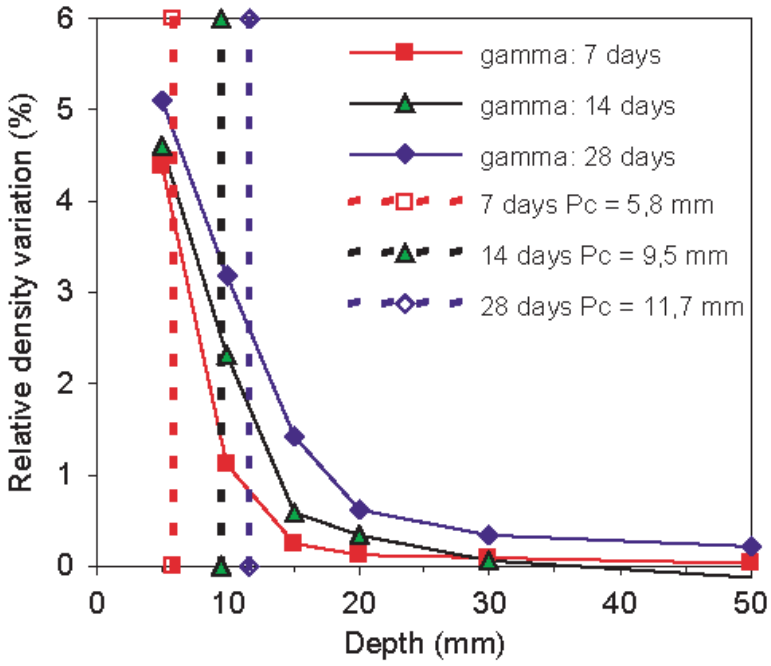

Figure 2-23: Gammadensimetry result of a carbonated concrete sample over

2.4.3.8 Discussion of carbonation test methods

Despite the new advancements in carbonation depth testing, controversially the phenolphthalein indicator test is still extensively used both within the laboratory and in practice. This can be attributed to the speed associated with this method, and as indicated earlier, the point that it is inexpensive, easy and reproducible. The other test methods investigated in this section are either expensive, time consuming, or require considerable expertise (Salvoldi, 2010).

Interpreting and measuring the colourmetric results are relatively easy. The carbonation depth is defined as merely the length from concrete surface to the carbonation front as indicated by a change in colour. This area is assumed to be uncarbonated as it appears after the application of the indicator solution, a process which does not require any sophisticated equipment. However, the actual migration of carbonation is more complex and thus it cannot be fully explained by such a basic method (Houst & Wittmann, 2002).

The phenolphthalein indicator test is viewed as being dependent on assumptions. Consequently, it is seen to reflect carbonation depth inaccurately. The controversy can be explained as follows. Firstly, based on the results, this test assumes that the carbonation front is steep. In fact, as pointed out earlier, the carbonation front is gradual, a phenomenon that can be observed and verified in the quantitative tests. After a certain time has elapsed the carbonation front may be regarded within three zones. The first zone is identified as the fully carbonated zone. The second zone or the transition zone is often referred to as the carbonation front, which is where a decreasing

magnitude of carbonation reaches zero. The third zone consists of entirely non-carbonated concrete (Villain, et al., 2007).

Secondly, based on the on the assumption that the carbonation front is steep it can lead to inaccuracy in the results. The study conducted by Chang and Chen (2006) compared the carbonation depth results from TGA, XRD and FTIR with those of the phenolphthalein indicator test. Their results showed on average that the colourmetric test reflected half the carbonation depth result. A similar observation was also observed in a study conducted by Villian and Thiery (2006). It was observed that carbonation depth results obtained by the gammadensitry test where greater than the results obtained from the phenolphthalein test. Additionally, Thiery et al (2007) investigated the comparison between TGA and phenolphthalein test. Similarly, the gammadensitry test results showed by the carbonation front was gradual, contrasting the steep carbonation front determined by the indicator solution. Additionally, the gradual carbonation front exceeded the depth of the steep carbonation front. This suggests that the carbon dioxide could have reacted beyond the carbonation front shown by the indicator test. It may therefore be deduced that the colourmetric can lead to an under-estimation of the carbonation depth.

2.4.4 Carbonation prediction models

There are numerous carbonation prediction models that exist in the literature, which range from simple enough for practice to very complex in application (Yam, 2004). For instance, a numerical model while accurate can still become heavily computer dependant. Within this range lie empirical-mathematical models, which consider the 'best attributes' sides of the spectrum. This model type provides relatively realistic predictions with less complexity (Ekolu, 2016).

The main objective of these carbonation prediction models is to estimate the carbonation depth in the concrete cover zone as far as is reasonably possible. This prediction gives the engineer an approximate value to use in the provision of adequate cover depth for the reinforcement; consequently, ensuring that carbonation-induced corrosion is theoretically avoided for its designated service life (Mackechnie & Alexander, 2002).

Carbonation prediction models are limited to providing precise approximates of carbonation depths as there are several influencing parameters to consider. Tests based on transport mechanisms are included within the prediction model as these are associated with deterioration mechanisms. Based on this, durability predictions of an empirical nature can be performed using correlations between early-age characterisation tests and carbonation durability results (Mackechnie & Alexander, 2002). The next section investigates commonly used carbonation prediction models and the correlations used within them.

2.4.4.1 Carbonation prediction models

While some variation is present within the literature, the equation that predicts the progression of the carbonation front within concrete is generally accepted as:

$$x = A\sqrt{t} \tag{2-10}$$

Where x = Carbonation depth (mm)

A = Carbonation coefficient (mm/years)

t = Time (years)

This model is derived from Fick's first law of diffusion, which assumes ideal diffusion conditions. The model suggests that the carbonation depth is directly proportional to the square root of time, taking into account that the progression of the carbonation front declines over time.

As explained in Section 2.4.2, carbonation is mainly governed by the internal relative humidity (RH), the amount of carbonatable material, external exposure conditions (such as temperature and RH) and carbon dioxide concentration. These factors are taken into account when determining the carbonation coefficient (Richardson, 2002).

Several researchers agree that the square root relationship provides a reasonable approximation for predicting carbonation behaviour (Mays, 1992; Houst & Wittmann, 2002; Ballim, et al., 2009). However, this square root relationship may appear conservative in the case of certain exposed conditions. In structures exposed to rain, observations in the field showed that the carbonation rate was lower than the result predicted in the square root model (Richardson, 2002).

In South Africa, this carbonation prediction model was adapted and expanded upon. This involved relating carbonation depth to an exponential function of 'n' to time where the n value changes depending on the composition of the concrete and the RH (Salvoldi, 2010). The equation is shown below:

$$x=At^{n} \tag{2-11}$$

The current SA carbonation model however was observed to have several limitations. It cannot differentiate between concrete with different cement extenders at various replacement ranges. The concrete compositions are limited to the conventional mineral admixture replacement types (30% fly ash, 50 slag, 10% silica fume). Also, it is calibrated to standard conventional concrete types for selective exposure environments only (RH of 60, 80 and 90%). This poses a problem when attempts are made to predict unconventional concrete types and within other environments (Salvoldi, 2010). Consequently, research conducted by Salvoldi (2010), sought to improve the existing South African carbonation model. The framework of this newly developed model was based on the model derived by Kropp (1995) and later modified by Audernaert (2007), here represented as follows:

$$x=\sqrt{\frac{2Dc\beta t_e}{a}} \tag{2-12}$$

Where D = Effective dry diffusion coefficient (mm^2/d)

C = Carbonation dioxide concentration (mol/m^3)

β = RH-reaction coefficient

t_e = Effective exposure time

a = Portlandite concentration (mol/m^3)

This model expanded on SA's previous model in that it considered varying exposure conditions such as RH, CO_2 concentration and average time of wetness as well as the chemical composition of the concrete. The chemical composition was accounted for by calculating the amount of calcium hydroxide using a mass balance equation developed by Papadakis (1991b). This equation considers the binder chemical makeup as well as the hydration and pozzolanic reactions thus making it a more adaptable model for a wider spectrum of concrete types.

2.4.4.2 Carbonation correlations

Two of the main concrete properties used by most empirical-mathematical carbonation models are permeability/diffusion and concrete strength. In prediction models, permeability/diffusion is more frequently used than concrete strength. Since carbonation progression in concrete is mainly affected by its microstructure, a correlation between permeability/diffusion and the carbonation depth is expected. Despite its popularity the high variability derived from the permeability characteristic makes its use questionable in relation to prediction modelling (Ekolu, 2016).

A related study conducted by Machkenie and Alexander (2002) investigated durability predictions using early age durability index testing. For carbonation predictions, the correlation between OPI and carbonation were investigated, as shown in Figure 2-24. The carbonation results were obtained from concrete samples, exposed to either dry laboratory conditions (average temperature 23°C and R.H 60%); and mild out conditions (average temperature 17°C and RH 80%) after being wet-cured for seven days. The OPI results were obtained after 28 days of wet curing. Moreover, conventional binder replacement values were investigated (that is, 30% FA, 50% BS and SF 10%). Results showed that the linear correlations between OPI and carbonation depths have been found to be good regardless of binder type.

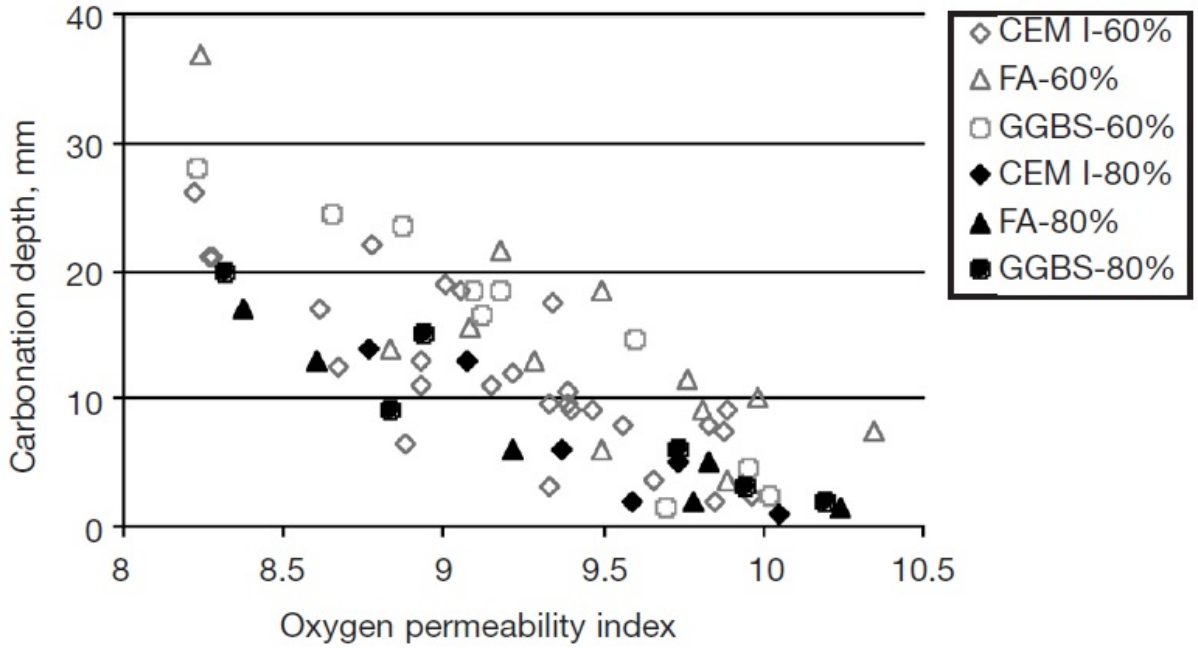

Figure 2-24: Correlation between carbonation depth and OPI (Mackechnie & Alexander, 2002)

Salvoldi (2015) further advanced this investigation into the correlation between carbonation and permeability by using the carbonation coefficient (carbonation depth over time). The carbonation coefficient correlated linearly well with both the D'Arcy's coefficient of permeability and the oxygen permeability index for each concrete type with a change in w/b ratio. Additionally, the carbonation coefficient correlated to a slightly greater degree with oxygen permeability. However, the correlation was weaker when compared to the correlations amongst the different concrete types (Refer to Figure 2-25).

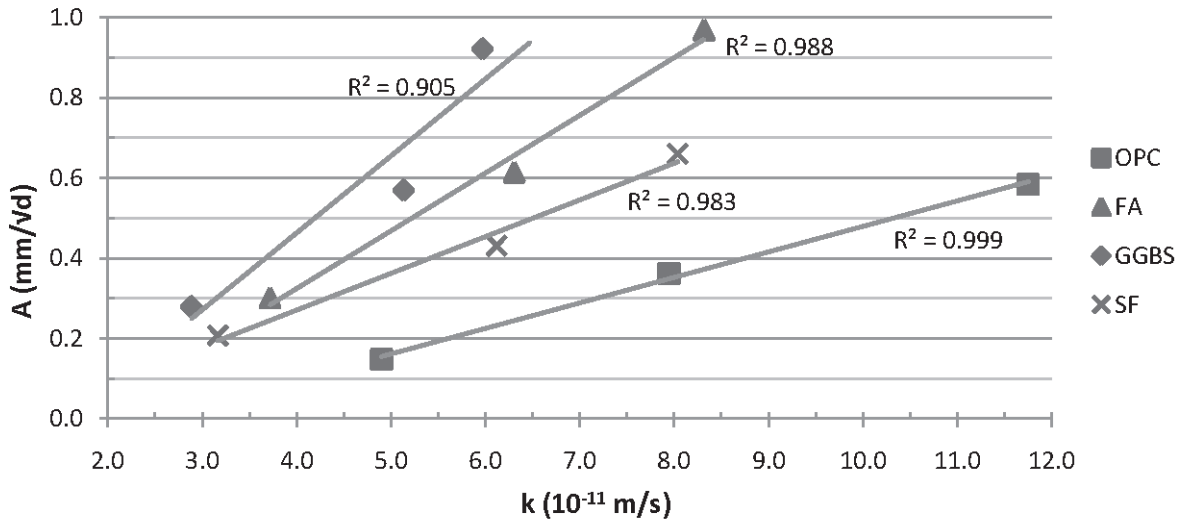

Figure 5-22: Permeability k vs. carbonation coefficient A

Figure 2-25: Correlation between carbonation coefficient and OPI (Salvoldi, 2010)

Explanation from the study done by Salvoldi (2010) of the contradictory results centres on the point that carbonation is governed by several factors, including concrete chemistry and environmental conditions. The argument is that these factors may cause an alteration of the slopes of regression of the individual concrete types. Subsequent use of this correlation has introduced difficultly when attempts have been made to predict the carbonation progression of various concrete types and exposure conditions, necessitating that each combination of exposure condition and concrete type be tested.

Similarly, in the old SA carbonation model upon which the research of Salvoldi (2010) relied, the OPI test acted as an input parameter and thereafter related to carbonation depth within this model. It was performed by investigating the correlation between diffusion and permeability as both transport mechanisms proceed in the same pore system. Both mechanisms are controlled by two different gradients, namely, pressure and concentration. The rationale was that if both mechanisms occur in the same pore structure both will describe the microstructure of the pore space and can thus be related. The correlation was investigated on the conventional concrete mixes for three different w/b ratios (0,4; 0,5 and 0,6), which underwent 28 days of wet curing. As shown in Figure 2-26, the results revealed that the correlation of the diffusion coefficient with oxygen permeability showed a general trend in the power relationship regardless of concrete type, leading to a regression equation correlating the permeability with the diffusion coefficient. The dotted lines indicated 95% confidence levels.

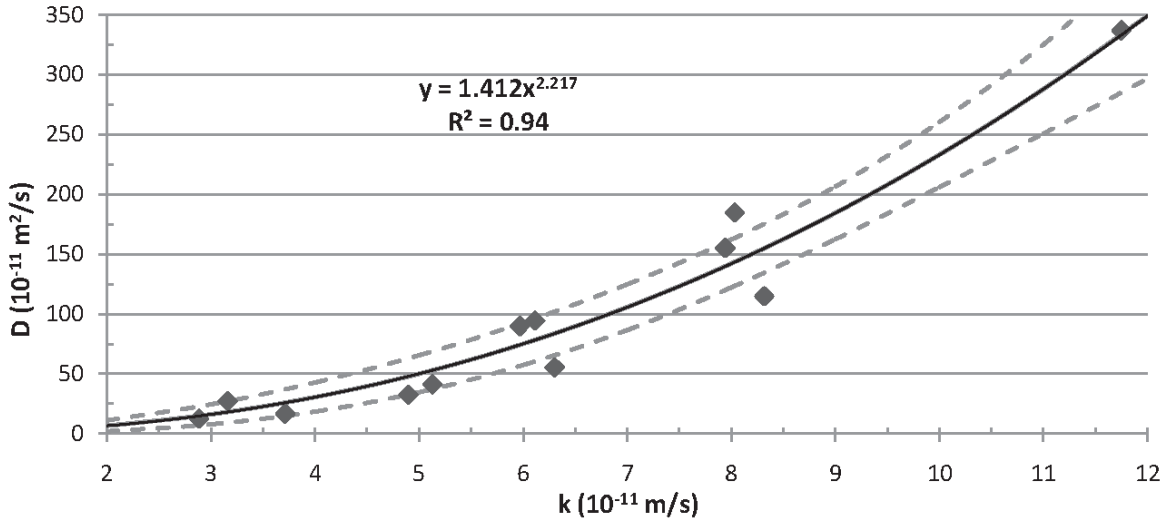

Figure 2-26: Correlation between diffusion and permeability (Salvoldi, 2010)

A further study conducted by Töpfer (2017) investigated the power relationship represented in research conducted by Salvoldi (2010). The study investigated concrete mixes of fly ash and slag at replacement levels of 20% and 80% for w/b ratios of 0,35 and 0,45. It found that a power correlation could not be confirmed for the concrete types. The calculation for CH value was negative for 80% SCM concrete mixes, which is impossible. Thus, this shows limitations in the mass balance equation when it is used to calculate the CH content in concrete. Additionally, even for mixes that had positive CH contents i.e. concrete mixes with 20% replacement levels, the power relation did not correlate adequately well with the observation shown in study conducted by Salvoldi (2010).

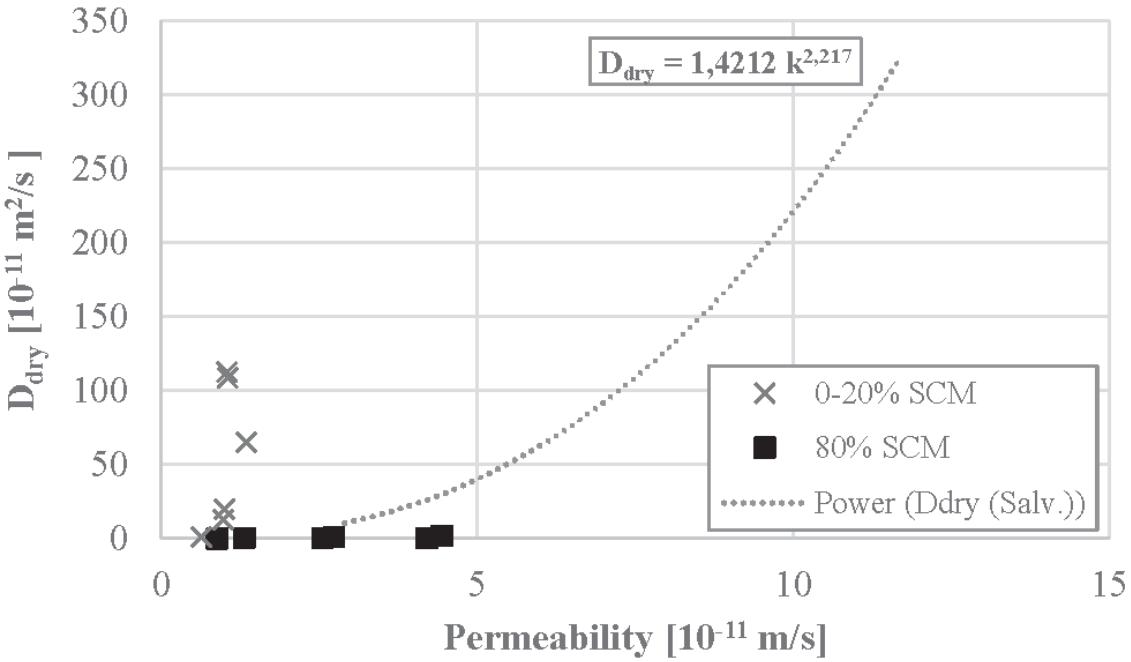

Figure 2-27: Correlation between diffusion and permeability (Töpfer, 2017)

2.5 Mineral additives

The term supplementary cementing materials (SCMs), also referred to as cement extenders or binders, is generally defined as a material used in combination with Portland cements (PC) which modifies the concrete properties through either hydraulic or pozzolanic activity, or through both (Thomas, 2013). SCMs come either as a component in blended cements, or as a manufactured product which includes PC inter grounded with one or more SCMs or fine filler. Alternatively, it can be included separately in the concrete mixer (Lothenbach, et al., 2011). Fine fillers, like SCMs are also integrated into blended cements or in the concrete mixer. They constitute any organic or inorganic materials used in concrete such as limestone or quartz. Generally, they are considered chemically inert. As a result, they cannot be considered as SCMs due to the absence of chemical inclusions in concrete (Thomas, 2013). Mineral additives can be defined as finely ground solid materials – other than the composition of water, stone, and PC – that are considered constituents of concrete or mortar and are included immediately before or during mixing (Elshafie, et al., 2016). For this study, the term mineral admixtures will be used to define the combination of SCMs and fine fillers.

Due to the adverse effects cement manufacturing has on the environment, partially replacing PC with mineral admixtures was considered as one of the viable options to address this concern. Popular mineral admixtures such as slag or fly ash are sourced from industrial manufacturing by-products and thus require no additional clinkering processes. Furthermore, they are relatively less energy intensive. This leads to a significant decrease in CO_2 emissions as well as a reduction in the overall cost in the manufacture of concrete (Boshoff, 2015).

The main reaction responsible for performance of concrete is known as cement hydration, involving the reactants, PC and water. This exothermic is considered as a complex process involving a series of reactions occurring concurrently at different rates and influencing each other (Hewlett, 1998). The main reactions occurring in hydration can be described by the reactions shown from Equations 2-13 to 2-16. Furthermore, typical chemical composition of South African PC (denoted as CEM I) is shown in Table 2.3 (Grieve, 2009).

Table 2-3: Compound composition of South African CEM I cements (Grieve, 2009)

Compound	Abbreviation	% by mass of cement
Tricalcium silicate	C_3S	60-73
Dicalcium silicate	C_2S	8-30
Tricalicum aluminate	C_3AH_{13}	5-12
Tetracalcium aluminoferrite	C_4AF_{13}	8-16
Magnesia	M	1,9-3,2
Gypsum	-	4,4-6,7
Free Lime	-	0,2-2,5

Calcium silica hydrate (CSH) is considered as the main constituent of cement. It is formed by the hydration of tricalcium silicate, C_3S (alite) and dicalcium silicate, C_2S (belite) (Refer to Equation 2-13 and 2-14) hydration (Emeritus, 1998; Hewlett, 1998; Newman & Choo, 2003). It has a needle and plate like structure and serves as the 'glue' of the concrete as it binds the sand and aggregate together (Newman & Choo, 2003). Furthermore, it is the main contributor the overall mechanical

strength, setting and hardening properties of the concrete (Neville, 2011). Besides the production of CSH, the hydration of alite and belite forms calcium hydroxide (CH) also referred to as Portlandite but unlike CSH, it does not contribute to the strength of the concrete. It is the second largest hydration product constituent after CSH. It takes on a crystal-like structure and has a soluble nature, which exists in the water-filled pores of the concrete (Grieve, 2009). The formation of tricalcium aluminate (C_4AH_{13}) and tetracalcium aluminoferrite (C_4FH_{13}) involves in the reaction between C_3A and C_4AF with water and CH which has been formed in the hydration of alite and belite (Hewlett, 1998) (Refer to Equation 2-15 and 2-16) (Aitcïn, 2000; Grieve, 2009).

$$2C_3S+6H_2O \rightarrow C_3S_2H_3+3CH \quad (2\text{-}13)$$

$$2C_2S+4H_2O \rightarrow C_3S_2H_3+CH \quad (2\text{-}14)$$

$$C_3A+H_2O + CH \rightarrow C_4AH_{13} \quad (2\text{-}15)$$

$$C_4AF+22H_2O + 4CH \rightarrow C_4AH_{13}+C_4FH_{13} \quad (2\text{-}16)$$

Blending mineral admixtures with PC produces a more complicated concrete system. Reactions from both PC and mineral admixtures occur concurrently, and the influences of mutual reactivity serve to modify the concrete's pore structure. Moreover, the physical attributes of the materials also have an influence on the reactions and consequently on the overall performance of the concrete (Lothenbach, et al., 2011). The focus of the next section thus entails an investigation into how the inclusion of mineral admixtures affects the concrete's performance. This is followed by an investigation into the common types of mineral admixtures used in concrete namely latent hydraulic binders, pozzolans, fine fillers as well as a short discussion on ternary mixes.

2.5.1 Effects of mineral admixtures

As stated in the previous section, mineral admixtures are partial substitutes for cement for reasons relating to the environment, the economy or performance. The processes associated with this phenomenon produce what is known as 'the dilution effect' as cement is partially substituted with another material: in this case, mineral admixtures of the same quantity (Cyr, et al., 2006). The dilution effect reduces the quantity of hydration products due to the partial exclusion of cement. This involves a consequential increase in the water:cement ratio. The amount of cement replaced by the admixture is a function of the dilution effect or the replacement level (Cyr, et al., 2006). This is expressed as a percentage of the total binder content.

Generally, the use of mineral admixtures may result in an improvement in the overall durability performance of the concrete. This can be attributed to the physical and chemical effects of the various material admixtures such as the size grading and mineral admixture chemical composition. However, there are cases in which their use produces negative effects. In such cases this could be due to the use of mineral admixtures of a poorly reactive nature, high replacement levels or insufficient curing duration (Pacheco-Torgal, et al., 2013). The section which follows investigates and discusses the various physical and chemical effects of mineral admixtures on the durability performance of the concrete.

2.5.1.1 Physical effects

The two main physical effects mineral additives have when used in concrete are the filler effect and heterogeneous nucleation. The degree of these physical effects is mainly dependent on the particle size distribution, density and the fineness of the particles (Cyr, et al., 2006). These properties are most clearly observed in the use of silica fume due to its high fineness (Emeritus, 1998).

Commonly, mineral additives have a higher surface area per unit volume as they consist of smaller particles relative to cement. It is thus possible to pack them between the cement grains. This is known as the filler effect, a phenomenon that results in a refinement of the concrete's overall pore structure of the concrete as there is an improvement to its compactness, decreasing the number of voids and potentially the number of interconnected pores (Moosberg-Butnes, et al., 2004). This decreases the permeability of the concrete, which is beneficial for aiding in the resistance to migration of deterioration mechanisms such as carbonation.

Although the focus of this section is on the physical effects of mineral admixtures, it is important to point out that these can also indirectly influence the chemical structure of the concrete positively. This physical effect is known as heterogeneous nucleation. Heterogeneous nucleation is a physical phenomenon whereby hydrates nucleate on foreign mineral particles or mineral additives, which in turn can promote the chemical activation of the hydration cements and have the general effect of fostering its hydration reaction. This serves to change the concrete's physical characteristics and mechanical behaviour (Moosberg-Butnes, et al., 2004). Additionally, its surface area governs the rate of the chemical reaction, an aspect which is discussed in the next section.

2.5.1.2 Chemical effects

The two main chemical effects mineral admixtures produce when used in concrete are the hydraulic and pozzolanic reactions. (The mineral admixtures used in this study excluded fillers as these are considered chemically inert) Each property requires an adequate alkaline environment within the concrete for its activation and progression. Consequently, the chemical attributes of mineral admixtures are considered to be secondary reactions and are negligible for the first few days until the alkaline environment within the concrete is adequate for the onset of secondary reactions (Newman & Choo, 2003). Note, this subsection will focus slags when referring to latent hydraulic binders.

Hydration in mineral admixtures such as latent hydraulic binders are similar to cement hydration. Normally, cement hydration reacts with water for the commencement of this exothermic reaction, but hydration in latent hydraulic binders requires an adequate alkali environment for its activation in addition to water. Without its activation, latent hydraulic binders will harden very slowly in the presence of water. Due to this slow reaction rate, the use of latent hydraulic binders as the only binder within the concrete mix are regarded as too slow for engineering use. The resistance applied to the hydraulic reaction is essentially caused by its own amorphous, glass-like structure. To increase the reactivity, an activator is required (Newman & Choo, 2003).

Slag activators can be divided into alkaline or sulphate activators. Alkaline activators include CH, sodium hydroxide, sodium carbonate or sodium silicate. Sulphate activators include calcium sulphate or phosphogypsum. The main alkali compound is CH, which is produced by the hydration reaction of Portland cement (PC) with water. Once a certain pH is reached, the glass structure is disrupted, increasing the reaction and subsequently producing its own cementitious gels independent of PC. The type of cementitious gels produced by the latent hydraulic binders is dependent on the nature of the activator (Hewlett, 1998).

The hydration of slag produces cementitious gels similarly to cement hydration except no CH is produced. It can undergo pozzolanic reactions as it contains an adequate silica component. After the hydration of slag, surplus acid components are liberated and react with CH to produce additional calcium silicate hydrate and calcium aluminate products (Emeritus, 1998).

A pozzolan is classified as siliceous or siliceous and aluminous material that itself has little to no cementitious qualities but that in the presence of adequate moisture can react chemically with calcium hydroxide (CH) to produce cementitious-like products. Pozzolans are either manufactured products such as fly ash or silica fume. Alternatively, they are sourced naturally as volcanic ash, shale, pumice, etc (Neville, 2011). The phenomenon where pozzolans react with CH to produce cementitious-like products is known as the pozzolanic reaction. CH required for the initiation of the pozzolanic reaction, which is mainly sourced from the hydration reaction of Portland cement (PC), or alternatively, from the insertion of hydrated lime into the concrete mix. Additionally, pozzolans are required to be in a finely divided state in the concrete mix. Equation 2.14 displays the simplified version of the pozzolanic reaction. This equation shows that the silica component of the mineral additive reacts with CH produced by cement hydration. Note, as mentioned previously slag can also exhibit pozzolan like characteristics due to its large silica component (Newman & Choo, 2003).

$$CH+SiO_2 \rightarrow C_3S_2H_3+H_2O \quad (2\text{-}14)$$

2.5.2 Types of mineral admixtures

There are several types mineral admixtures used in concrete today. This research focuses its investigation on the following: ground granulated blastfurnace slag (BS), Corex slag (CS), fly ash, (FA), silica fume (SF) and fine fillers, specifically limestone (L). SCMs can be divided into two categories: latent hydraulic and pozzolans. This section investigates latent hydraulic binders, pozzolans and fine fillers. The use of ternary mixes is also discussed.

2.5.2.1 Ground granulated blastfurnance slag (BS)

BS is sourced from the by-products of the blastfurnace process within iron manufacturing industries. To become usable for construction practices, the slag needs to be cooled rapidly to assume a glassy, reactive state. If this condition is not fulfilled, that is, if it is cooled down slowly, it is likely to form a more stable, non-reactive structure (Newman & Choo, 2003). Table 2-4 shows the typical chemical composition of BS produced in South Africa.

Table 2-4: Typical chemical composition of South African GGBS (Grieve, 2009)

Oxide	% by mass in GGBS
SiO_2	34-40
CaO	32-37
Al_2O_3	11-16
MgO	10-13
FeO	0.3-0.6
MnO	0.7-1.2
K_2O	0.8-1.3
SiO_2	1.0-1.7
TiO_2	0.7-1.4

To stimulate its reactive nature, during manufacture slag is commonly ground finer than Portland cement (Aïtcin, 2008). For this reason, it can locate itself in-between cement particles, further refining the pore structure, and thus confirming its contribution as a fine filler. Other improvements include a

slight enhancement of workability, retardation of the alkali-silica reaction and increased resistance to chloride-induced corrosion due to the binding of chlorides (Grieve, 2009).

BS is alkali-activated as it is a latent hydraulic binder, and it can thus react with and in water to form cementitious compounds similar to those achieved through PC hydration reaction, except that no CH is produced. In concrete, the activation may mainly commence with the formation of CH, a product of cement hydration. Alternatively, other alkalis including NaOH and KOH or sulphates may also contribute to the activation (Grieve, 2009).

2.5.2.2 Corex slag (CS)

Originally discovered in Germany in 1862, Ground Granulated Corex Slag – referred to in this study as Corex slag (CS) – is a relatively new mineral additive that has more recently become available in South Africa. Corex slag is mainly sourced from the Saldanha Steel Plant in the Western Cape. The chemical composition is similar to BS as shown in Table 2-4. This was revealed in an XRF analysis conducted by Jaufeerally (2001) on CS, as illustrated in Table 2-5.

Table 2-5: Chemical composition of study based on XRF analysis (Jaufeerally, 2001)

Oxide	% by mass in GGCS
CaO	34
SiO_2	35.5
Al_2O_3	15.4
MgO	9.4
TiO_2	1.2
Fe_2O_3	1.0
MnO	0.9
K_2O	0.9
Na_2O	0.2
SO_3	2.5

In many ways, CS is similar to BS regarding physical properties, chemical composition and source. However, there are two key differences. The first is that the manufacturing process used to produce the iron differs from the traditional blastfurnace process. Known as the Corex process, it is considered to be a more environmentally friendly iron-production process whereby the coke ovens and the blastfurnace are replaced by a direct reduction shaft and a melter-gasifer (Alexander, et al., 2003).

The second difference concerns its reactivity. In certain cases, CS is more reactive than BS in relation to hydraulic activity. This is based on the former having higher calcium oxide (CaO) and lower SiO_2 content and other formulae that determine the degree of hydraulic activity. However, this assumes equivalence between the fineness of the binders. It is argued that not only the chemical composition, but also the mineralogical composition and glass content of slag could have a significant influence on the hydraulic activity (Alexander, et al., 2003).

2.5.2.3 Fly ash (FA)

Fly ash falls under the pozzolanic family and is sourced from electrostatic precipitators or filters from coal-powered factories Table 1.4 illustrates the typical chemical composition of FA sourced in the South African region. It is considered the most common artificial pozzolana, possessing little to no cementing value as it does not react with water. However, it is able to produce insoluble cementing compounds by reacting with CH in the presence of water. This phenomenon is known as the pozzolanic reaction (AitcÏn, 2000).

Table 2-6: Typical chemical composition of South African FA (Grieve, 2009)

Oxide	% by mass in FA
SiO_2	48-55
Al_2O_3	28-34
CaO	4-7
Fe_2O_3	2-4
MgO	1-2
$Na_2O + 0{,}658\ K_2O_2$	1-2

In terms of their geometry, the particle size of FA is generally finer than Portland cement (PC), thus presenting as a fine filler. In addition, their normally spherical shape can improve the fluidity and workability of fresh concrete. These grey spheres function as 'ball hearings' within fresh concrete, which can reduce the amount of water needed for a specific workability (Newman & Choo, 2003).

ASTM C618-17a (2017)) classifies both natural pozzolans and fly ashes under three categories: Class F, C and N. These are based on the value of the sum of SiO_2 (S), Al_2O_3 (A) and Fe_2O_3 (F), referred to in this study as S + A + F. Alternatively, they may be based on the source from which they derive whether natural or artificial. Class F fly ash, the most common type is artificially sourced from burning anthracite or bituminous coal. At less than 10% its CaO content is fairly low. Moreover, its S + A + F sum is greater than 70% despite it exhibiting a pozzolanic character, which is quite rare (Neville, 2011).

Class C pozzolans are generally produced from lignite or sub-bituminous coal. Class C fly ash differs from Class F fly ash as not only does it possess pozzolanic activity, but it also has the potential to self-produce cementing-like products because it commonly has more than 15% CaO content. Additionally, it contains mainly calcium alumino silica glass which is considered highly reactive. Class N comprises typically raw or calcined natural pozzolans such as shale, volcanic ashes or pumice (Neville, 2011).

2.5.2.4 Silica fume (SF)

Silica fume (SF), also referred to as microsilica or condensed silica fume, is a by-product of the ferrosilicon or silicon smelting process. As part of the pozzolanic group, its chemical properties within concrete entail reacting with calcium hydroxide in the presence of water to produce cementitious - like compounds. Its typical chemical composition is shown in Table 2-7 (Grieve, 2009).

Table 2-7: Typical chemical composition of SF (Grieve, 2009)

Oxide	% by mass in SF
SiO_2	92-96
Al_2O_3	1-1.5
Fe_2O_3	1-1.6
CaO	0.3-0.6
MgO	0.6-0.8
K_2O	1.2-2.0
H_2O	0.4-0.8

Concerning its geometry, SF particles are spherical in nature and are extremely fine with an average particle size of approximately 150 nm where more than 95% of the particles are finer than 1 µm. This makes SF particles effective fine fillers since they can fit in-between cement particles, refining the pore structure, especially at the interfacial transition zone (Siddique & Khan, 2011). The spherical geometrical shape of SF particles does not aid in improving the fluidity and workability of fresh concrete. Due to its fineness, concrete containing SF tends to be relatively more cohesive and exhibits greater resistance to segregation (Newman & Choo, 2003). Consequently, its inclusion can reduce the workability of the fresh concrete (Grieve, 2009).Silicon dioxide, also referred to as silica, is highly reactive in an amorphous state. SF has a high amorphous silica content, generally containing more than 90%. Table 1.5 displays the typical SF chemical composition in South Africa. Coupling the chemical nature of SF with its fineness and providing a large surface for the onset of reactions, allows it to be a highly reactive pozzolanic material (Neville, 2011).

The chemical and physical properties of SF can have beneficial influences on the performance of the concrete, specifically during early ages. Early age improvement of the concrete's mechanical properties such as compressive strength and tensile strength can be observed, added to which there is an overall improvement in the durability of the concrete (Newman & Choo, 2003).

2.5.2.5 Fine fillers

Fine fillers or fillers are either naturally sourced or processed inorganic materials. They are typically finely-ground to the same fineness as Portland cement. Furthermore, they are considered as being nominally ‘inert’ so their influence on concrete performance is mainly owing to their physical properties. These physical properties include acting as a fine filler, enhancing the pore structure and acting as nucleation sites, subsequently accelerating the hydration reaction. The most commonly used fine filler is limestone (Neville, 2011).

Limestone, which can be naturally found in the environment, is used to produce calcium oxide, one of the main constituents of cement clinker. However, it may be used to partially replace cement, making the concrete more economical. It does not participate in any hydration reactions and thus it is merely considered as a fine filler to improve the permeability of the concrete serving as a reaction nucleation point (Grieve, 2009). However, some researchers do argue that it is not totally inert as calcium carbonate can react with C_3A to form a carboaluminate (Newman & Choo, 2003).

2.5.2.6 Ternary blends

Ternary blended concrete is composed of two mineral additives in addition to Portland cement. A growing interest in the use of ternary mixes arose in response to the limitations of binary mixes, despite the beneficial factors of the incorporation of SCMs as outlined earlier. The limitating factors include low early age strength, prolonged curing times, increased admixture use and plastic shrinkage, depending on the SCM used (Thomas, 2013).

In certain cases, the use of a single SCM can improve one performance attribute of concrete but at the cost of another. Examples include SF which can be used to decrease ASR expansion but an increase in the replacement levels can result in difficulties with workability. The use of reasonably proportioned ternary blends can potentially allow for the effects of one SCM to compensate for the shortcomings of the other and vice versa, for example, the combination of fly ash and silica fume (Thomas, 2013).

2.6 Summary

The review of literature has shown that reinforcement corrosion is one of the pervasive concerns in the world today as it is the main cause of deterioration in concrete structures. Thus, the nature of the covercrete is important if it is to protect the underlying steel from harmful substances that may enter. Carbonation-induced corrosion, one of the main deterioration mechanisms that cause reinforcement corrosion, is a chemical reaction wherein carbon dioxide in the atmosphere reacts with the alkaline species in the concrete thus depassivating the steel. It is mainly affected by the prevailing relative humidity, the concrete composition, ambient temperature, and carbon dioxide concentration in the atmosphere. Carbonation depth can be tested using the phenolphthalein indicator test. It is the most commonly used in practice as it is quick, easy and reproducible. In addition, the results obtain this test is used as an input parameter in several carbonation models. Controversy concerns the phenolphthalein indicator test as it assumes that the carbonation front is a steep front but in fact it is gradual.

Commonly, the use of the mineral admixtures results in a general improvement in the permeability performance of the concrete. However, there as cases in which it can produce contrasting results. This can be attributed to a weak reactive nature, high replacement level or insufficient curing duration. In terms of carbonation performance, the inclusion of mineral admixtures may result in a decrease in carbonation resistance. This is due to the dilution effect, reducing the degree of hydration products due to the partial exclusion of cement. Moreover, binders which have pozzolanic attributes increase the rate of carbonation as these binders consume CH to produce cementing compounds.

Several carbonation models were discussed in the literature review, notably those related to Salvoldi's (2010) and Mackechnie and Alexander's (2002) research. These models investigated the correlation between the carbonation depth or carbonation coefficient and concrete's permeability to determine the carbonation model’s viability in estimating the progression of carbonation in concrete. The key attribute within these mod+els allows for the use of early-age characterisation testing, that is oxygen permeability index (OPI) testing, to determine the design life of a structure with respect to carbonation within a given environment. It is used to determine the coefficient of permeability and has a good correlation with other common permeability tests, suggesting that they have similar merit in assessing concrete cover quality.

Previous research for formulating the South African carbonation prediction model has been based on conventional binder combinations. For example, concrete containing PC replacement levels of 30% fly ash, 50% slag or 10% silica fume. Therefore, it is not confirmed whether the use of permeability and carbonation parameters of modern concretes still hold true in an existing South African carbonation model, and to determine whether adjustments are required. This enquiry concerns modern concretes made with modern cement types, varying binder replacement levels and binder combinations, including binary and ternary cement blends. The need to investigate this further presented itself.

3 Experimental methodology

This chapter provides a detailed outline of the experimental component undertaken in this study. In this section an overview of the experimental approach is provided, and the aim of the study is explained. Also outlined are parameter variations, mix proportions, preconditioning and curing regimes, sample specifications, and details of laboratory experiments conducted. Additionally, a brief reasoning behind and use of statistical tools in the interpretation of the results is elaborated. A summary of the experimental work is presented in Figure 3-1.

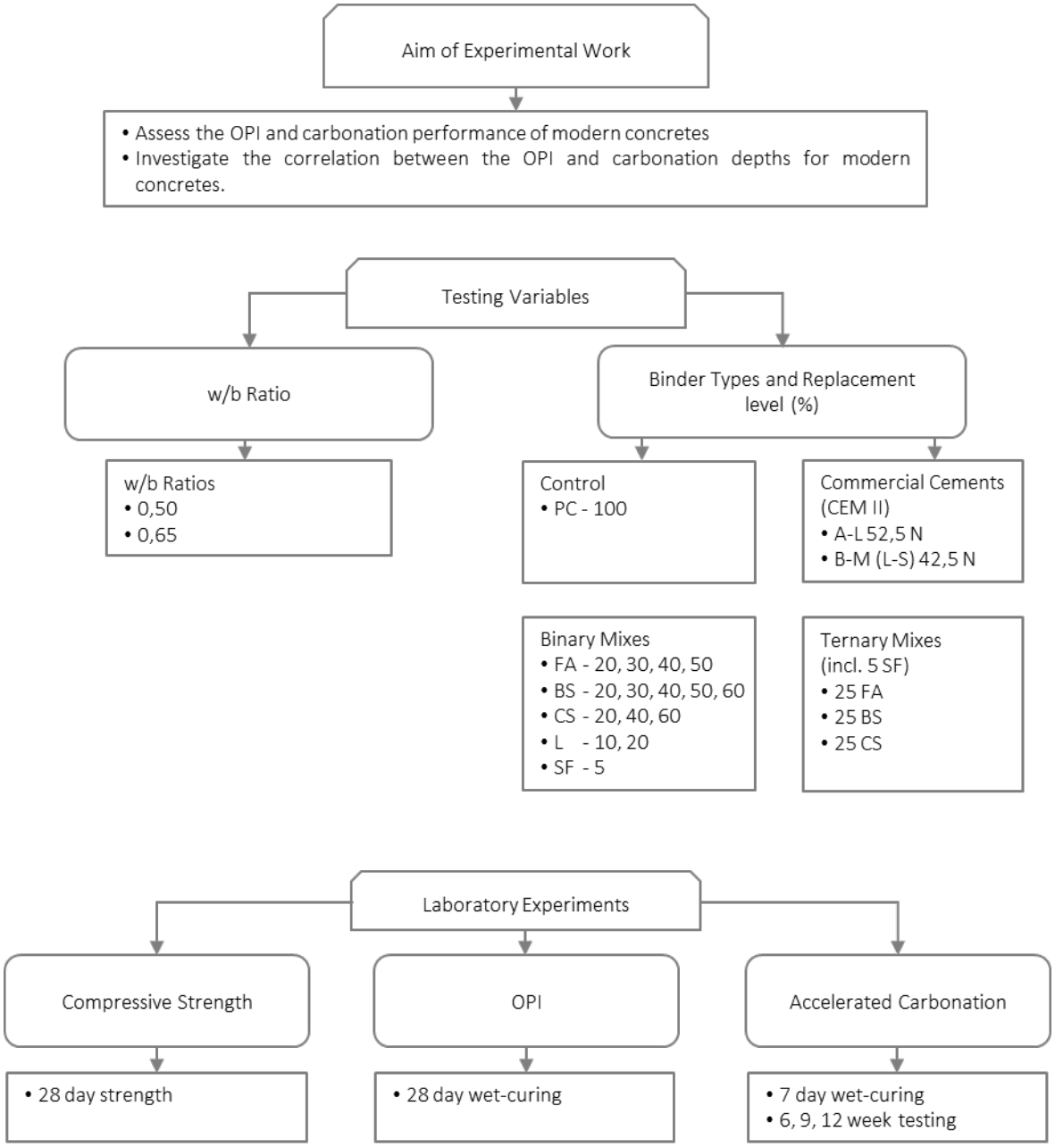

Figure 3-1: Overview of experimental work

3.1 Aims of the experimental work

Using the results from the laboratory experiment, this study seeks to investigate whether the use of permeability and carbonation parameters of modern concretes still hold true in an existing South African carbonation model, and to determine whether adjustments are required. This enquiry concerns modern concretes made with modern cement types, varying binder replacement levels and binder combinations, including binary and ternary cement blends. Noting that previous research has been based on conventional binder combinations. For example, concrete containing PC replacement levels of 30% fly ash, 50% slag or 10% silica fume. The need to investigate this further presented itself.

While the literature contains adequate information on the durability performance of conventional concretes, there is limited information regarding the statistical significance of the difference in results obtained from different modern concrete mixes. Thus, the aim of this research is to determine the effects of varying cement replacement percentages of different mineral admixtures on the concrete's durability performance regarding permeability and carbonation. Using the permeability and carbonation parameters, this research seeks to assess any correlations that could be used in the carbonation-related service life modelling of reinforced concrete structures.

3.2 Experimental variables

The influence of mineral admixture type, replacement levels and water-binder (w/b) ratios was investigated to determine their effects on carbonation and oxygen permeability respectively. The variables were selected on the basis of an investigation that had been conducted on the various mix designs used in the past at the University of Cape Town's (UCT's) concrete laboratory. The selection of variables was also informed by the literature, various codes and standards as well as information received from several companies within the field of civil engineering. The three variables (mineral admixture type, replacement level and w/b ratio) are explained in further detail in the section that follows.

3.2.1 Mineral admixture type

For the control concrete mix, CEM I 52,5N was used. It is known that currently this cement type is rarely used without the inclusion of a mineral admixture in industry due its high clinker content and the inclination amongst cement companies to more sustainable production practices. However, as it contains minimal to no mineral additives, it serves as an adequate reference concrete mix for comparison with mixes of varying binder replacement levels.

As this study focuses on South African concretes, the mineral admixtures used in concrete mixes were sourced in South Africa. As a result, the binders chosen comprised the following: Fly ash (FA) supplied by Ash Resources, Ground Granulated Blast Furnace Slag (BS) and Ground Granulated Corex Slag (CS), both sourced from PPC, Silica Fume (SF) sourced from Ferro Atlantic, and Limestone (L) sourced from Kulubrite. More information regarding their mineral components and related properties is detailed in Appendix B.

In this research commercial blended cement products were used, namely CEM II A-L, and CEM II B-M (L-S) 42,5N, referred to as A-L and B-M respectively hereafter. Both were sourced from PPC. A-L and B-M cement nominally contain 8% limestone, and 8% limestone coupled with 25% GGCS respectively – information which was discussed in personal communication with the cement producer.

Lastly, ternary blended mixes were investigated. Commonly, ternary mixes include SF and an additional binder. For this study the ternary mixes consisted of FA, BS or CS, with the inclusion of SF. The replacement percentages of each binder are presented in the next section.

3.2.2 Binder replacement percentages

The selected variables for the replacement levels are tabulated in Table 3-1. The ternary mixes include 5% SF replacement levels in addition to the binders stated.

Table 3-1: Cement replacement levels

Variable	Symbol	Replacement Levels (%)
Fly Ash	FA	20, 30, 40, 50
Blastfurnance Slag	GGBS	20, 30, 40, 50, 60
Corex Slag	GGCS	20, 40, 60
Limestone	L	10, 20
Silica Fume	SF	5
Ternary Mixes	SF FA	SF 5; FA 25
	SF BS	SF 5; BS 25
	SF CS	SF 5; CS 25

3.2.3 Water-binder ratio

Two water-binder (w/b) ratios were investigated: 0,5 and 0,65. The w/b ratios chosen for this study were expected to provide a reasonable spectrum in terms of strength and durability. For all concrete mix designs, the water content was kept constant at 170 l/m^3. Therefore, alterations were made to the binder content to obtain the required w/b ratio. Furthermore, the w/b ratio selection was based on mixes commonly used in practice. Grieve (2009) states that the range of conventional concrete lies between 0,45 and 0,80. Therefore, the selected w/b ratios comply with what is used in practice.

The w/b ratio is not intrinsically an indicator of durability. However, varying the w/b ratio can refine the concrete's pore matrix, and can subsequently influence the transport mechanisms of diffusion and permeation. Furthermore, altering the w/b ratio affects the rate of carbonation. Calcium hydroxide (CH), is governed by the w/b ratio. Hence, the hydration reaction rate determines the amount of CH produced. As noted in Section 0, CH serves as a 'buffer' since it is one of the dominant reactants involved in the carbonation reaction.

For prescriptive approaches, the service life of the concrete structures is usually expected to be 50 years provided various threshold values of parameters are complied with (Bertolini, et al., 2013). According to EN 206-1 (2002), Structural class 4, also referred to as S4, is denoted for concrete structures with a design life of 50 years, which is the conventional design life for most concrete structures. Table 3-2 presents the minimum concrete cover required for various exposure classes in relation to carbonation-induced corrosion. XC4 is regarded as the most severe exposure class for the progression of carbonation-induced corrosion.

Table 3-2: Minimum cover depth for S4 (carbonation-induced corrosion)

Exposure Class	Minimum cover (mm)
XC1, XC2	15
XC3	25
XC4	30

According to EN 206-1 (2001), the maximum w/b ratio for exposure class XC4 is 0,55. The w/b ratios selected for this study will thus provide a representation from both ends of the spectrum – below and higher than the recommended limit.

3.2.4 Workability and superplastizer

A slump range of 75 ± 25 mm was chosen for this study, the same range used in Salvoldi's (2010) study. Chryso Premia 310 Superplastizer (SP) was used to promote workability of the fresh concrete, and trial mixes were conducted to determine the amount of SP required. The SP was added incrementally (approximately 5 ml) until the slump lay within the specified range. Slump values and SP dosage for the concrete mixes are shown in Appendix B.

3.3 Mix proportions

The concrete mix designs were done in accordance with the C & CI Method (Addis & Goodman, 2009). Before a full-scale design was made, trial mixes were performed, including slump testing, to determine whether the mixes were within a specific slump range of 75 ± 25 mm and to observe the overall cohesiveness, consistency and bleeding. Modifications were made if the fresh properties of the trial mixes were not deemed satisfactory. Detailed information regarding the trial mixes is presented in Appendix A.

Initially, calculation of the coarse aggregate (referred to as stone content in this study) was based on the Compacted Bulk Density (CBD). However, after trial mixes had been conducted the stone was altered, which changed the fine aggregate content. Greywacke stone was used for the coarse aggregate with a nominal maximum aggregate size of 19 mm, whereas the sand content was a 50/50 blend of Philippi Dune sand and Greywacke crusher sand. The mass of fine aggregate was then calculated based on the remaining volume required to achieve a mix volume of 1 cubic metre. The sieve analysis and grading curves of the fine aggregates are shown in Appendix A.

Table 3-3: Detailed concrete mix design

Type	w/b	CEM I	FA	BS	CS	L	SF	Water	GW	Sand	Density	Slump	SP
		kg									kg/m^3	mm	%
CEM I	0,5	340						170	1050	452	2464	55	0,3
	0,65	262						170	1050	485	2452	85	0,1
20 FA	0,5	272	68					170	1054	439	2442	55	0,5
	0,65	209	52					170	1054	476	2437	80	0,0
30 FA	0,5	238	102					170	1055	433	2431	60	0,0
	0,65	183	78					170	1055	471	2428	80	0,0
40 FA	0,5	204	136					170	1056	427	2420	95	0,0
	0,65	157	105					170	1056	466	2420	75	0,0
50 FA	0,5	170	170					170	1057	421	2409	70	0,2
	0,65	131	131					170	1057	461	2411	85	0,0
20 BS	0,5	272		68				170	1050	449	2458	55	0,5
	0,65	209		52				170	1050	484	2449	65	0,2
30 BS	0,5	238		102				170	1050	448	2456	50	0,5
	0,65	183		78				170	1050	483	2447	60	0,2
40 BS	0,5	204		136				170	1050	447	2454	50	0,5
	0,65	157		105				170	1050	481	2444	55	0,2
50 BS	0,5	170		170				170	1050	446	2452	60	0,5
	0,65	131		131				170	1050	480	2442	60	0,2
60 BS	0,5	136		204				170	1050	444	2448	50	0,3
	0,65	105		157				170	1050	479	2440	65	0,3
20 CS	0,5	272			68			170	1050	449	2458	50	0,6
	0,65	209			52			170	1050	484	2449	60	0,3
40 CS	0,5	204			136			170	1050	447	2454	60	0,8
	0,65	157			105			170	1050	481	2444	75	0,1
60 CS	0,5	136			204			170	1050	444	2448	60	0,8
	0,65	105			157			170	1050	479	2440	55	0,0
10 L	0,5	306				34		170	1050	449	2458	60	0,2
	0,65	235				26		170	1050	484	2449	50	0,3
20 L	0,5	272				68		170	1050	447	2454	60	0,2
	0,65	209				52		170	1050	482	2445	50	0,3
SF	0,5	323					17	170	1050	448	2456	50	0,6
	0,65	248					13	170	1050	483	2447	55	0,8
SF FA	0,5	238	85				17	170	1052	433	2428	80	0,6
	0,65	183	65				13	170	1052	471	2425	50	0,2
SF BS	0,5	238		85			17	170	1050	445	2450	45	0,6
	0,65	183		65			13	170	1050	480	2441	55	0,6
SF CS	0,5	238			85		17	170	1050	445	2450	50	0,6
	0,65	183			65		13	170	1050	480	2441	50	0,6
A-L	0,5	340						170	1050	452	2464	55	0,4
	0,65	262						170	1050	485	2452	50	0,5
B-M	0,5	340						170	1050	452	2464	50	0,5
	0,65	262						170	1050	485	2452	55	0,4

3.4 Casting and curing regime

The curing regimes adopted were dependent on the laboratory experiment conducted, namely, the compressive strength test, the OPI test and the accelerated carbonation test. All specimens were placed into a water bath (referred to as wet curing) and kept at a constant temperature range of 22°C to 25°C in accordance with SANS 5861-3 (2006).

Both compressive strength and OPI tests involved a 28-day wet curing. 28-day curing was used as this is generally the industry standard for compressive strength testing. Moreover, SANS 3001-C02 (2015) and the Durability Index Testing Procedure Manual (2017) state that OPI specimens cast under laboratory conditions should be prepared (cored and cut) after 28 ± 3 days of curing unless otherwise required by the project specifications. Therefore a 28-day wet curing regime for OPI specimens can be considered as the convention in practice.

Accelerated carbonation specimens were wet cured for seven days prior to the preconditioning regime which is explained in Section 3.5.3. For locations that experience hot summers coupled with strong winds, such as the Western Province, a suggested seven-day moist curing regime is recommended as a construction practice (Kellerman, 2009). This curing regime was therefore chosen as it simulates conditions that structures may experience on site.

3.5 Specimen preparation

This section details the number of specimens required for the laboratory experiments, as well as the precondition regimes conducted for the OPI test specimens.

3.5.1 Samples required

For this study a total of 42 mixes were produced. For all the laboratory experiments only 100 mm cube specimens were required. A minimum of 10 L of fresh concrete was required for each mix. One extra cube was made per test as a contingency and to consider any wastage or concrete loss during casting. A total of 420 100-mm cubes were cast for the 42 mixes used in this study. Table 3-4 summarises the number of cubes required for each test.

Table 3-4: Number of 100 mm cubes required per mix

Test	Concrete Required (L)
Compressive strength (28 Days)	3
OPI	2
Accelerated carbonation test	2
Contingency (1 per test)	3
Total	10

3.5.2 OPI specimens

OPI specimens were prepared in accordance with SANS-C03-1 (2015). Four concrete discs (70 ±2mm diameter; 30 ±2mm thickness) were prepared from two 100 mm cube specimens. After a 28-day wet curing period, two cores were extracted perpendicular to the casting direction from the cube specimens by means of a coring drill.

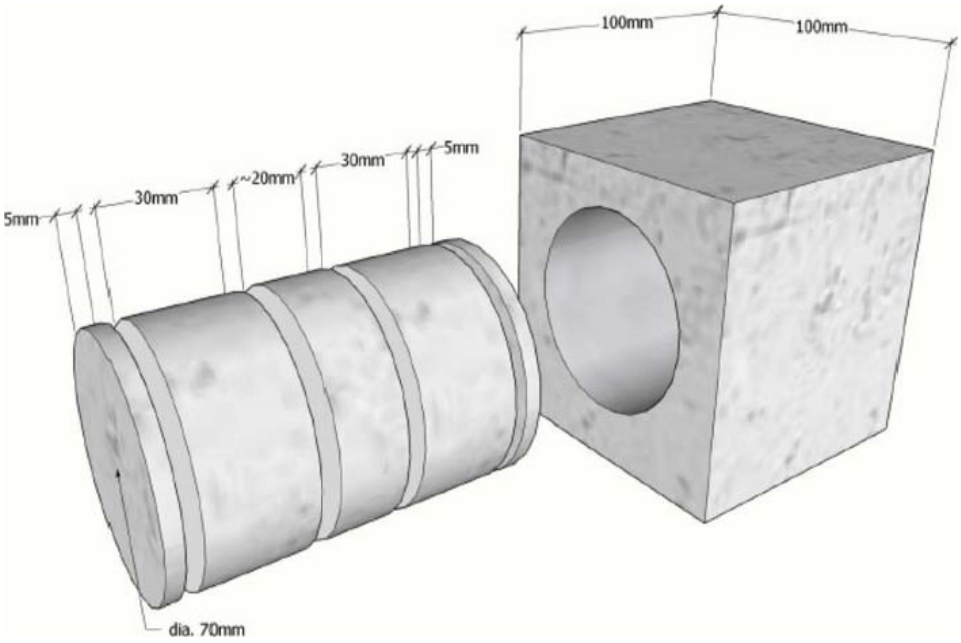

Figure 3-2: Details of cutting discs from 100 mm cube (Alexander, 2017)

The cores were saw-cut into the specified thickness of 30 ±2mm. It should be noted that the disc was made after 5 mm had been removed from both sides of the core, as illustrated in Figure 3-2. The concrete discs were preconditioned in an oven at 50 ± 2^0 C for 7 days immediately after coring and cutting. After 7 days, the discs were then cooled down in a desiccator at 23 ± 2^0C for 2-4 hours prior to the commencement of the test.

3.5.3 Accelerated Carbonation specimens

As stated in Section 2.4.2.1, one of the factors affecting the rate of carbonation is the internal relative humidity (RH) because it affects both the diffusion and the reactivity of carbon dioxide (CO_2) as it enters the specimen. It is for this reason that a preconditioning regime was adopted to ensure that the resulting internal RH in the samples has a minimal effect on the carbonation rate in the accelerated carbonation test

The preconditioning regime conducted by Salvoldi (2010) was adopted for this experiment with a few minor adjustments. He based his preconditioning regime on the internal relative humidity equation proposed by Parrot (1988) to approximately the internal humidity level in the concrete:

$$RH_{internal}=100-\left(1-e^{\left(\frac{-1.42t}{(d+0.01)^2}\right)}\right)(100-RH_{ambient}) \quad (3\text{-}1)$$

Where t = Drying time (days)

d = Depth of humidity front from surface (mm)

By mere observation, this equation is very limited as it does not account for factors such as w/b ratios or different binder types. However, determining the performance of this preconditioning regime on the internal humidity can be time consuming and lies outside the scope of this investigation.

This experiment required two 100-mm cube specimens. After the 7-day wet curing, the specimens were placed in an environmentally controlled room for 63 days (instead of 60 days in

Salvoldi's study) at a relative humidity of 45% ± 5% and a temperature of 20°C ± 2°C. Thereafter the specimens were sealed on four sides normal to the CO_2 ingress, using Sika Sikadur 45N epoxy and were left to dry overnight. This was performed to ensure unidirectional carbonation in the specimens as can be seen in Figure 3-3. The specimens were placed in another environmental room with a relative humidity of 65% ± 5% and a temperature of 20°C ± 2°C for 14 days. They were subsequently ready for accelerated carbonation testing.

The preconditioning regime conducted in Salvoldi's (2010) study resulted in the drying front not impeding the carbonation front. This was made apparent as similar carbonation coefficient values were observed after each testing day (3,6,9 and 12 weeks). For this reason, it is suspected that adopting this preconditioning regime would result in a similar nature. Details regarding whether the drying front has impeded the carbonation front are investigated in Chapter 4.

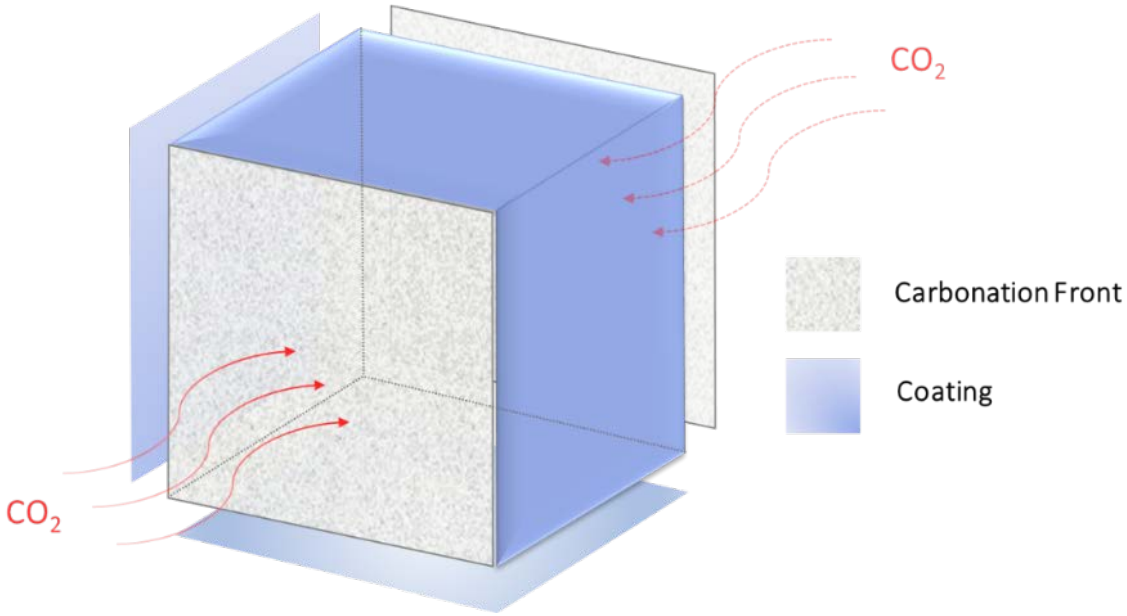

Figure 3-3 Sample preparation of accelerated carbonation specimens

3.6 Laboratory experiments

3.6.1 Slump test

The slump test was conducted in accordance with SANS 5862-1 (2006). The cohesiveness and workability of the concrete mix needed to be determined before it could be made at a full-scale level. If the mix was deemed inadequate, it had to be redesigned. Therefore, a trial concrete mix (10L) was used to determine these properties. A steel cone was filled in thirds with the fresh concrete compacted 25 times with a steel rod after each phase. Workability was determined by measuring the distance between the top of the slump and the bottom of the tapping rod as depicted in Figure 3-4.

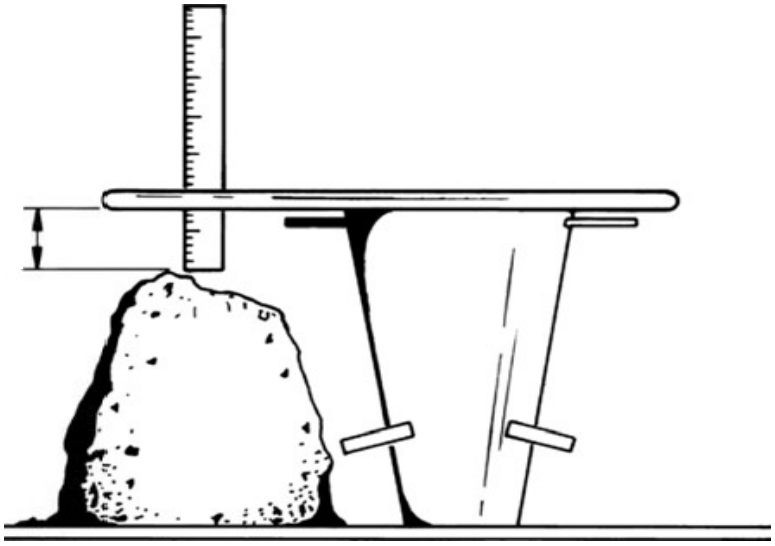

Figure 3-4:Measuring the slump (Kellerman & Croswell, 2009)

3.6.2 Compressive Strength test

The compressive strength test was conducted in accordance with SANS 5863 (2006). This was required mainly for concrete mix characterisation purposes. Three saturated, surface-dried 100 mm x 100 mm x 100 mm cubes were crushed at a uniform rate of 0,3 MPa/s ± 0,1 MPa/s to determine the average compressive strength of the respective concrete mixes. The test was conducted 28 days after casting. The cube specimens were to be water-cured and their dimensions and weight were to be recorded prior to testing. Finally, the Amsler compression machine was used to conduct the compressive strength test.

Figure 3-5: Amsler compressive machine

3.6.3 OPI test

The OPI test was conducted in accordance with SANS 3001-C03-2 (2015). Four concrete disks, also prepared in accordance with SANS-C03-1 (2015), were used for this test as described in detail in Section 3.5.2. Once the dimensions of the specimens had been measured, the specimens were placed in the compressible collar within the rigid sleeve, and thereafter inserted into the permeability cell with the exterior surface facing the bottom, as shown in Figure 3-6.

Figure 3-6: Permeability cell

Unwanted gases were purged from the cell. Afterwards the cell was supplied with oxygen until the pressure reached 100 ± 5 kPa. During the test, readings were taken periodically and was terminated either when the pressure had dropped to 50 kPa or after six hours if the pressure had not yet reached the limit. The results were then tabulated and processed. The Darcy coefficient of permeability was determined using the following equation:

$$k = \frac{\omega V g d z}{R A \emptyset} \qquad (3\text{-}2)$$

Where ω = molecular mass of oxygen = 32 g/mol;

V = Volume of oxygen under pressure in permeameter (m^3);

g = acceleration due to gravity (9.81 m/s^2);

R = universal gas constant = (8.313 Nm/K mol);

d = average specimen thickness (m);

$\emptyset$ = Temperature (K);

z = slope of the line determined in the regression analysis

Finally, the oxygen permeability index (OPI) for each concrete mix could be calculated which is the negative log of k-permeability.

3.6.4 Accelerated carbonation test

The method described in CPC-18: Measurement of hardened concrete carbonation depth (1988) was adapted for the accelerated carbonation test used in this study. Two 100-mm cube specimens were used for this test. Testing was done after 6, 9 and 12 weeks.

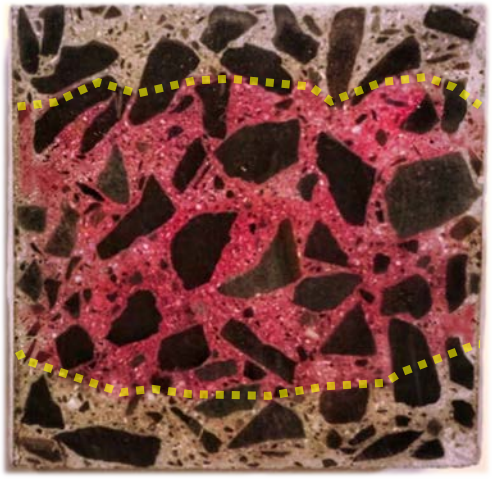

Figure 3-7: Concrete specimen with phenolphthalein applied

After the preconditioning regime, the specimens were placed in the carbonation chamber at an RH of 65% ± 5%, and a temperature of 20°C ± 2°C, applying a CO_2 concentration of 2 ± 0.1%, as stated in the fib Model Code for Service Life Design (2007). Carbonation depth measurements consisted of removing the specimen from the chamber and slicing approximately 15-20 mm off its side. Phenolphthalein indicator solution was then applied to the freshly cut surface, causing the uncarbonated section of the concrete to turn pink in colour as shown in Figure 3-7. The carbonation depth was then measured using a Vernier calliper with a precision to the nearest millimetre. Measuring was done approximately 24 hours after the indicator solution had been applied to the specimen to ensure the boundary between the carbonated and uncarbonated concrete was rendered more explicit.

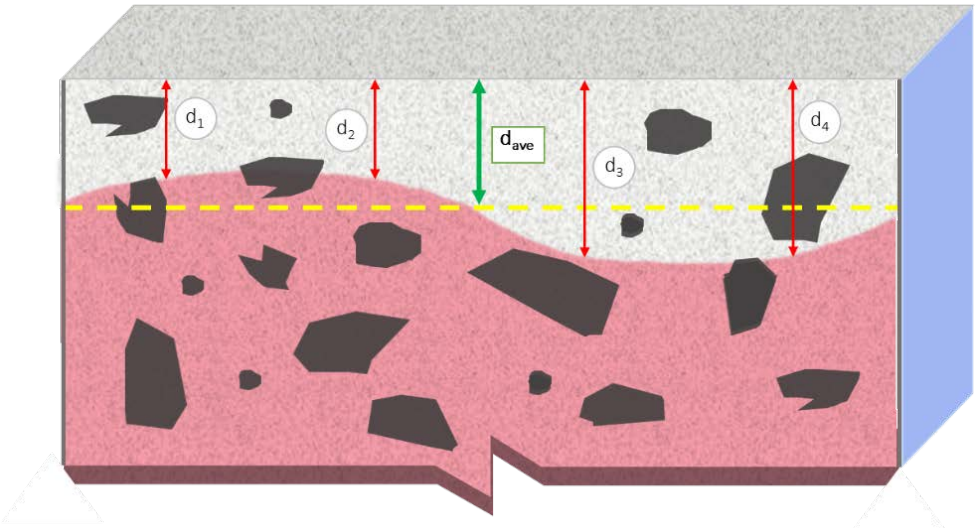

Figure 3-8: Measuring of carbonation depth after phenolphthalein is applied

Determination of the carbonation depth value is depicted in Figure 3-8. Four sites, shown as d_1 to d_4, approximately equally spaced across the specimen were measured. Thereafter, an average depth, d_{ave} was taken from the four measurements and was reported as the mean carbonation depth. A total of four mean carbonation depth measurements were gathered per mix per testing.

3.7 Statistical analysis of results

Significant differences in the experimental results could not be identified by merely visually observing trends in the graphs. A more in-depth analysis of the results was therefore required. Consequently, the results obtained from the laboratory experiments were analysed statistically. The various statistical tools provided by Walpole et al. (2012) are stipulated here as the t-test, rank sum test, ANOVA, and the Kruskal Wallis Test. Based on the statistical tools stated, a statistical approach was selected. The decision-making is conventionally dependent on a determination of the significance in the change of results, specifically through:

- Observing the significance in change of the OPI and carbonation depth with the increase in binder replacement percentage;
- Ascertaining the significance between results obtained with different binders of the same binder replacement percentage; and
- Determining the significance of using ternary mixes, compared to binary blends.

3.7.1 Hypothesis testing

The null hypothesis, denoted as H_0, refers to any hypothesis that is to be tested. It is usually used to propose that no statistical significance exists in a given set of observations. In a case where H_0 is rejected, an alternative hypothesis, denoted as H_1 is subsequently accepted. H_1 is considered as the logical complement to H_O as it nullifies or opposes it. For example, if H_0 states that the SF (5%) air permeability mean result is not significantly different from the control mix's (CEM I) air permeability mean, then H_1 would be that SF's mix is significantly different from the control in terms of their respective means.

The rejection or acceptance of the null hypothesis investigated is dependent on the chosen significance level (α). The significance level is expressed as a percentage (%) and can be interpreted as the percentage risk of concluding that a significant difference exists when there is no difference, which is the hypothesis being tested. This is referred to as a Type 1 error. To build on the foregoing example, if α equals 5%, it means that there is a 5% chance that there is a difference and thus H_0 is rejected, in other words SF's mix is significantly different from the control in terms of their respective means. In this study, an α value of 5% was chosen.

3.7.2 Analysis-of variance – ANOVA

The ANOVA test is done when there are more than two samples in the comparative process. It assumes that the samples are normally distributed that is, that the measurements derived from an equal-interval scale H_1 are accepted when there is no significance between the sample means. H_o, is rejected when at least one of the means is significantly different. However, this test does not have the ability to point out which means are significantly different.

3.7.3 T-test

The T-test is considered as the precursor to ANOVA. The advantage of this test is that it can be used to determine the significance between two sample means with limited sets of data, for a set of observations less than 30 or when the variance is unknown. This test was designed to determine

whether the means of two samples are different, assuming that both groups' data are normally distributed.

3.7.4 Kruskal Wallis test

The Kruskal Wallis test, referred to as the H-test, is similar to the ANOVA test as it is used to determine the significance of the means when there are more than two samples being compared. However, the difference lies within the distribution of the results. The ANOVA test is limited to parametric values or results that are normally distributed. When this condition does not hold, the H-test is used as it is the non-parametric counterpart. An example of a non-parametric distribution is the permeability coefficient (k-values) obtained from the OPI test (Nganga, 2012).

3.7.5 Wilcoxon rank-sum test

The Wilcoxon Rank-sum test – also referred to as the Wilcoxon two-sample test – is the non-parametric alternative to the t-test as it compares the means of two samples in which the results are non-normally distributed.

The test procedure is briefly described here. Let n_1 and n_2 be the number of observations from the smaller and larger sample respectively. Alternatively, n_1 and n_2 can be either one in cases where the number of observations is equal. The determinations from both samples are compiled together and thereafter ranked in ascending order. The ranks from each sample are summed up and denoted as either w_1 or w_2. If the observed u_1 or u_2 is less than or equal to the established critical value, the null hypothesis is rejected for the respective level of significance.

3.7.6 Statistical tools chosen

The permeability coefficient (k-value) results obtained from the OPI test follow a log-normal distribution or non-parametric distribution (Nganga, 2012). Thus, the use of statistical tools based on the parametric ANOVA and t-test is not suitable for these results. The non-parametric alternatives, that is, the Rank-sum and Kruskal Wallis tests can be used. However, the Kruskal Wallis test like the ANOVA test does not have the ability to distinguish which means are significantly different from a sample set of more than two. Hence the statistical tool used for the OPI test was the Rank-Sum test.

The T-test was used on the accelerated carbonation results as well as to supplement and verify the non-parametric test results for the OPI (log-scale) results. As the sample size for both the OPI and accelerated carbonation is less than 30 and the results are normally distributed, the T-test is suitable

3.7.7 Statistical test procedure

This section stipulates the statistical procedure that was conducted in this study. This analysis revolves around the acceptance or the rejection of H_O. Worked examples of the statistical tools used and the critical values outlined here can be found in Appendix E. The steps for the statistical test procedure are as follows:

1. State the null hypothesis (H_o): Mix A is not significantly different to Mix B regarding OPI and accelerated carbonation.

2. State alternative hypothesis (H_1): Mix A is significantly different to Mix B regarding OPI and accelerated carbonation.

3. Choose significance level, alpha = 0,05, so there is a 5% probability of rejecting H_o when it is true. This is a common value to use among researchers.

4. Statistical tests:

- Rank-Sum test (U): used for concrete permeability coefficient (k-value) results
- T-test (t): used for OPI (log scale) values and accelerated carbonation results.

5. Critical region: sourced from the statistical tables

- If $U < U_{crit}$ then fail to reject Ho or alternatively if $U > U_{crit}$ then reject H_o in favour of H_1.
- If $|t| < t_{crit}$ then fail to reject HO or alternatively if $|t| > t_{crit}$ then reject H_o in favour of H_1.

3.8 Summary

In this chapter, a detailed experimental programme was explained whose aim it was to potentially achieve a better understanding of concrete's long-term carbonation performance. This entails investigating the effects of different binders on the resistance to carbonation and the permeability coefficient of concrete. The variables coupled with the test methods presented in this chapter aimed at investigating the performance of the varying cement replacement percentages of different mineral admixtures regarding oxygen permeability and carbonation resistance. Moreover, the objective was to investigate whether the use of permeability and carbonation parameters of modern concretes still holds true in an existing carbonation model. To get a deeper understanding and interpretation of the results, statistical tools were utilised. The results of the experimental investigation explained in this Chapter are discussed in Chapter 4.

4 Results and discussion

This chapter discusses the results obtained from the experimental testing described in Chapter 2 namely, the 28-day compressive strength oxygen permeability index (OPI) and accelerated carbonation. Section 4.1 presents a brief discussion on the 28-day compressive strength results. In Section 4.2, the OPI results focus on the influence of water:binder ratio (w/b) and various binder types at specific replacement percentages (by mass of cement). This is followed by a discussion centred on further investigative tests on the influence of ternary mixes, the transitioning from binary to ternary mixes, comparison of the different binders at the same replacement level and commercial cements. Section 4.3 analyses the results obtained from the accelerated carbonation test. Similar analysis to that applied in the OPI tests was used on the carbonation results, as well as an evaluation of the impact of the preconditioning regime on carbonation. The chapter concludes with an investigation into the correlation between the carbonation depth and the permeability results, as shown in Section 4.4.

Both the OPI and the accelerated carbonation results were supplemented with a statistical analysis which includes a Rank-sum and t-test for the OPI results, and a t-test for the accelerated carbonation results. A statistical analysis (t-test) was also conducted on the compressive strength results in which a discrepancy in results was observed. Information regarding variables tested and the notations used for the various mixes will be discussed in brief throughout the course of this chapter. Conclusions drawn, and recommendations based on these results are presented in Chapter 5. Detailed experimental results and worked statistical analysis examples are shown in Appendix A to E.

4.1 Compressive strength

The 28-day compressive results for concretes with w/b ratios of 0,50 and 0,65 are shown in Figure 4-1 and Figure 4-2 respectively. The test was conducted merely for characterisation and consistency. The error bars shown in the figures represent first standard deviation error (STDV). Detailed compressive strength results are shown in Appendix B.

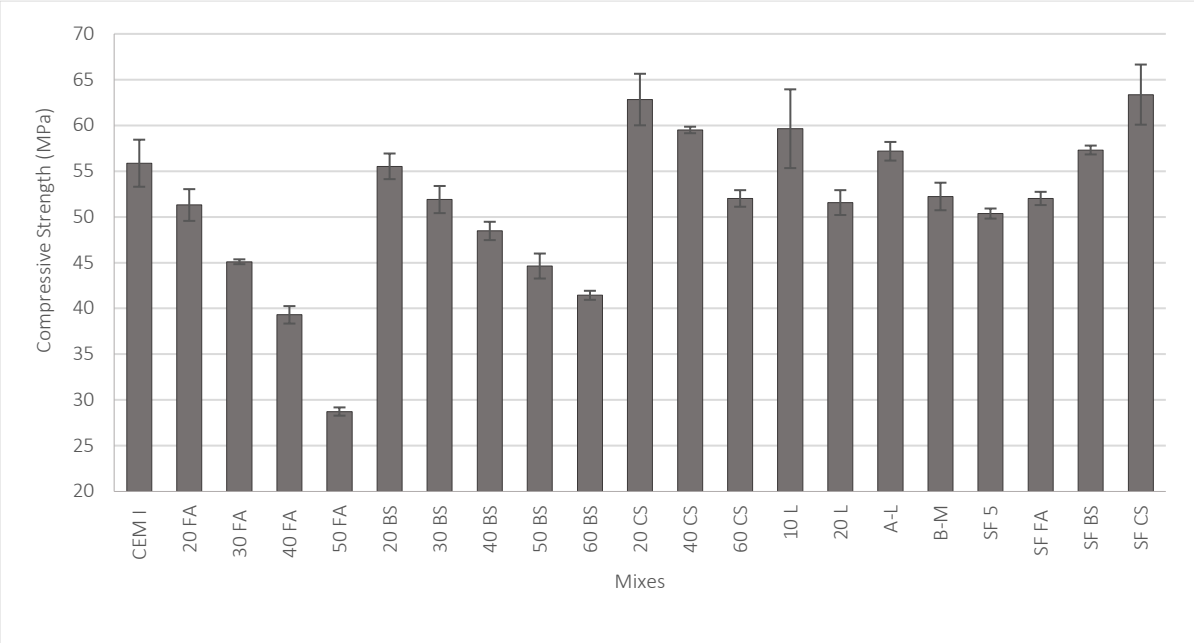

Figure 4-1: 28-day compressive strength results of concretes with w/b = 0,5

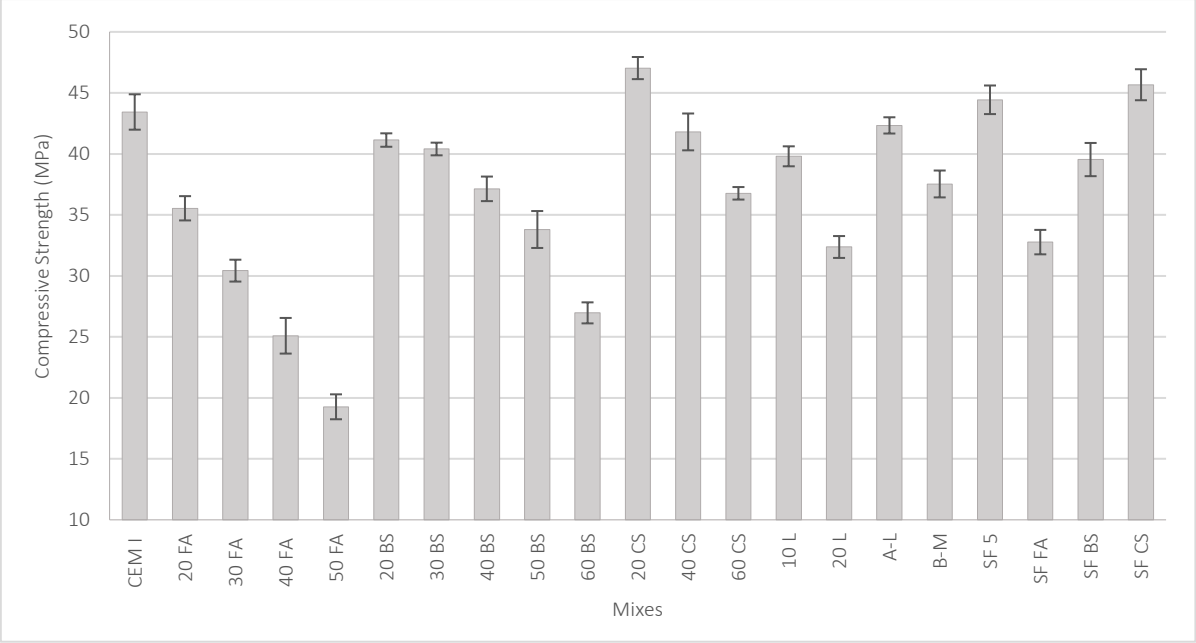

Figure 4-2: 28-day compressive strength results of concretes with w/b = 0,65

In comparing the 28-day compressive strength results between Figure 4-1 and Figure 4-2, it became evident that as expected, the w/b ratio has a marked influence on the compressive strength of concrete. The results showed that an increase in w/b ratio causes a decrease in compressive strength and that in general, an increase in binder replacement (with a few noticeable exceptions) resulted in a decrease in compressive strength. This trend can be attributed to the dilution effect resulting in a lesser degree of hydration reaction especially at early ages. At increasing replacement levels fewer hydration products, specifically calcium silica hydrate (CSH), the main hydration product contributing to the concrete's strength, are typically formed. It should be noted that this trend is more common for early-age compressive strengths (28 days or fewer) excluding concrete that includes silica fume. Although, long-term compressive strength of concretes containing blended cements tends to be higher, compared to concrete made without mineral admixtures (Grieve, 2009).

Exceptions to the trend observed of decreasing strength with increased binder replacement levels could be found in the w/b 0,50 mixes. Firstly, the control mix (containing 100% CEM I) had a compressive strength lower than the 10 L mix, that is, concrete with 10% limestone replacement. As stated in Section 2.5.2.5, limestone is regarded as an inert filler, and so contributes mainly to the dilution effect, consequently decreasing compressive strength. A t-test comparing the two means showed that the results were statistically insignificant and therefore the discrepancy was considered negligible.

Secondly, the 5% silica fume replacement level mix (referred to as SF 5) had a lower compressive strength in comparison to the control mix. A t-test conducted confirmed that there was a statistical significance between the two mixes. As indicated in Section 2.5.2.4, the positive influence of SF on compressive strength is attributed to its fine filler effect coupled with its highly reactive pozzolanic nature. Additionally, in contrast to the results shown in this study, a study conducted by Alexander & Bagee (1999) showed that the addition of silica fume from a 5% replacement level can result in an increase in compressive strength. With this in mind, the present results were considered an anomaly.

Finally, the 20% and 40% Corex slag (CS) replacement level mixes namely, 20 CS and 40 CS for a w/b ratio of 0,50 and 20 CS for a w/b ratio of 0,65, had greater strength than the control mix. This result was similar to what was seen in Jauferally's (2001) study, where the optimum CS replacement levels with respect to compressive strength were approximately 45% and 50% for w/b ratios of 0,4 and 0,6 respectively. This phenomenon could be attributed to the highly reactive nature of CS, which produces additional hydration products within an adequate alkaline environment.

4.2 Oxygen permeability index

The discussion in this section concerns the influence of the w/b ratios and different binders at specific replacement levels on the concrete's permeability using the results obtained from the OPI test. Also incorporated are an investigation of ternary mixes, a comparison of the transition from binary to ternary mixes, and a discussion on the influence of different binder types and commercial cements. The OPI results presented were obtained after 28 days of wet curing and preconditioning in accordance with SANS 3001-CO1 (2017). Both the D'Arcy coefficient of permeability, k (m/s) and the OPI index results are presented in this section. These are initially shown in table format (refer to Table 4-1).

The results are then illustrated in bar graph form. The error bars on the graphs represent first order standard deviation (STDV). This approach was implemented as OPI index values typically range from 8 to 11. The range lies over three orders of magnitude and was determined by calculating the negative logarithm of k-permeability. The rationale is that showing the k-permeability results allows for a better evaluation regarding the numerical differences among the mixes, in comparison to the OPI (log scale) values (Beushausen & Alexander, 2008). Detailed test results are included in Appendix C.

In addition, the results are supplemented with statistical analysis tests namely, the Rank-Sum test and t-test, which are presented and discussed in this section. The statistical analysis results are presented in table format. Either one or two results are shown when comparing the statistical significance between the mean results of the mixes. One test result indicates that the results from both statistical tests (rank-sum and t-test) are in agreement. Conversely, two test results are shown if they are contradictory. If the null hypothesis is accepted it was denoted as the symbol 'O'; if not, the symbol 'X' was used.

4.2.1 Influence of w/b ratio

The results of both OPI (log scale) and k-coefficient for the concretes at w/b ratios of 0,5 and 0,65 are presented in Table 4-1. Column 6 shows the ratio between the permeabilities obtained from the two w/b ratios (w/b ratio of 0,5 over 0,65) in terms of percentage. On average, the ratio was at 50%, indicating that the increase in w/b ratio from 0.50 to 0.65 doubled the permeability performance in this study. Increasing the w/b ratio increases the porosity and permeability. This is due to the lower degree of hydration as well as extending the initial spacing between cement particles (Grieve, 2009). Consequently, this leads to an increase in the size and connectivity of the pores within the hardened concrete.

Table 4-1: Permeability results for concrete mixes of different w/b ratios

Type	OPI		k (m/s)		k(0,50)/k(0,65)
	log scale		(10^(-11))		%
w/b	0,5	0,65	0,5	0,65	
CEM I	10,70	10,46	2,1	3,5	60
20 FA	10,65	10,32	2,4	4,9	48
30 FA	10,70	10,44	2,2	3,7	59
40 FA	10,79	10,31	1,7	5,3	32
50 FA	10,46	9,77	3,5	19,3	18
20 BS	10,85	10,54	1,5	3,0	49
30 BS	10,94	10,61	1,2	3,2	37
40 BS	10,97	10,66	1,1	2,3	48
50 BS	10,99	10,63	1,0	2,4	44
60 BS	11,06	10,81	0,9	1,6	55
20 CS	10,70	10,65	2,0	2,6	78
40 CS	11,08	10,34	0,7	4,5	16
60 CS	10,66	10,60	2,2	2,8	78
10 L	10,72	10,47	1,9	3,4	57
20 L	10,69	10,36	2,0	4,5	45
A-L	10,76	10,52	1,8	3,1	57
B-M	10,93	10,68	1,2	2,1	57
SF 5	10,76	10,48	1,9	3,4	56
SF FA	10,93	10,62	1,2	2,4	49
SF BS	10,91	10,62	1,4	2,5	55
SF CS	11,02	10,70	1,0	2,0	48
				AVERAGE	50

4.2.2 Influence of FA

Figure 4-3 and Figure 4-4 illustrate the influence of Fly Ash (FA) on the permeability from 20 to 50% FA replacement levels in 10% increments (referred to as 20 FA to 50 FA) in terms of k-permeability and OPI values respectively. The results are supplemented with statistical analysis test results, shown in Table 3.2. Detailed results are shown in Appendix C.

Observations as read from Figure 4-3 and Figure 4-4 show no explicit differences in permeability among the mixes with a w/b ratio of 0,5 at different FA replacement levels. This is due to overlapping of the error bars among the mixes. A similar trend can be seen for the mixes with a w/b ratio of 0,65 except that a slight decreasing trend in permeability was observed with increasing FA replacement levels until the 40 FA mix. Thereafter, a significant increase in permeability was seen for the 50 FA mix in comparison with the other FA mixes (as no overlapping of error bars was observed). Therefore, this result does not correspond to the overall trend and could be considered as an outlying observation.

Table 4-2 shows that the two statistical analysis tests were in agreement. The results showed no statistical significance was observed between the control mix (CEM I) and the FA mixes up to 40% FA replacement for both w/b ratios thus accepting the null hypothesis, H_o. However, the null hypothesis was rejected for the 50 FA mix of both w/b ratios when compared to the control mix.

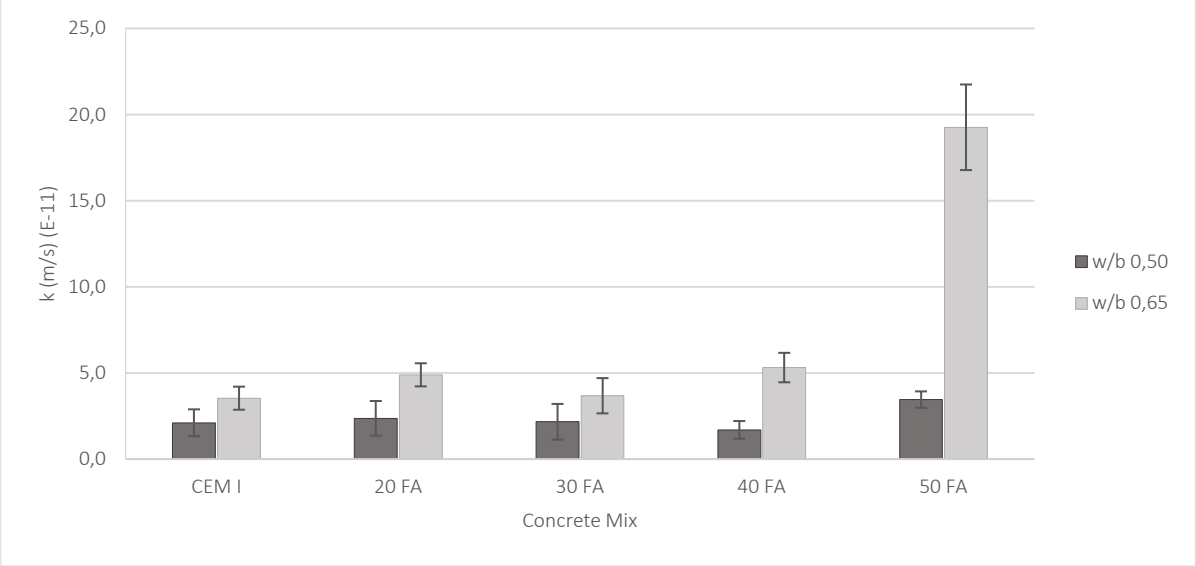

Figure 4-3: k-permeability of FA of varying replacement percentages

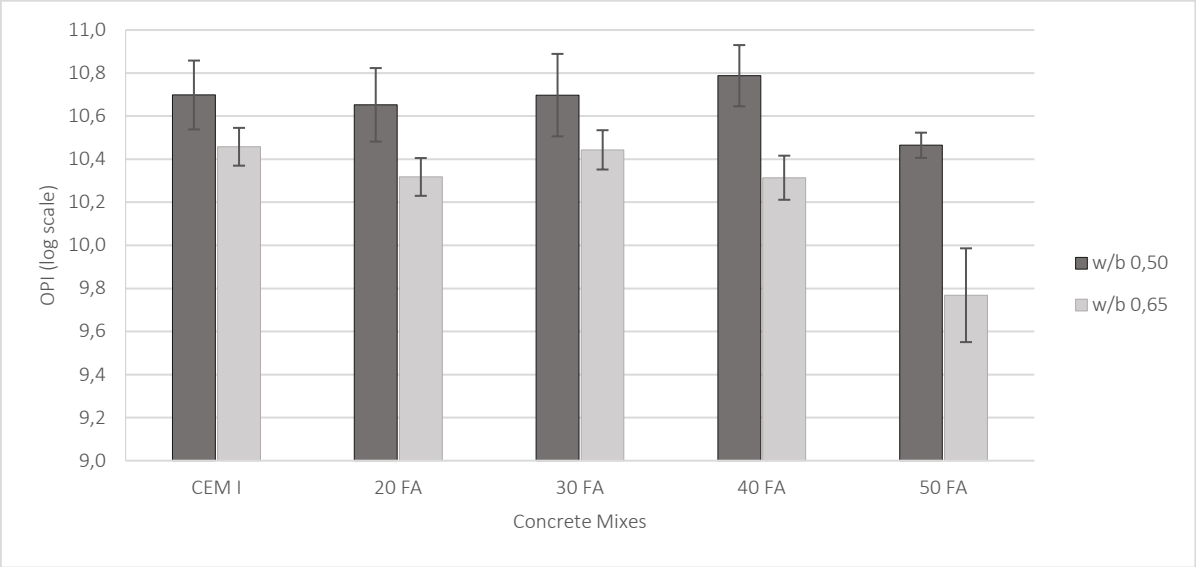

Figure 4-4: OPI values of FA at varying replacement percentages

Table 4-2: Statistical analysis results for FA mixes

Type	CEM I	20 FA	30 FA	40 FA	CEM I	20 FA	30 FA	40 FA
	w/b 0,50				w/b 0,65			
20 FA	O				O			
30 FA	O	O			O	O		
40 FA	O	O	O		O	O	O	
50 FA	X	O	O	X	X	X	X	X

Similar observations were seen in a study conducted by Zulu & Allopi (2015) where the influence of FA, from 30% to 60% replacement levels in 10% increments on permeability after 28 days of wet curing was investigated, although no control was considered. Results showed no difference between the 30% and 40% FA replacement mixes. Furthermore, a clear increase in permeability was observed with FA replacement levels reaching and exceeding 50%. A study conducted by Khan & Lynsdale (2012) reported that the addition of FA had limited influence on the permeability. In this study FA

replacement levels of 20%, 30% and 40% on permeability after 28 days of curing were investigated. No significant difference or trend in the permeability result could be seen for FA replacement levels of 20% to 40%.

The literature (refer to Section 2.4.4) states that usually the addition of mineral admixtures results in a refinement of the pore structure, potentially increasing the permeability performance. However, this was not explicitly observed in the results. It is suspected that due to the permeability for the control mixes having already obtained results of impermeable concrete; the addition of FA could not have a significant effect.

Due to FA's pozzolanic behaviour, it is suspected that the OPI results will increase significantly with age (permeability being reduced) as is to be expected with a refinement of the pore structure over time. Research conducted by Golden (2015) showed almost identical permeability performance between the 30% FA replacement and the control mixes (CEM II A-L 52 ,5N) for both w/b ratios of 0,50 and 0,65 after 28 days of wet-curing. After 90 days, the OPI results of the FA mixes significantly increased in comparison to the control mixes. A similar trend was also observed in the study conducted by Khan & Lynsdale (2012).

In conclusion, it can be argued that the fine filler and pozzolanic effects were approximately equal but opposite to the dilution effect in terms of their influence on the permeability performance up to a replacement level of 40%. At the FA replacement level of 50%, a decreased permeability performance was observed due to the dilution effect becoming the dominant effect. Additionally, as the control mixes exhibited low permeabilities, it was suspected that the addition of FA could not further improve the permeabilities significantly.

4.2.3 Influence of BS

Figure 4-5 and Figure 4-6 illustrate the influence of ground granulated blastfurnace slag (BS) on the permeability performance from 20% to 60% BS replacement levels in 10% increments (referred to as 20-60 BS) in terms of k-permeability and OPI values respectively. The results are complemented with the statistical analysis test results shown in Table 4-3. Detailed results are shown in Appendix C.

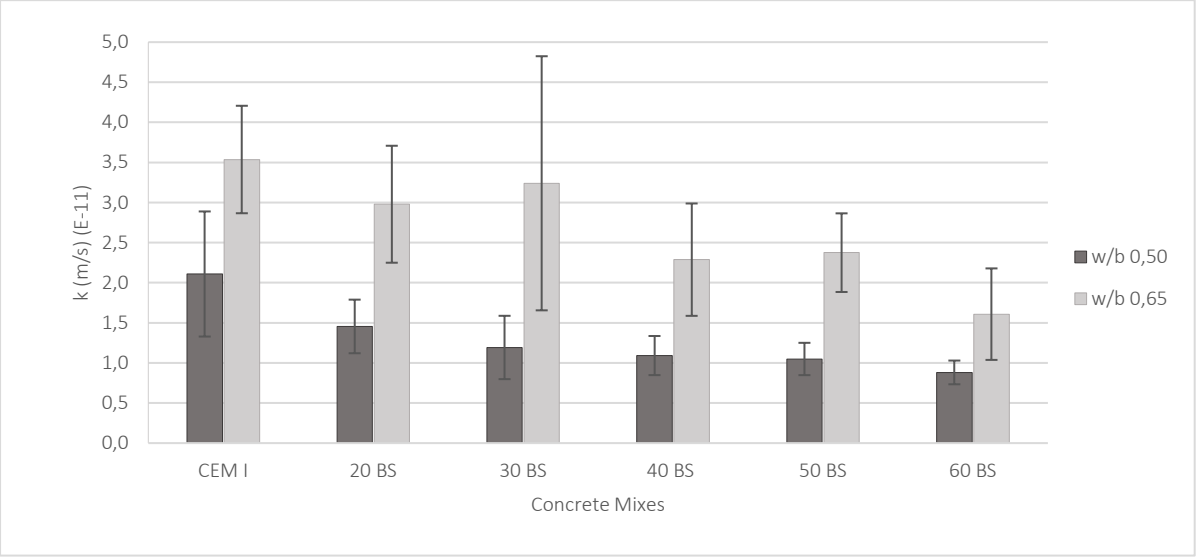

Figure 4-5: k-permeability of BS of varying replacement percentages

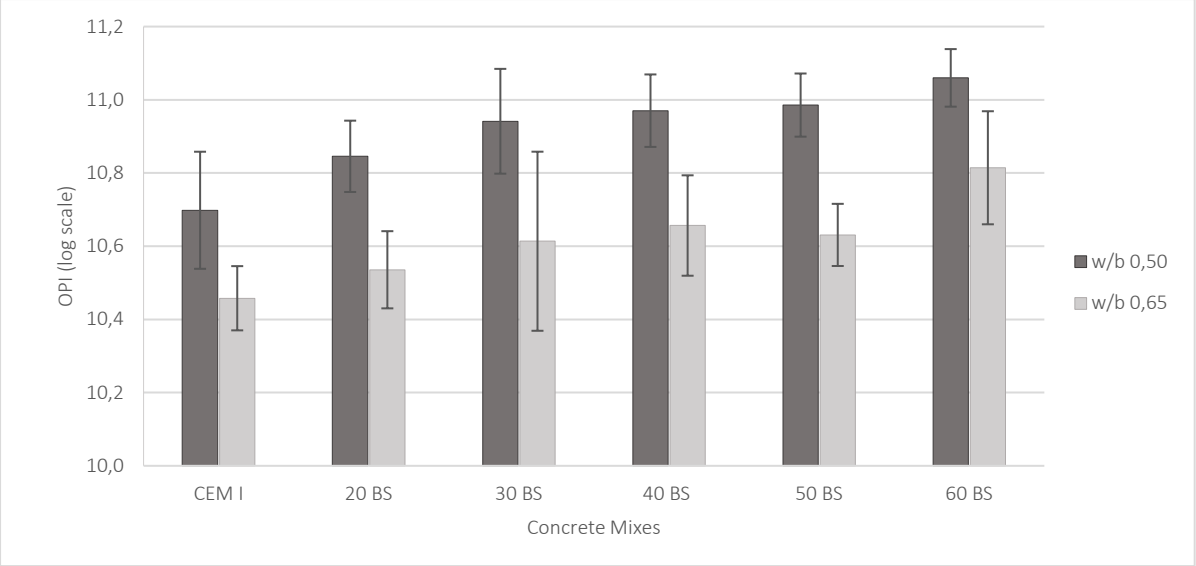

Figure 4-6: OPI values of BS at varying replacement percentages

Figure 4-5 and Figure 4-6 showed that there was a general decrease in permeability with the addition of BS to both w/b ratios. However, overlapping of the errors bars, it can be argued that the numerical differences of the means could be insignificant. Statistical analysis results in Table 4-3 showed that inclusion of BS is statistically insignificant up to a replacement level of 30% and 50%, for a w/b ratio of 0,5 and 0,65 respectively. It is suspected that due to the permeability for the control mixes already indicating relatively impermeable concrete, the addition of BS could not result in a significant effect of reducing permeability further. A similar decreasing trend in permeability was observed in a study conducted by Akram & Raza (2015). The performance of BS on concrete permeability was tested at 35% and 50% binder replacement after 28 days of wet curing.

Table 4-3: Statistical analysis results for BS mixes

Type	CEM I	20 BS	30 BS	40 BS	50 BS	CEM I	20 BS	30 BS	40 BS	50 BS
	w/b 0,50					w/b 0,65				
20 BS	O					O				
30 BS	O	O				O	O			
40 BS	X	O	O			O	O	O		
50 BS	X	O	O	O		O	O	O	O	
60 BS	X	X	O	O	O	X	X	O	O	O

It is suspected that both the chemical and physical properties of BS contributed positively to the permeability performance. BS is a latent hydraulic binder, activated in the presence of an alkaline environment to produce hydration-like cementing products, refining the concrete's pore structure. Moreover, slag is generally ground more finely than Portland cement (PC), contributing to the fine filler effect. BS's inclusion can also have a negative influence on the concrete's permeability as it contributes to the dilution effect. Nevertheless, its inclusion did not result in a net increase in permeability even at a replacement level of 60% where the dilution effect was most prominent compared to the other BS mixes in this study.

4.2.4 Influence of CS

Figure 4-7 and Figure 4-8 illustrate the influence of ground granulated Corex slag (CS) on the permeability performance from 20% to 60% CS replacement levels in 20% increments (referred to as 20-60 CS) in terms of k-permeability and OPI values respectively. The results are supplemented with statistical analysis test results shown in Table 4-4. Detailed results are shown in Appendix C.

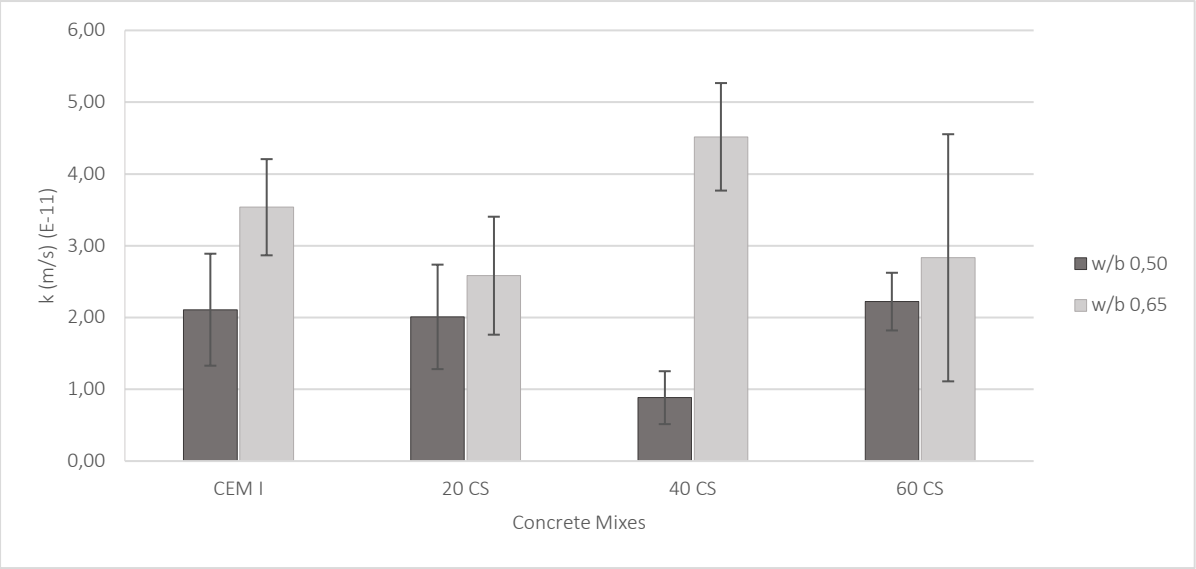

Figure 4-7: k-permeability of CS of varying replacement percentage

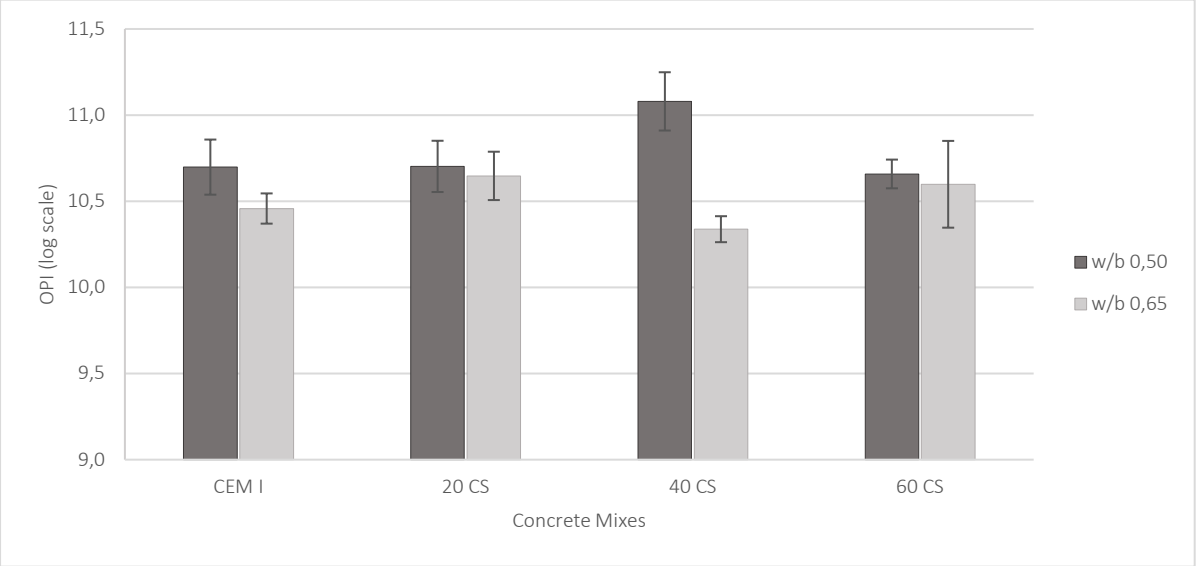

Figure 4-8: OPI results of CS of varying replacement percentages

Observations from Figure 4-7 and Figure 4-8 showed that no clear trend could be deduced by comparing the results and it was suspected that anomalies exist. In addition, it was observed that generally CS had no significant influence on the permeability. Statistical analysis results in Table 4-4 showed that for the mixes with a w/b ratio of 0,65 there was no significant difference amongst all the CS mixes when compared to the control mix. However, amongst those with a w/b ratio of 0,50, a significant difference was observed for the 40 CS mix in comparison to the control mix, although no statistical significance was observed between the latter and 60 CS. Therefore, it is assumed that an anomaly exists among the mixes with a w/b ratio of 0,5.

Table 4-4: Statistical analysis results for CS mixes

Type	CEM I	20 CS	40 CS	CEM I	20 CS	40 CS
	w/b 0,50			w/b 0,65		
20 CS	O			O		
40 CS	X	X		O	X	
60 CS	O	O	X	O	O	O

It was predicted that an observed decreasing trend of permeability should have been observed for CS similar to that which was manifest in the BS results shown in Section 4.2.3. This relates to what was pointed out in Section 2.5.2.2 – that CS has a similar chemical composition to BS. For this reason, a similar decreasing trend in permeability was expected.

4.2.5 Influence of L

Figure 4-9 and Figure 4-10 illustrate the influence of limestone (L) on the permeability performance of 10% and 20% L replacement levels (referred to as 10 L and 20 L) in terms of k-permeability and OPI values respectively. The results are supplemented with statistical analysis test results shown in Table 4-4. Detailed results are shown in Appendix C.

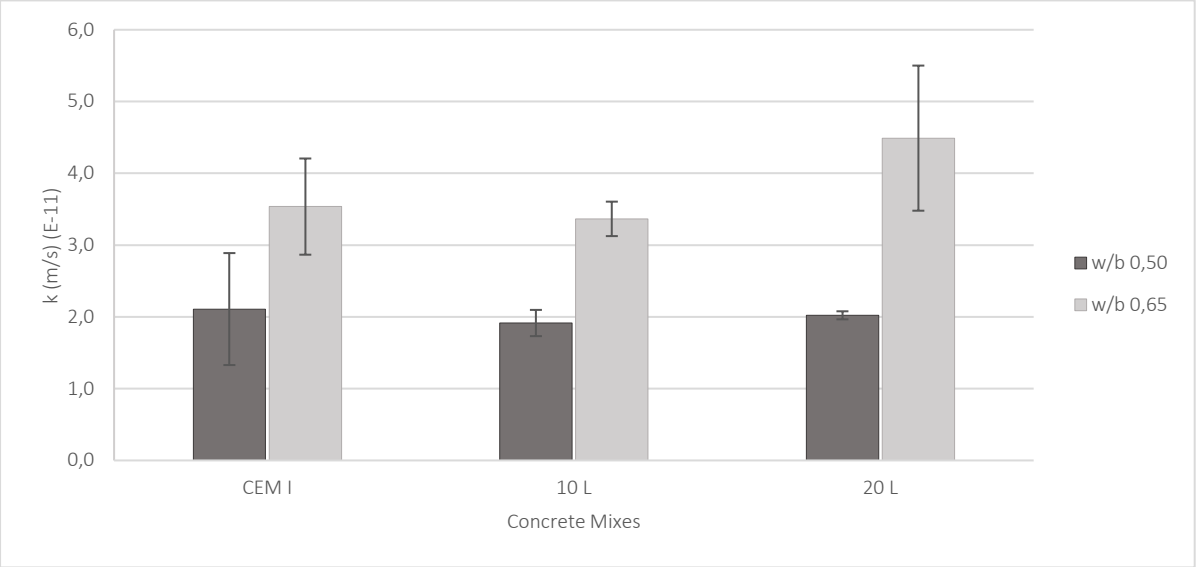

Figure 4-9: k-permeability of L of varying replacement percentages

Observations read from Figure 4-9 and Figure 4-10 show no clear significance for mixes of either w/b ratio, as the error lines of the mixes with various replacement levels of L overlapped. However, for the mixes with a w/b of 0,65 a slight increase in permeability could be observed with an L replacement of 20%. The statistical analysis in Table 4-4 showed that for both w/b ratios the inclusion of L had not resulted in a significant change in permeability in comparison to the respective control mixes.

As indicated in Section 2.5.2.5, limestone is considered to be an inert fine filler as it does not participate chemically in the various reactions in the concrete. For the L mixes, it is suggested that two attributes affected the concrete pore system: dilution and fine filler effect. These attributes oppose each other in terms of the way they affect the concrete pore system.

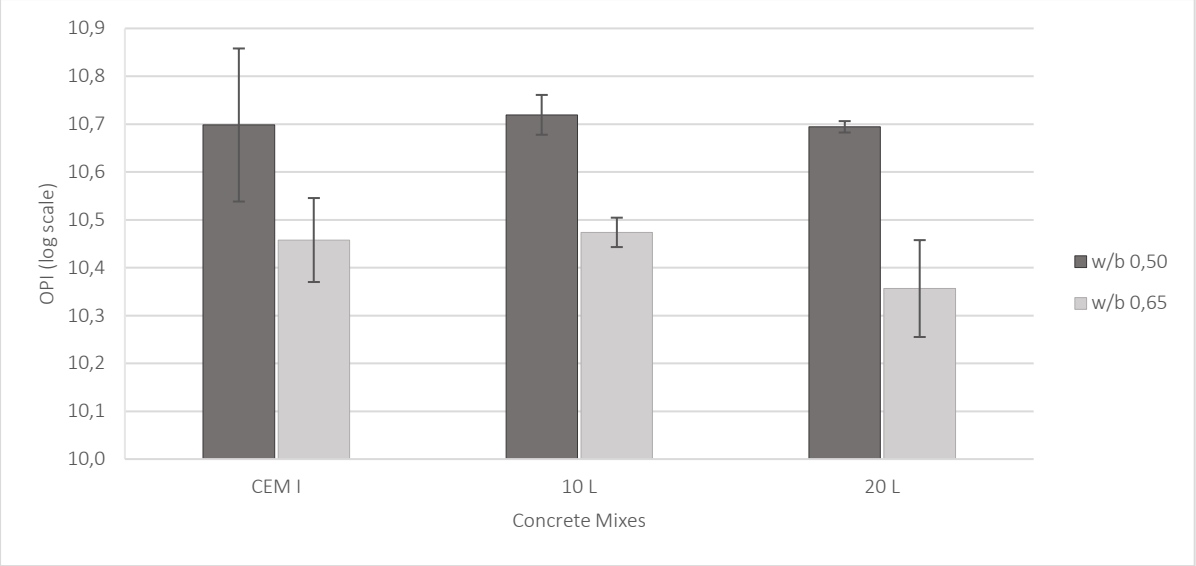

Figure 4-10: OPI (log scale) results of limestone of varying replacement percentage

Based on these reasons and results, it was concluded that replacement levels of L up to 20% had no significant influence on the concrete's permeability. It appeared that limestone's two affecting attributes counteract each other, approximately cancelling each other out until to a L replacement level of 20% and consequently causing no significant change in permeability.

Table 4-5: Statistical analysis results for L mixes

Type	CEM I	10 L	CEM I	10 L
	w/b 0,50		w/b 0,65	
10 L	O		O	
20 L	O	O	O	O

4.2.6 Influence of SF and ternary mixes

Figure 4-11 and Figure 4-12 illustrate the influence of silica fume (SF) at 5% replacement (referred to as SF 5), and ternary mixes in terms of k-permeability and OPI values respectively. The ternary mixes all consist of 5% SF and either fly ash, blastfurnace slag or Corex slag, referred to in this study as SF FA, SF BS and SF CS respectively. Statistical analysis results are shown in Table 4-6. Detailed results are shown in Appendix C.

In interpreting Figure 4-11 and Figure 4-12, a minor decrease in permeability with the inclusion of SF for both w/b ratios was observed. A similar trend is observed in a study conducted by Alexander & Bagee (1999). However, the change in permeability in the latter study was greater than the one observed in this study. It is suspected that the SF used in this study may have had a weaker reactive nature in comparison.

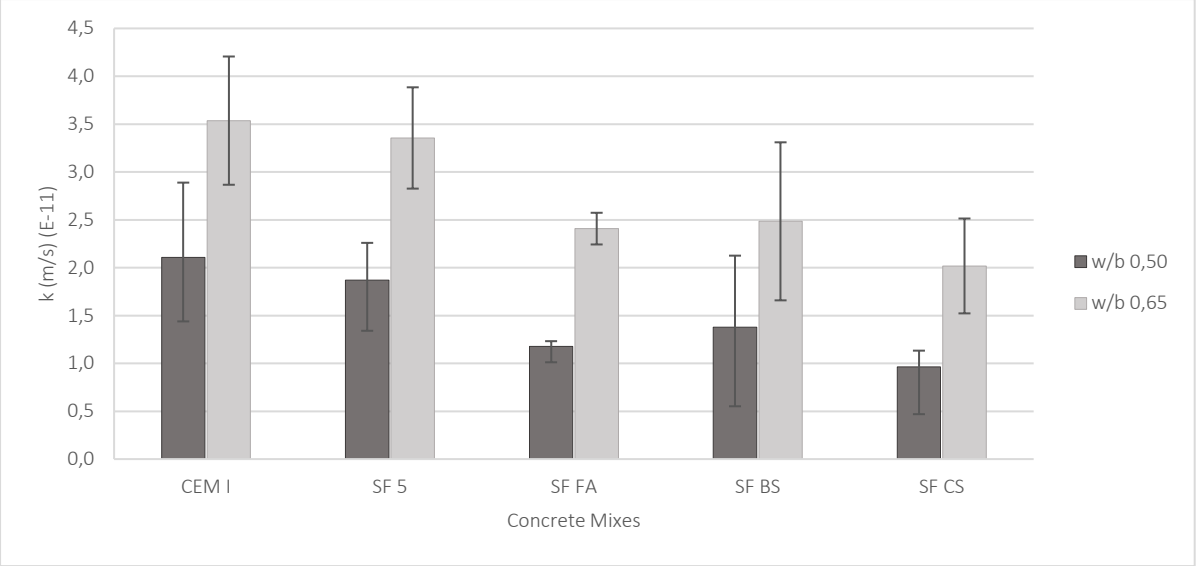

Figure 4-11: k-permeability results of SF and ternary mixes

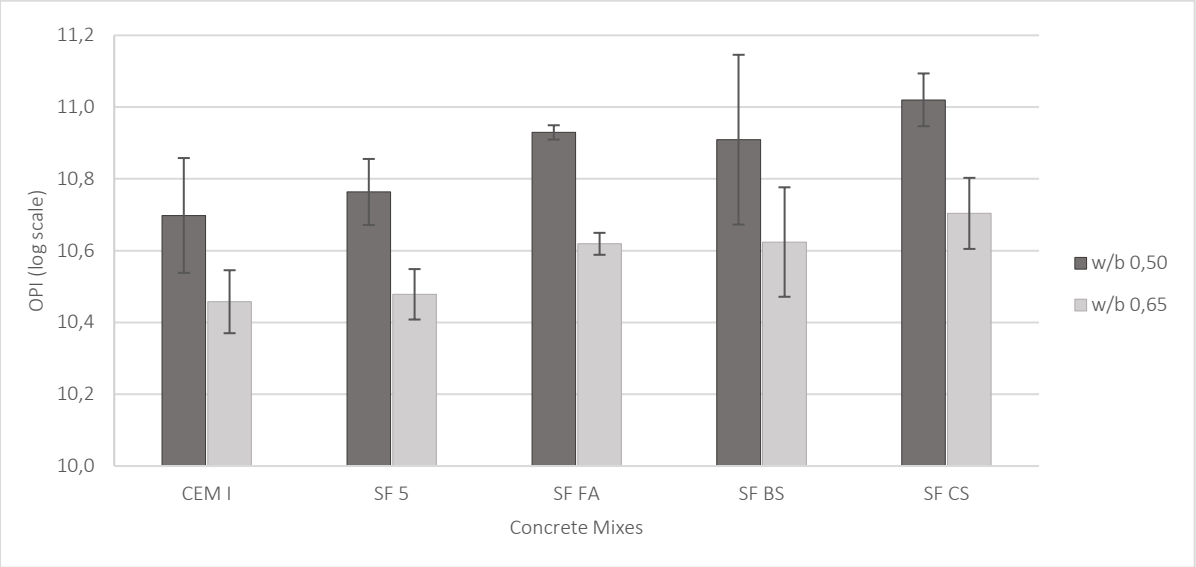

Figure 4-12: OPI results of SF and ternary mixes

The overlapping of the error bars implies that there was no significant difference between the results obtained from various mixes at a certain w/b ratio. Statistical analysis in Table 4-6 results showed that there was no statistical significance between SF 5 and CEM I for the w/b ratios of the mixes. Therefore, the null hypothesis was not rejected.

Table 4-6: Statistical analysis results for SF and ternary mixes

``Type	CEM I	SF 5	SF FA	SF BS	CEM I	SF 5	SF FA	SF BS
	w/b 0,50				w/b 0,65			
SF 5	O				O			
SF FA	X	X			X	X		
SF BS	O	O	O		O	O	O	
SF CS	X	X	O	O	X	X	O	O

As indicated in Section 2.5.2.4, SF is a highly reactive pozzolanic material due to its high amorphous silicon dioxide content. In addition, SF particles are extremely small (with an average particle size of 15 nm), thus making it an effective fine filler. Despite these beneficial factors, results showed that a 5% SF replacement level was not adequate to be statistically significant to the control mix. It appears that the SF replacement level and/or the reactive nature of SF was not sufficient to cause a statistically significant change in the permeability performance. Like FA, SF is a pozzolan, and it will therefore continue to produce cement-like hydration products with calcium hydroxide (CH) over time. This will lead to further improving of the pore structure over time.

Results from statistical analysis showed that the ternary mixes (excluding the SF BS mix) were statistically significant in comparison to the control mix and the SF 5 mix, thus refuting the null hypothesis. Among the ternary mixes, SF CS had the best permeability performance followed by SF FA and thereafter SF BS. However statistically, no significance was observed among the mixes for both w/b ratios.

4.2.7 Binary versus ternary mixes

Figure 4-13 and Figure 4-14 illustrate the contrast between the binary and ternary mixes in terms of k-permeability and OPI values respectively. The binary mixes are 30% replacement (by mass) of fly ash (FA) and blast-furnace slag (BS) that is, 30 FA and 30 BS. The ternary mixes both consist of 5% silica fume (SF) and either 25% of FA or BS, referred to as SF FA and SF BS respectively. Statistical analysis results are shown in Table 4-7. Detailed results are shown in Appendix C.

Although differences pertaining to the number of binders are apparent between the binary and ternary mixes, similarities still exist. Both concrete mix types replace the same percentage of cement. This section thus investigates the effects of adding the additional extender to a binary concrete mix whilst maintaining the same replacement level. In other words, its focus is a comparison between binary and ternary concrete mixes.

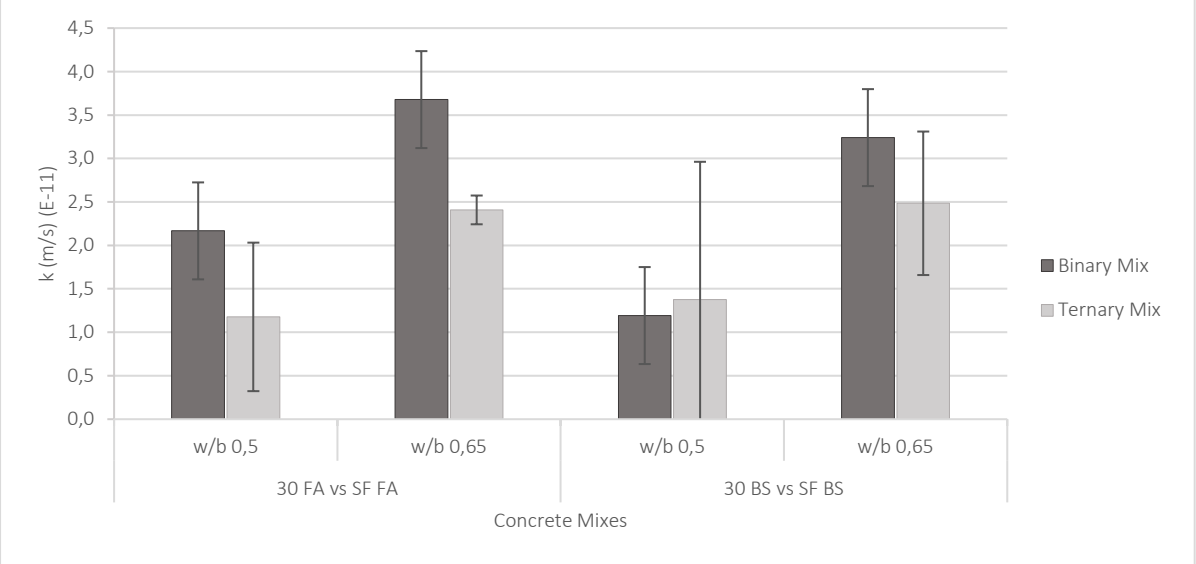

Figure 4-13: The k-permeability results of binary and ternary mixes

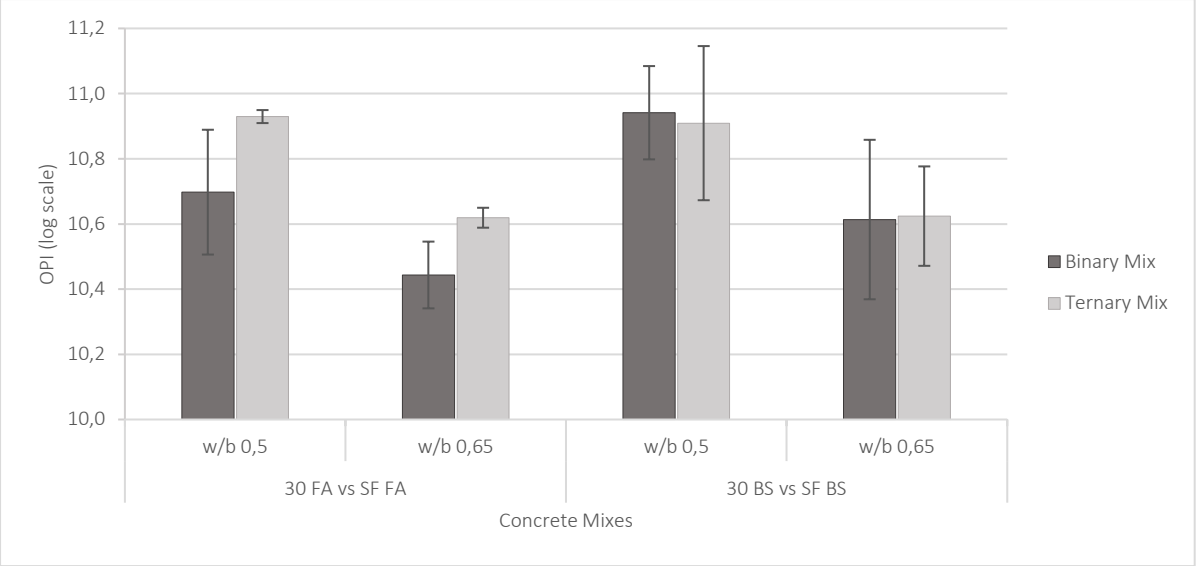

Figure 4-14: OPI results of binary and ternary mixes

Observations deduced from Figure 4-13 and Figure 4-14 revealed an increase in permeability performance from 30 FA to SF FA for both w/b ratios. This suggests that the synergy between the FA and SF for this specific replacement proportion has a positive influence on the concrete's permeability performance. However, the same cannot be said for the comparison between 30 BS and SF BS. A slight increase in permeability was observed for the w/b ratio of 0,50. However, overall a general increase in permeability performance was observed in comparing the binary and ternary mixes.

The statistical analysis results of the significance between 30 BS and SF BS revealed that for both w/b ratios no statistical significance was detectable, although a statistical significance was observed between the FA and SF FA mixes with a w/b ratio of 0,65. However, contradictory statistical analysis results emerged in observations of the mixes with a w/b ratio of 0,50. The null hypothesis is effectively validated by the Rank-sum test and refuted by the t-test results. Reasons for this phenomenon may be found in the high variability of the results, specifically 30 FA's having a coefficient of variation of 48% outside the suggested range outlined in Section 2.3.1.1. This indicates that further investigation is required, which would involve the testing of a greater number of specimens.

Table 4-7: Statistical analysis for binary and ternary mixes

Type	30 FA	30 BS	30 FA	30 BS
	w/b 0,65		w/b 0,65	
SF FA	O[1]/X[2]		X	
SF BS		O		O

As stated in Section 2.5.2.6, the use of reasonably proportioned ternary blends can potentially allow for the effects of one mineral admixture to compensate for the shortcomings of the other and vice versa. Based on the results, it emerged that the transition from binary to ternary mix, while maintaining the same replacement level, can potentially achieve a slight improvement in the concrete's permeability, despite the observation that this effect was not found to be statistically significant for the mixes investigated. Further investigation into binder properties such as mineral composition, heat of hydration, particle size distribution, degree of pozzolanic behaviour, etcetera,

were not considered in this study. For this reason, a further investigation is recommended as it could shed more light on the uncertainties which emerged in this section.

4.2.8 Comparison of the same binder replacement level

Figure 4-15 and Figure 4-16 illustrate a comparison of the different binders at the same replacement percentage levels in terms of k-permeability and OPI values respectively. The binders fly ash, blast-furnace slag, Corex slag and limestone, denoted as FA, BS, CS, and L respectively were investigated. Statistical analysis results are shown in Table 4-8. Detailed results are shown in Appendix C.

Observations taken from Figure 4-15 and Figure 4-16 showed that the inclusion of the latent hydraulic binders BS and CS mixes had the greatest positive effect on the permeability performance for replacement levels of 20-50% in comparison to the other mixes. This occurrence could possibly be attributed to the reactive nature of the different binders. However, this requires a chemical analysis which lies outside of this study. However, it should be considered in a future study.

Despite permeability superiority of the latent hydraulic binders, the statistical analysis results in Table 4.8 showed that this superiority is not entirely statistically significant. When comparing BS to the FA mixes, its performance is only generally significant (with the exception of 40 FA) for a w/b ratio of 0,65 whereas for a w/b ratio of 0,50, the comparison is only insignificant after a replacement level of 40%. No clear trend of a statistical nature could be identified for comparative purposes between CS and FA. This could be attributed to the high variability.

Despite L being an inert filler, the statistical analysis results showed that in certain cases mixes were insignificant when compared to L. Generally, results obtained with mixes containing slag were statistically significantly different, in comparison to the results obtained with mixes containing L. This was to be expected because L does not have any chemical function in the concrete. It is interesting to note that for both w/b ratios, differences in results obtained with L and FA were considered statistically insignificant. Although FA has chemical attributes (pozzolanic in nature), which can contribute to improving permeability, it remained similar in permeability performance to limestone. However, FA will continue to react if cured for longer, by contrast to L, resulting in a long-term improvement in permeability.

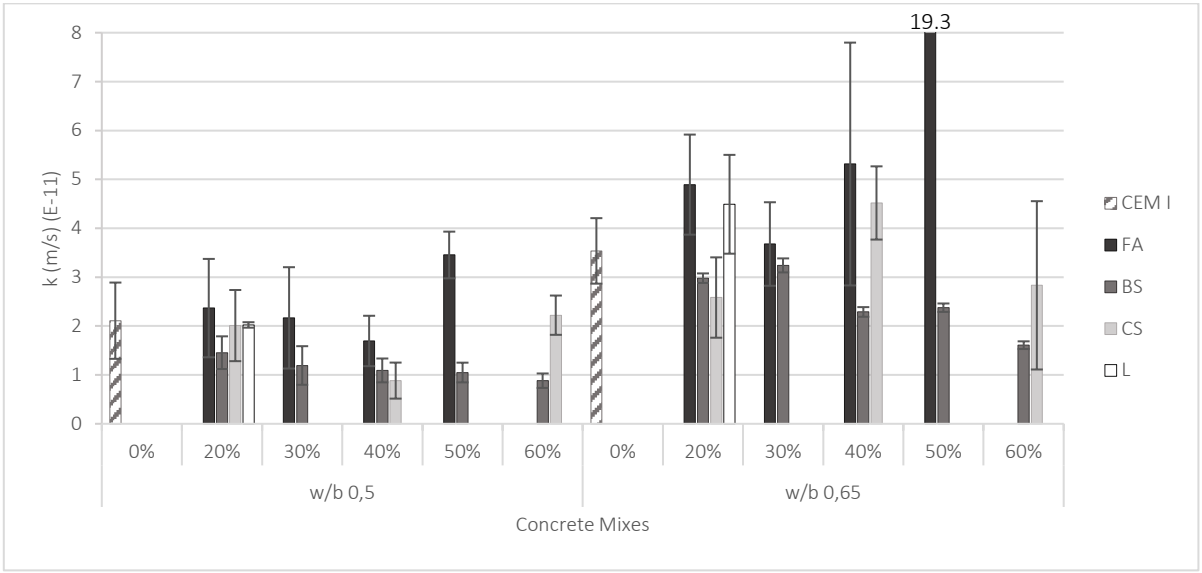

Figure 4-15: k-permeability results of binders with the same replacement levels

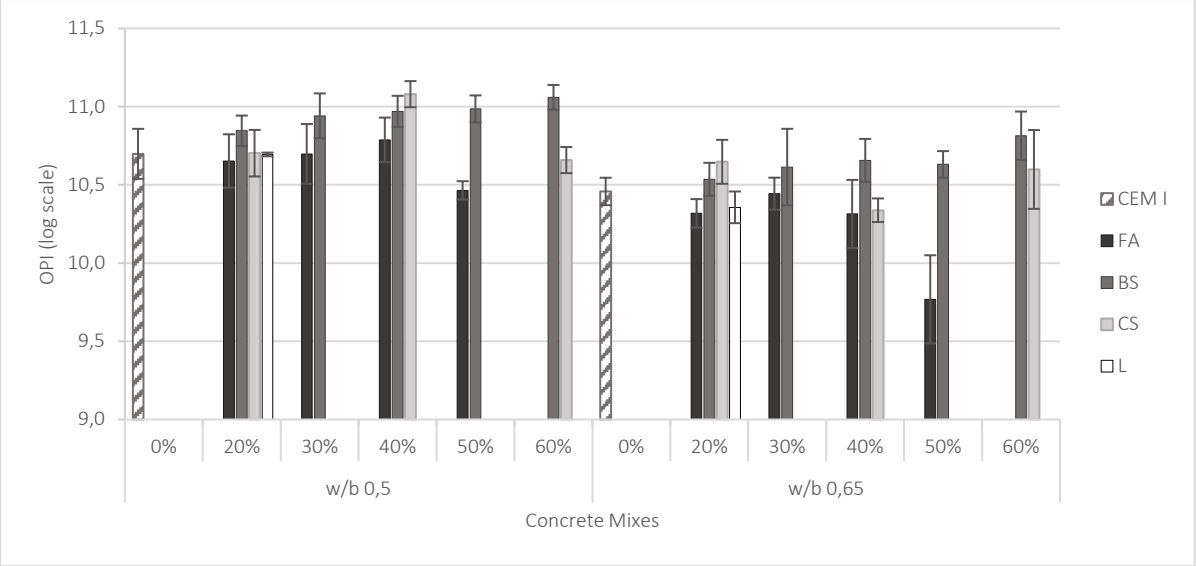

Figure 4-16: OPI results of binders with the same replacement levels

Despite permeability superiority of the latent hydraulic binders, the statistical analysis results in Table 4.8 showed that this superiority is not entirely statistically significant. When comparing BS to the FA mixes, its performance is only generally significant (with the exception of 40 FA) for a w/b ratio of 0,65 whereas for a w/b ratio of 0,50, the comparison is only insignificant after a replacement level of 40%. No clear trend of a statistical nature could be identified for comparative purposes between CS and FA. This could be attributed to the high variability.

Despite L being an inert filler, the statistical analysis results showed that in certain cases mixes were insignificant when compared to L. Generally, results obtained with mixes containing slag were statistically significantly different, in comparison to the results obtained with mixes containing L. This was to be expected because L does not have any chemical function in the concrete. It is interesting to note that for both w/b ratios, differences in results obtained with L and FA were considered statistically insignificant. Although FA has chemical attributes (pozzolanic in nature), which can contribute to improving permeability, it remained similar in permeability performance to limestone. However, FA will continue to react if cured for longer, by contrast to L, resulting in a long-term improvement in permeability.

Table 4-8: Statistical analysis for mixes with the same replacement levels

Type	20 FA	20 BS	20 CS	20 FA	20 BS	20 CS
	w/b 0,50			w/b 0,65		
20 BS	O			X		
20 CS	O	O		X	O	
20 L	O	X	O	O	X	X
	30 FA			30 FA		
30 BS	O			O		
	40 FA	40 BS		40 FA	40 BS	
40 BS	O			X		
40 CS	X	O		O	X	
	50 FA			50 FA		
50 BS	X			X		
	60 BS			60 BS		
60 CS	X			O		

4.2.9 Influence of commercial products

Figure 4-17 and Figure 4-18 illustrate the influence of the commercial concrete mixes in terms of k-permeability and OPI values respectively. The commercial products tested were CEM II A-L 52,5N, and CEM II B-M 42,5N – referred to as A-L and B-M respectively. Statistical analysis of these results is shown in Table 4-9. Detailed results are shown in Appendix C.

Observations made of Figure 4-17 and Figure 4-18 show a minor decrease in permeability of A-L in comparison to the control for both w/b ratios. The statistical analysis results in Table 4-9 interprets this minor decrease as having no statistical significance difference. Thus, the null hypothesis was not rejected.

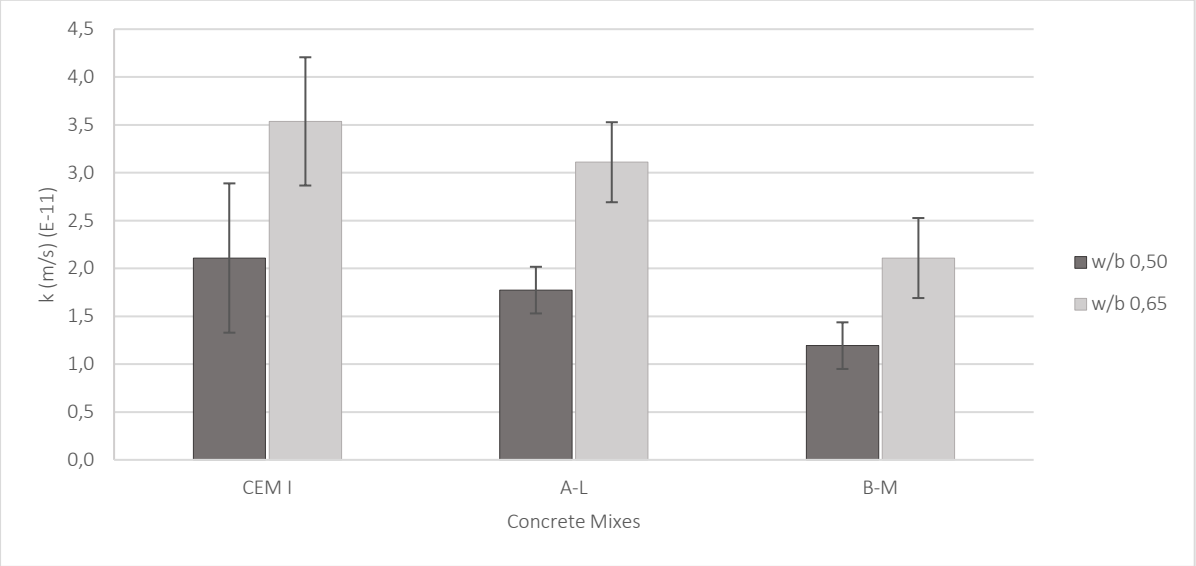

Figure 4-17: k-permeability of commercial concrete mixes

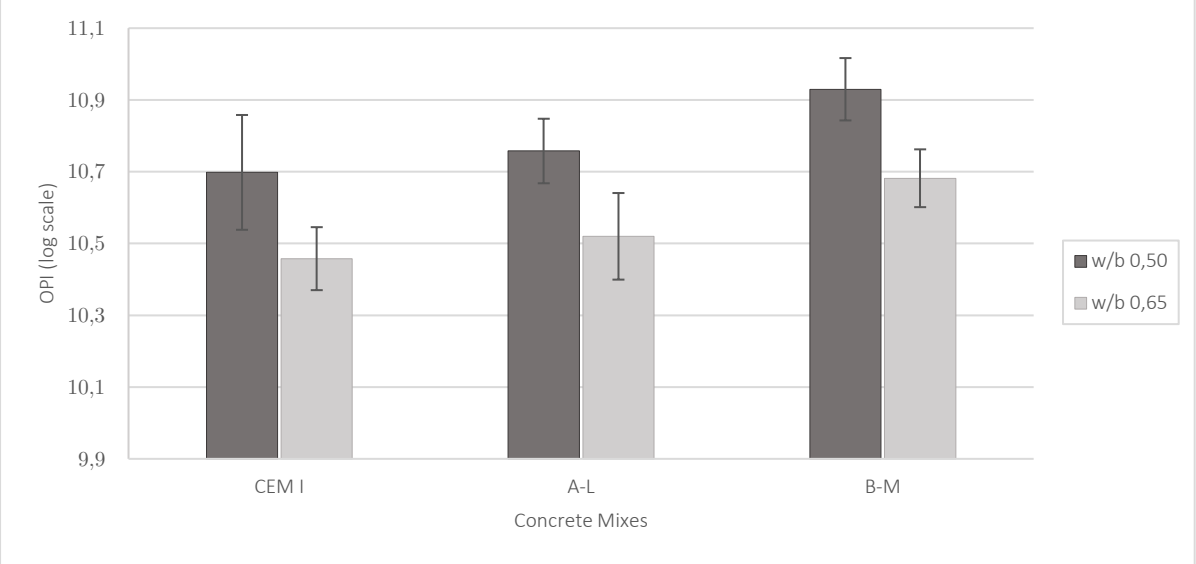

Figure 4-18: OPI results of commercial concrete mixes

For the comparison between B-M and the control mix (CEM I), observations were derived from Figure 4-17 and Figure 4-18, which showed a decrease in permeability for the B-M mixes of both w/b ratios. A similar decreasing trend was observed in study conducted by Mukkadam (2015). For w/b ratios of 0,40 and 0,50 a decrease in permeability was noted in the usage of B-M, in comparison to the control

mix. However, for 0,65 there was an increase in permeability, which contrasts the results obtained in this study. It is suspected that the reactivity of the CS component of the cement and the alkali intensity were not sufficiently adequate to contribute towards the decrease in permeability.

The Rank-sum test is based on ranking a set of observations or results from both samples that are being compared. Because the sample size of the OPI test was relatively small (four specimens per sample), there was a higher likelihood of this test accepting the null hypothesis than would have been the case with the t-test. The only way the Rank-sum test will reject the null hypothesis is if all the test results from one sample are either higher or lower than those from the other. In other words, there can be no overlap between the four results from the two mixes being compared. By contrast, the t-test uses the actual value of the test results and the variances in the samples for an evaluation of the size of the differences between results (Mukadam, 2014). Owing to this, it can be concluded that there is a significant difference between these two mixes.

Table 4-9: Statistical analysis for commercial mixes

Type	CEM I	CEM I
	w/b 0,50	w/b 0,65
A-L	O	O
B-M	X[1]/O[2]	X

B-M nominally consists of 8% L and 25% CS, hence factors affecting the permeability performance derive from the synergistic combination of both binders. Possible reasons for the decrease in permeability in relation to the inclusion of CS are similar to those relating to BS as they are both latent hydraulic binders and are similar in chemical composition.

Both the chemical and the physical properties contribute to a decrease in permeability. In an adequate alkaline environment, CS can produce hydration-like cementing products, refining the concrete's pore structure. Moreover, CS has finer particles than PC, thus contributing to the fine filler effect. Additionally, limestone can further improve the permeability performance via the fine filler and heterogeneous nucleation attributes.

4.3 Carbonation depth

Presented in this section is a discussion of the accelerated carbonation test results that were taken at 6, 9 and 12 weeks despite the fact that only the '12 weeks' results are shown in graph form. The error bars on the graphs represent first order standard deviation (STDV). The discussion begins with a validity assessment of the accelerated carbonation results, through an investigation into the carbonation coefficient results. Thereafter, the focus shifts to the influence of the w/b ratios and the various binders at different replacement levels. Also incorporated is an investigation of ternary mixes, a comparison of the transition from binary to ternary mixes and the influence of different binder types. These results are supplemented with a statistical analysis using the t-test. More detailed results are shown in Appendix D.

4.3.1 Carbonation coefficient

Table 4-10 shows the average carbonation coefficient calculated from the three measurements taken at 6, 9 and 12 weeks. The calculation of the carbonation coefficient (A) was done using Equation 4-1, which is a variation of Equation 2-9. Thereafter the standard deviation (S.D) and coefficient of variation (CoV) are shown for each concrete mix.

$$A = \frac{x}{\sqrt{t}} \quad (4\text{-}1)$$

Section 2.4.4.1 mentioned that carbonation is mainly governed by the internal relative humidity (RH), the amount of carbonatable material, external exposure conditions and carbon dioxide concentration. These factors are taken into account when determining the carbonation coefficient. Therefore, if the carbonation coefficient value changes significantly, it suggests that one of the variables affecting carbonation were altered. The accelerated carbonation specimens were tested in a controlled environment (65% RH, temperature of 23°C and CO_2 concentration of 2%) and thus a significant change to the carbonation coefficient value among the testing days (6,9 and 12 weeks) suggests that there was a change in internal humidity meaning that the carbonation front has impeded the drying front. Additionally, it could mean that there was an occurrence of hydration or pozzolanic activity.

Table 4-10: 12-week Carbonation depth (x) and carbonation coefficient (A) results for concrete mixes of different w/b ratios

Type	$x_{12\ weeks}$	A	S.D	CoV	$x_{12\ weeks}$	A	S.D	CoV
	(mm)	(mm/√t)		%	(mm)	(mm/√t)		%
	w/b 0,50				w/b 0,65			
CEM I	6,5	0,70	0,05	6,6	10,0	1,14	0,05	4,1
20 FA	9,4	1,04	0,03	2,5	14,9	1,69	0,16	9,4
30 FA	11,7	1,35	0,14	10,6	19,7	2,20	0,13	5,8
40 FA	14,1	1,64	0,17	10,6	23,3	2,78	0,26	9,2
50 FA	20,4	2,48	0,23	9,1	32,7	3,74	0,15	4,1
20 BS	8,7	0,92	0,04	4,6	13,4	1,48	0,04	2,7
30 BS	9,1	1,05	0,06	5,3	14,4	1,75	0,17	9,7
40 BS	10,0	1,14	0,09	7,7	16,4	1,84	0,11	5,9
50 BS	10,3	1,10	0,06	5,9	18,7	2,13	0,11	5,0
60 BS	14,2	1,59	0,05	23,	21,4	2,50	0,15	6,0
20 CS	6,2	0,62	0,08	13,4	12,5	1,44	0,11	8,0
40 CS	6,7	0,75	0,02	2,1	14,3	1,65	0,08	4,8
60 CS	9,3	1,07	0,06	5,2	18,3	2,00	0,12	6,0
10 L	7,4	0,75	0,05	7,2	14,8	1,62	0,02	1,5
20 L	9,3	1,02	0,04	4,0	16,5	1,81	0,09	4,9
A-L	6,5	0,64	0,09	13,6	10,7	1,23	0,11	9,0
B-M	6,4	0,69	0,02	2,4	14,4	1,52	0,05	3,0
SF 5	7,2	0,72	0,10	13,2	10,8	1,22	0,06	5,2
SF FA	9,6	1,08	0,04	3,7	17,6	2,09	0,16	7,7
SF BS	9,00	1,00	0,05	4,9	13,5	1,59	0,11	7,2
SF CS	8,33	0,91	0,01	0,7	10,5	1,22	0,14	11,4

Based on the results displayed in 4-10., no trend was apparent from the measured values (i.e. A). It was deduced that the drying front had minimal or no effect on the carbonation front, that is, there was no intersection between the two fronts. It was also surmised that no further hydration or pozzolanic reactions had taken place in the time between the measurements (6, 9 and 12 weeks).

4.3.2 Influence of w/b ratio

The accelerated carbonation results measured at 12 weeks for w/b ratios of 0,5 and 0,65 are presented in Table 4-10. As expected, the results showed that the w/b ratio is inversely proportional

to the carbonation depth. This correlation is imputed to the amount of the calcium hydroxide (CH) produced with a change in w/b ratio, as indicated in Section 2.4.2.3.

The progression of the carbonation front is the result of the reaction between carbonation dioxide (CO_2) and CH. As a result, CH can be considered as a sacrificial layer opposing the carbonation front's migration. As mentioned, CH is formed in the concrete because of cement hydration. And the degree of hydration is a function of the w/b ratio of the concrete. Therefore, altering the w /b ratio influences the rate of the carbonation front. Also, the w/b ratio influences the concrete's permeability as they are inversely proportional to each other: permeability affects the progression carbonation front as this concrete property determines the ease with which CO_2 can penetrate the interconnected pores of the concrete.

4.3.3 Influence of FA

Figure 4-19 illustrates the influence of Fly Ash (FA) on the 12-week carbonation depth from 20 to 50% replacement levels in 10% increments (referred to as 20 – 50%). The statistical results from the t-test are displayed in Table 4-11. Detailed results of the carbonation results are shown in Appendix E.

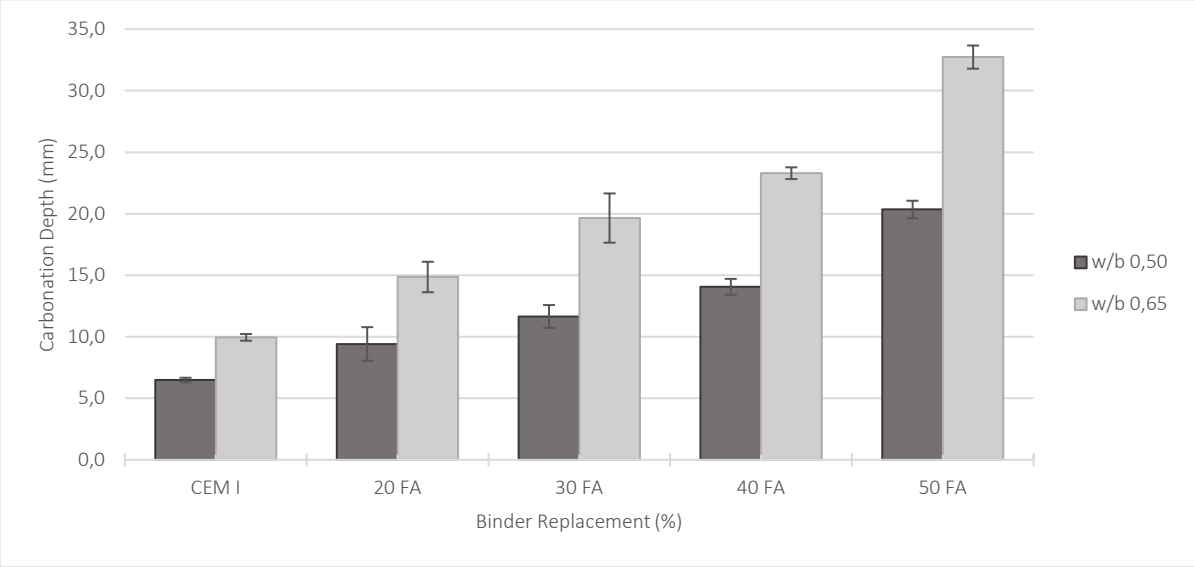

Figure 4-19: 12-week accelerated carbonation results of FA mixes

An analysis of Figure 4-19 showed a clear increase in carbonation depth with an increase in FA replacement level, as expected. The t-test statistical analysis results presented in Table 4-11 complement this as the results reveal that the carbonation depth readings amongst all the FA mixes were all statistically significant for both w/b ratios. The augmentation of the t-test results indicates a clear correlation between the inclusion of FA and carbonation depth for the specific regime used in this study.

Table 4-11: Statistical analysis for FA 12-week accelerated carbonation results

Type	CEM I	20 FA	30 FA	40 FA	CEM I	20 FA	30 FA	40 FA
	w/b 0.50				w/b 0,65			
20 FA	X				X			
30 FA	X	X			X	X		
40 FA	X	X	X		X	X	X	
50 FA	X	X	X	X	X	X	X	X

The relationship between FA and carbonation depth is mainly attributable to the dilution effect. By increasing the FA content, the cement content in the concrete is decreased. Consequently, the carbonation resistance lessens as the amount of CH has reduced. The likelihood exists that the pozzolanic nature may have influenced the carbonation progression due to its consumption of CH.

4.3.4 Influence of BS

Figure 4-20 illustrates the influence of blast-furnace slag (BS) on the carbonation depth from 20 to 60% replacement levels in 10% increments (referred to as 20-60% BS). The statistical results from the t-test are displayed in Table 4-12. Detailed results of the carbonation results are shown in Appendix E.

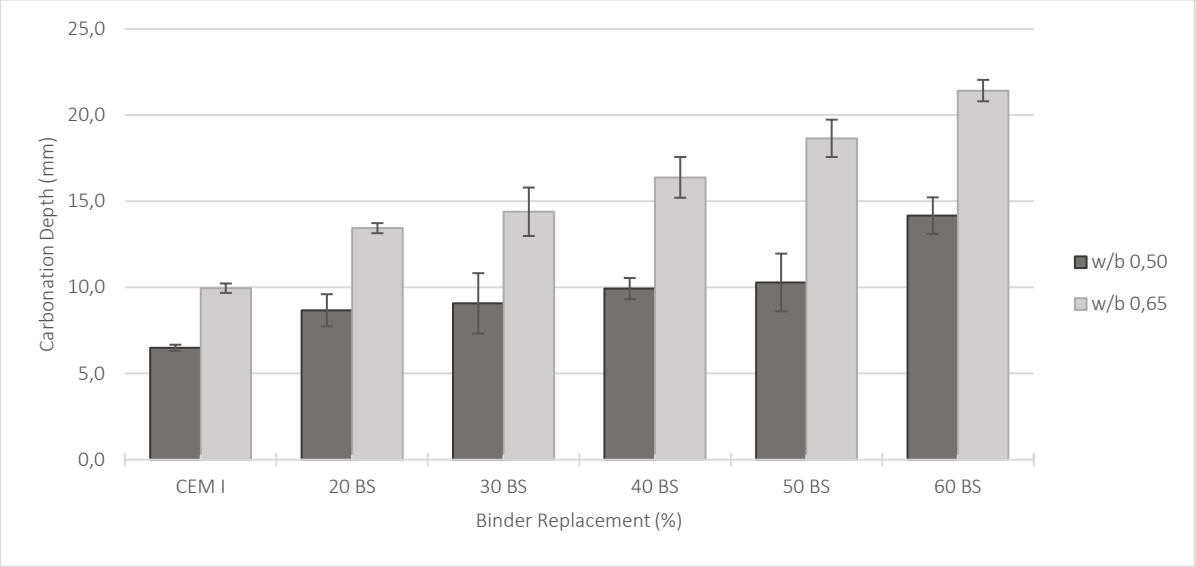

Figure 4-20: 12-week accelerated carbonation results of BS mixes

An assessment of Figure 4-20 renders a general increase in carbonation depth with the expected increase in BS. The results from the t-test presented in Table 4-12 show that the carbonation results for the BS mixes in both w/b ratios are statistically significant in comparison to the control mixes (CEM I). This indicates that carbonation depth is directly proportional to the increase in BS replacement. However, the significance among the BS concretes is not entirely insignificant.

Table 4-12: Statistical analysis for BS 12-week accelerated carbonation results

Type	CEM I	20 BS	30 BS	40 BS	50 BS	CEM I	20 BS	30 BS	40 BS	50 BS
	w/b 0,50					w/b 0,65				
20 BS	X					X				
30 BS	X	O				X	O			
40 BS	X	X	O			X	X	O		
50 BS	X	O	O	O		X	X	X	X	
60 BS	X	X	X	X	X	X	X	X	X	X

In reading Table 4-12, it is interesting to note the decrease in w/b ratio leads to more mixes being statistically insignificant to one other. Lowering the w/b ratio increases the sacrificial CH layer concentration and improves the concrete's permeability, which are both attributes governed by altering of the w/b ratio. Therefore, the progression rate of the carbonation font will be slower and subsequently decreases the difference in carbonation depth between the BS concrete mixes leading to some mixes being statistically insignificant.

BS's chemical and physical attributes can positively contribute to the carbonation resistance because as explained in Section 2.5.2.1, BS is a latent hydraulic binder which is activated in an alkaline environment. In turn, it produces hydration-like cementing products, refining the concrete's pore structure. Moreover, it is an effective fine filler. However, the dilution effect is assumed to be the dominating contribution to the carbonation depth performance.

4.3.5 Influence of CS

Figure 4-21 illustrates the influence of Corex slag (CS) on the carbonation depth at 12 weeks from 20 to 60% replacement in 20% increments (referred to as 20 - 60% CS). The statistical results from the t-test are displayed in Table 4-13. Detailed results are shown in Appendix E.

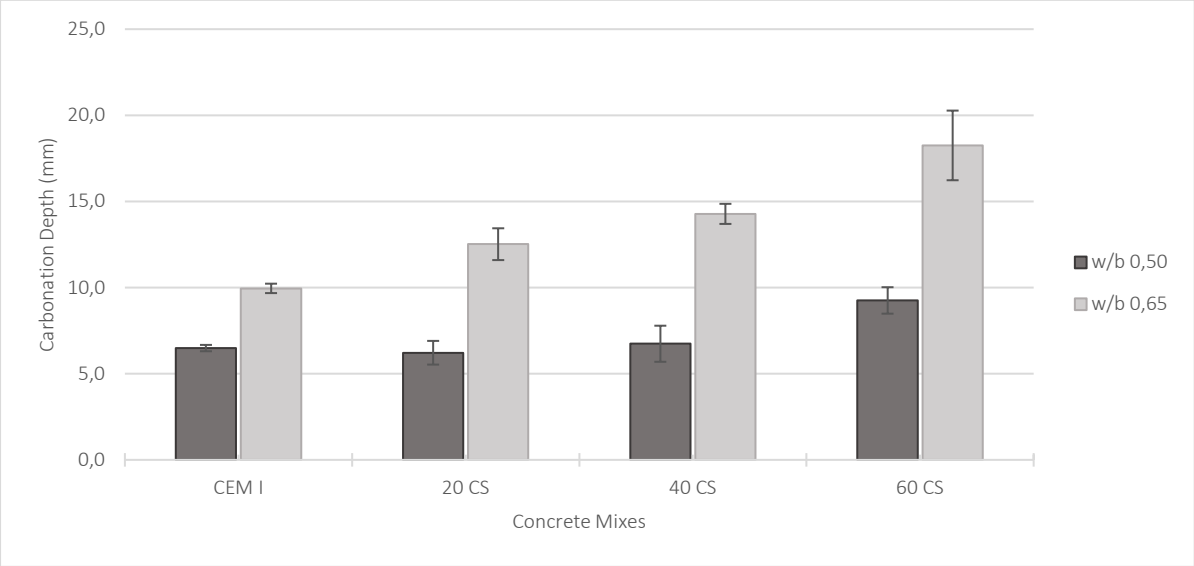

Figure 4-21: 12-week accelerated carbonation results of CS mixes

An evaluation of Figure 4-21 revealed a general increase in carbonation depth with the expected increase in CS. The results from the t-test presented in Table 4-13 showed that the results of the mix with a w/b ratio 0,65 are statistically significant in relation to one another including the control mix. This further indicates a definite increasing trend in carbonation depth with respect to CS replacement level. Yet the same cannot be said for the w/b 0,50 mixes as the statistical significance was observed only at the introduction of 60% CS replacement level.

Table 4-13: Statistical analysis for CS 12-week accelerated carbonation results

Type	CEM I	20 CS	40 CS	60 CS	CEM I	20 CS	40 CS	60 CS
	w/b 0,50				w/b 0,65			
20 CS	O				X			
40 CS	O	O			X	X		
60 CS	X	X	X		X	X	X	

As stated in Section 2.5.2.2, CS is a latent hydraulic binder which is activated in the presence of an alkaline environment. In turn it produces hydration-like cementing products, refining the concrete's pore structure. Lowering the w/b ratio increases the sacrificial CH layer concentration and improves the concrete's permeability. The combination of the pore refinement and the more concentrated CH sacrificial layer provided greater resistance to the inward diffusion of carbon dioxide into the

concrete, consequently slowing down the rate of carbonation leading to some mixes being statistically insignificant.

4.3.6 Influence of L

Figure 4-22 illustrates the influence of limestone (L) on the carbonation depth for replacement level of 10 to 20% (referred to as 10 and 20 L). The statistical results from the t-test are displayed in Table 4-14. Detailed results are shown in Appendix E.

An analysis of Figure 4 22 revealed a clear increase in carbonation depth with an increase in L replacement level, as predicted. The results from the t-test presented in Table 4-14 are in agreement with the observation analysis. All the L mixes as well as the control mixes, are statistically significant amongst one another. This indicates that there was a clear decreasing trend in carbonation depth with the inclusion of L.

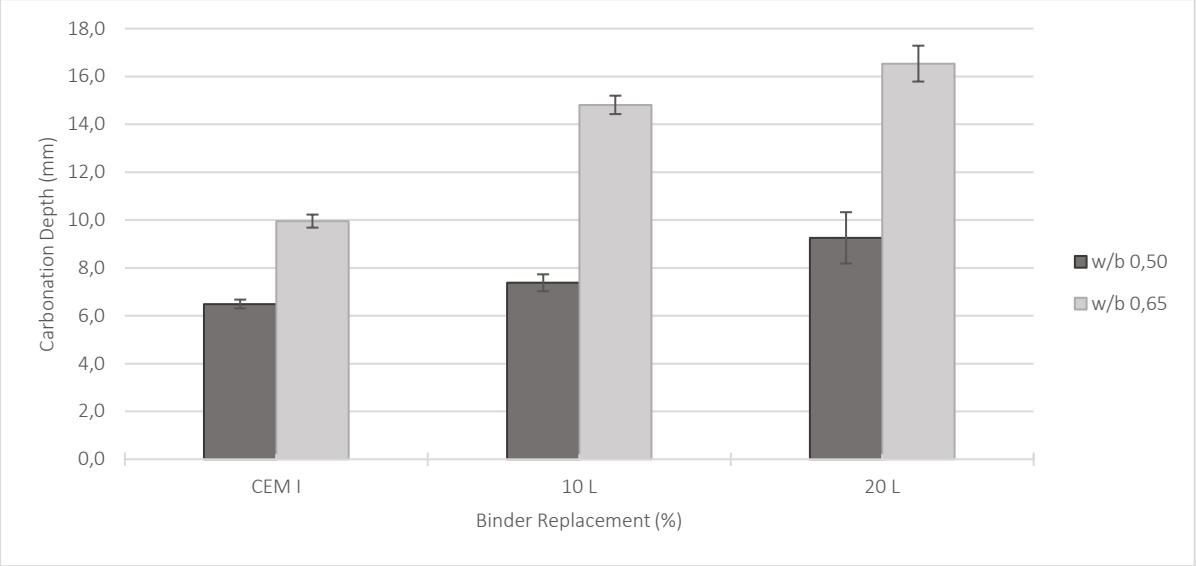

Figure 4-22: 12-week accelerated carbonation results of L mixes

An analysis of Figure 4-22 revealed a clear increase in carbonation depth with an increase in L replacement level, as predicted. The results from the t-test presented in Table 4-14 are in agreement with the observation and statistical analysis. All the L mixes as well as the control mixes, are statistically significant amongst one another. This indicates that there was a clear decreasing trend in carbonation depth with the inclusion of L.

Table 4-14: Statistical analysis for L 12-week accelerated carbonation results

Type	CEM I	10 L	CEM I	10 L
	w/b 0,50		w/b 0,65	
10 L	X		X	
20 L	X	X	X	X

L used in this study was considered chemically inert and used mainly as a fine filler and reaction nucleation point which can potentially increase the carbonation resistance. However, the trend of increasing carbonation depth with the introduction of L is mainly attributed to the dilution effect. Replacing cement with L lessens the amount of CH being reduced. This weakens the sacrificial CH layer which leads to an increase in carbonation as less CH is available for this reaction. Its fine filler

and reaction nucleation effects can potentially increase the resistance of carbonation progression, but this was no observed in this study.

4.3.7 Influence of SF and ternary mixes

Figure 4-23 illustrates the influence of silica fume (SF) and ternary mixes on the carbonation depth at 12 weeks. The ternary mixes all consist of 5% SF and either fly ash, blastfurnace slag or Corex slag, referred to as SF FA, SF BS and SF CS respectively in this section. The statistical results from the t-test are shown in Table 4-15. Detailed results are shown in Appendix E.

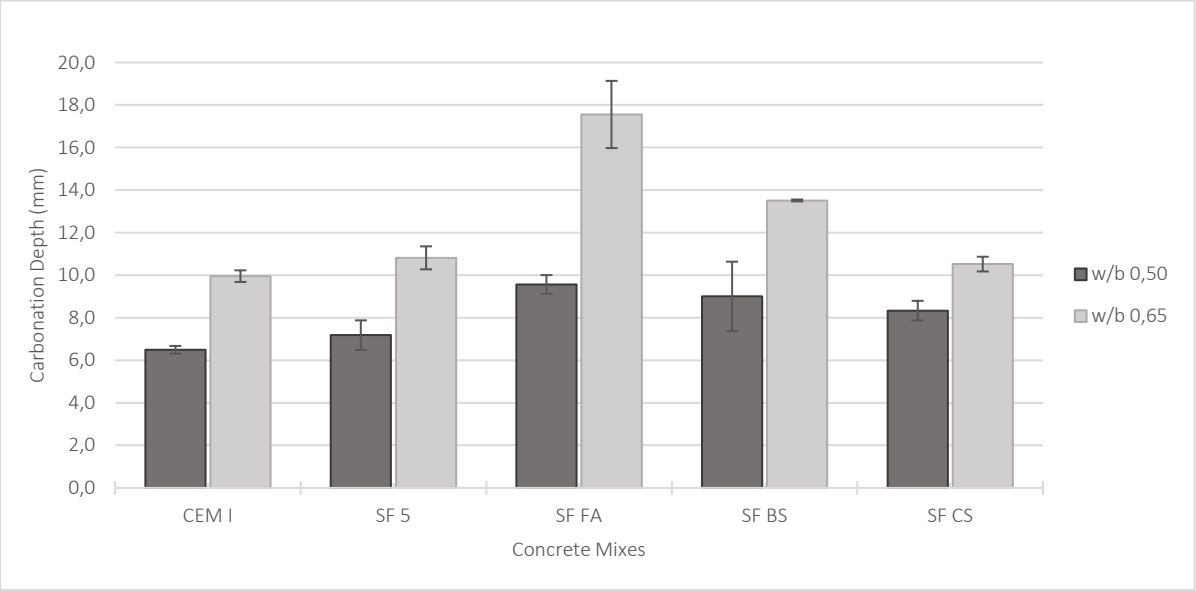

Figure 4-23: 12-week accelerated carbonation results of SF and ternary mixes

Comparative inspection of the SF and control mix (CEM I) showed a slight increase in carbonation depth with the inclusion of SF, as expected. The statistical analysis results depicted in Table 4-15 show that the increase in carbonation is only statistically significant for the mixes with a w/b of 0,65.

Besides the decrease in w/b ratio, it is surmised that SF's physical and chemical characteristics might also play a role in establishing the insignificance between the control mix and SF for the w/b ratio of 0,5. As explained previously, SF is considered to be a highly reactive pozzolanic material due to its high amorphous silicon dioxide content. In addition, SF particles are extremely small, making it an effective fine filler. Both aspects aid in refining the concrete structure, thus increasing its resistance to the onset of CO_2 diffusion through the interconnectedness of the pores.

Table 4-15: Statistical analysis for SF and ternary mixes 12-week accelerated carbonation results

Mix	CEM I	SF	SF FA	SF BS	CEM I	SF	SF FA	SF BS
	w/b 0,50				w/b 0,65			
SF	O				X			
SF FA	X	X			X	X		
SF BS	X	O	O		X	X	X	
SF CS	X	X	X	O	X	O	X	X

Figure 4-23 showed a general increase of the ternary mixes in carbonation depth with the transition from SF 5 to the ternary mixes. The t-test supplemented this observation as its results showed a general statistical significance in carbonation depth between the SF mix and each of the ternary mixes

for both w/b ratios. This phenomenon contributes to the dilution effect due to the inclusion of another binder to the concrete mixes.

Among the ternary mixes, SF CS performed the best with respect to carbonation; followed by SF BS; and then by SF FA for both w /b ratios. The t-test showed statistical significance in carbonation depth amongst the mix with a w/b ratio of 0,65. However a statistical insignificance was generally observed for the w/b ratio of 0,5. It was assumed to be attributed to the reactive nature of the binders. However, this requires a chemical analysis which lies outside of this study. However, it should be considered in a future study.

4.3.8 Binary versus ternary mixes

Figure 4-24 illustrates a comparison between the binary and ternary mixes on the carbonation depth at 12 weeks. The binary mixes constitute 30% replacement (by mass) of fly ash (FA) and blastfurnace slag (BS) that is, 30 FA and 30 BS. The ternary mixes both consist of 5% silica fume (SF) and 25% of either FA or BS, referred to as SF FA and SF BS respectively. The statistical results from the t-test based on the significance between the mixes are shown in Table 4-16. Detailed results are shown in Appendix E.

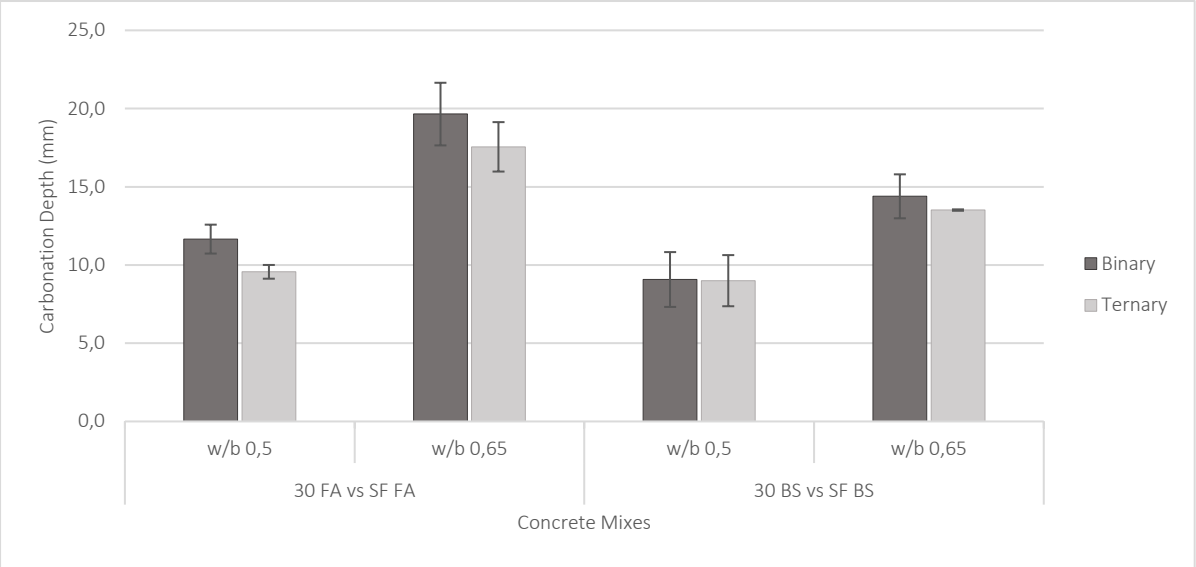

Figure 4-24: 12-week accelerated carbonation results of binary and ternary mixes

Observation of the ternary mixes in Figure 4-24, showed a general decrease in carbonation depth in the transition from a binary to a ternary mix. However, the t-test results showed that the decreasing trend in carbonation depth is statistically insignificant for both w/b ratios. The decrease in carbonation depth from the binary to ternary mixes could be attributed to the inclusion of SF. SF is an effective fine filler, which contributes to refining the concrete pore structure. Subsequently it increases the carbonation resistance. Additionally, its high pozzolanic reactive nature can produce more cementitious-like compound, further improving the pore structure. That notwithstanding, the inclusion of SF at 5% replacement was not sufficient to cause a significant effect. To draw sound conclusions in this respect, further investigation is required on the amount of carbonatable material in the mixes.

Table 4-16: Statistical analysis for binary and ternary mixes 12-week accelerated carbonation results

MIx	30 FA	30 BS	30 FA	30 BS
	w/b 0,50		w/b 0,65	
SF FA	O		O	
SF BS		O		O

4.3.9 Comparison of the same binder replacement level

Figure 4-25 illustrates a comparison between the different binders used in the study at the same replacement percentage levels on the carbonation depth at 12 weeks. The mineral admixtures fly ash, blast-furnace slag, corex slag and limestone are denoted as FA, BS, CS, and L respectively. Statistical analysis results are shown in Table 4-17. Detailed results are shown in Appendix E.

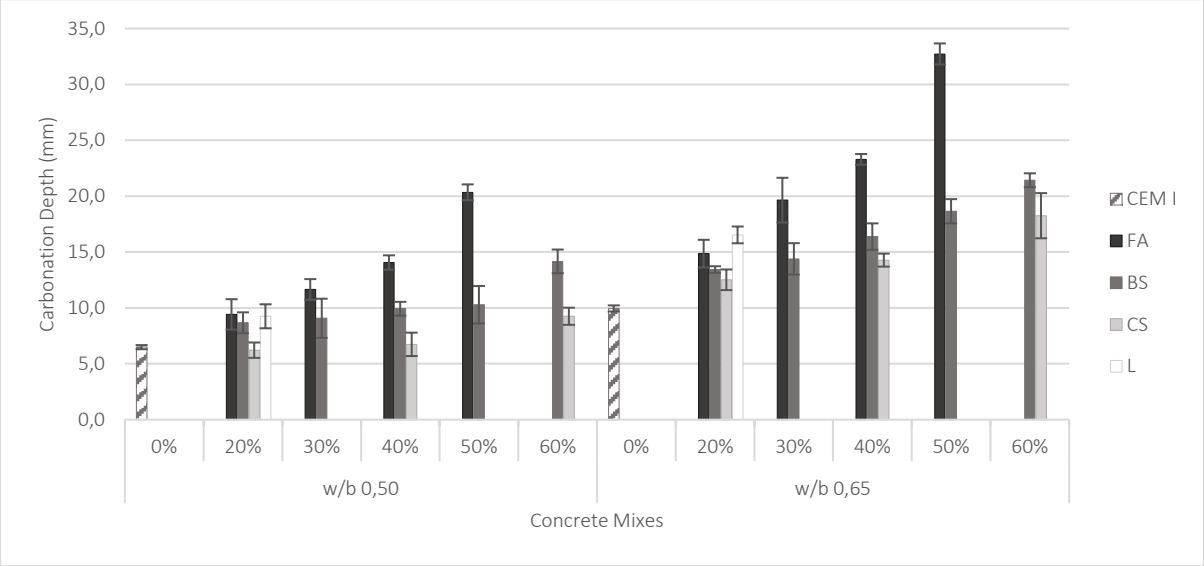

Figure 4-25: 12-week accelerated carbonation results of binders with the same replacement levels

Figure 4-25 showed that the latent hydraulic binders, BS and CS were generally superior in carbonation resistance, followed by FA and then L. It is suspected that this trend could be due to the amount of carbonatable material within the concrete. However, this requires a chemical analysis which lies outside the scope of this study. It should however be considered in a future study.

Despite carbonation resistance superiority of the latent hydraulic binders, the statistical analysis results showed no general statistical significance difference for a replacement level of 20%. However, in higher binder replacement levels, statistical significance of the carbonation resistance of the latent hydraulic binders against the others was more evident.

It is interesting to note that for both w/b ratios, the difference in results obtained from mixes containing L and FA (at 20% replacement level) was statistically insignificant. Additionally, the null hypothesis was accepted between L and BS for the w/b ratio of 0,5. This phenomenon could be due to L's fine filler attribute, refining the concrete's permeability and its lack of chemical reactivity resulting in no consumption of CH.

Table 4-17: Statistical analysis for binders with the same replacement levels for the 12-week accelerated carbonation results

Type	20 FA	20 BS	20 CS	20 FA	20 BS	20 CS
	w/b 0,50			w/b 0,65		
20 BS	O			O		
20 CS	X	X		X	X	
20 L	O	O	X	O	X	X
	30 FA			30 FA		
30 FA						
30 BS	X			X		
	40 FA	40 BS		40 FA	40 BS	
40 BS	X			X		
40 CS	X	X		X	X	
	50 FA			50 FA		
50 FA						
50 BS	X			X		
	60 BS			60 BS		
60 BS						
60 CS	X			X		

4.3.10 Influence of commercial products

Figure 4-26 illustrates the influence of commercial concrete mixes on the 12-carbonation depth. The commercial products tested were CEM II A-L 52,5N, and CEM II B-M 42,5N – referred to as B-M and A-L respectively. The statistical results from the t-test are displayed in Table 4-18. Detailed results are shown in Appendix E.

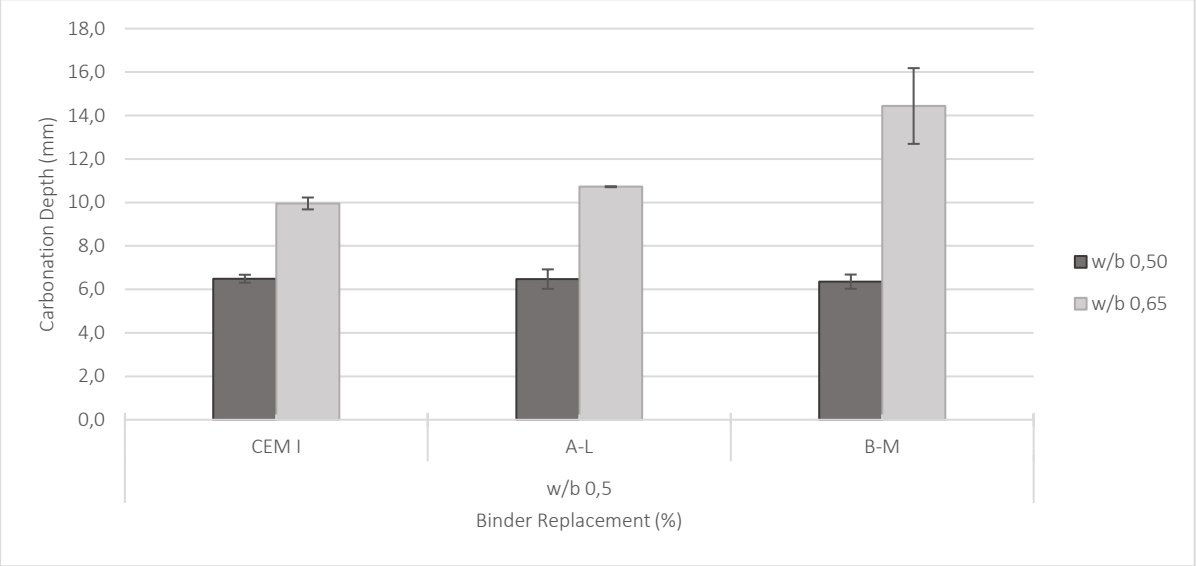

Figure 4-26: 12-week accelerated carbonation results of commercial mixes

Figure 4-26 indicates a minor increase in carbonation depth between A-L and the control mix (CEM I) for both w/b ratios. Furthermore, for the w/b 0,5 mixes, despite A-L having lower clinker content in comparison to the control, the t-test results showed that there was no statistical significance.

Table 4-18: Statistical analysis for commercial mixes 12-week accelerated carbonation results

Type	CEM I	CEM I
	w/b 0,50	w/b 0,65
A-L	O	X
B-M	O	X

Two factors would have influenced this phenomenon. The first is that the fine filler effect refining the pore structure of the concrete provided greater resistance to the diffusion of CO_2. The second is that the nucleation effect accelerated the hydration subsequently producing more CH and thus improving the sacrificial layer. Also, the decreasing w/b consequently produced additional CH products.

B-M contains both L and CS (nominally 8% and 25% respectively), although the statistical insignificance among some of the BS mixes could be attributed to the chemical nature of CS and the change in w/b ratio. As a latent hydraulic binder, CS is activated in the presence of an alkaline environment. In turn it produces hydration-like cementing products, refining the concrete's pore structure while decreasing the w/b ratio. This process results in the increase in CH concentration which may simultaneously hinder the progression of carbonation. The combination of the pore refinement and the more concentrated CH sacrificial layer provides greater resistance to the inward diffusion of carbon dioxide into the concrete, consequently slowing down the rate of carbonation. The addition of L contributes to the refinement of the pore structures through the fine filler and the nucleation effect.

4.4 Correlation between carbonation coefficient and permeability

The deterioration of concrete is affected by the ease with which gases or ions of fluids can migrate through the concrete's micro-structure. Consequently, a correlation between the carbonation coefficient and permeability is expected. The current South African carbonation prediction model relies on this correlation to predict the service life of concrete structures. This section of the chapter displays the correlation between the 12-week carbonation coefficient and permeability in the form of the k-permeability and oxygen permeability index (OPI) for all the mixes used in this study. Followingly, the study focuses on the correlation between carbonation depth and individual binder types.

Figure 4-27 and Figure 4-28 illustrate the scatterplots between the 12-week carbonation coefficient plotted against the k-permeability and the OPI respectively of all the mixes conducted in this study. The linear correlation coefficient (R^2) was displayed on each of the graphs. 50% fly ash replacement concrete mix (50 FA) with a w/b ratio of 0,65 was omitted from the correlation as it was considered an outlier.

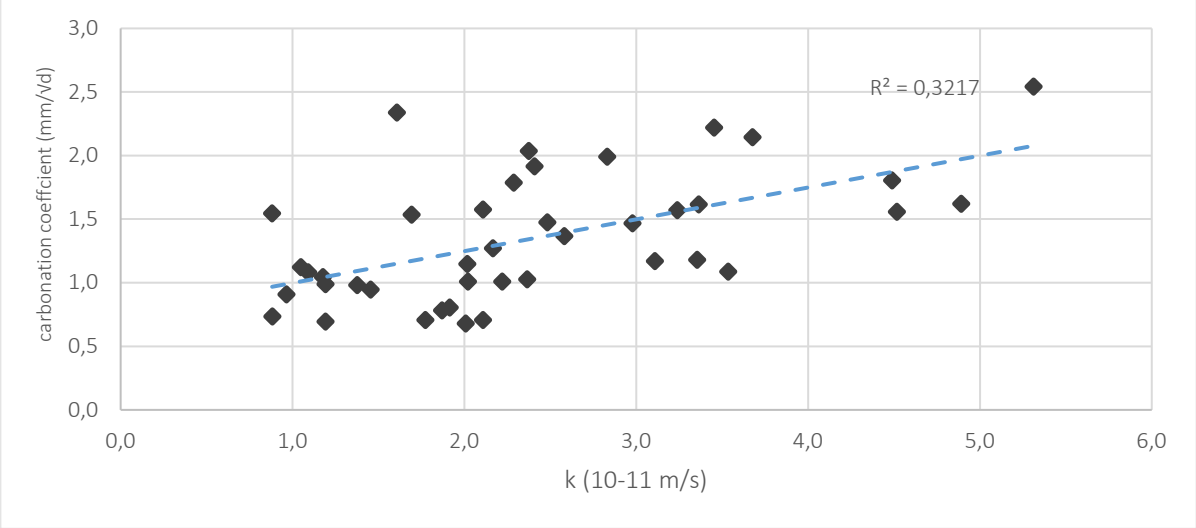

Figure 4-27: Correlation between carbonation coefficient and k-permeability

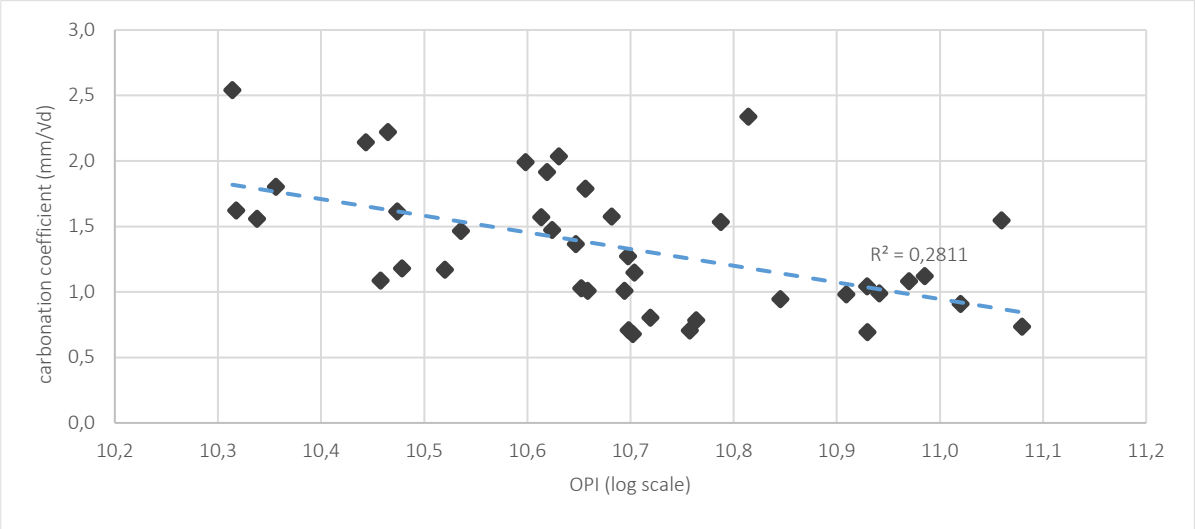

Figure 4-28: Correlation between carbonation coefficient and OPI

Observation of the scatterplots correlations could be seen. The direction of the trend showed a positive and negative association when the carbonation coefficient is plotted against k-permeability and OPI, respectively. This indicates that the decrease in permeability results in an increasing resistance to carbonation, as expected. It also indicates that the permeability results may provide a reasonable measure for carbonation performance for modern concretes despite the fact that the two variables are based on two different transport mechanisms. However, further investigation is needed to support this statement.

It was also observed that the scatter of the values was quite dispersed where results lie far from the regression line. This observation concurs with the linear correlation values (R^2) achieved which were 0,32 and 0,28 for k-permeability and OPI respectively, indicating that the regression line would provide 'poor' prediction in relation to using permeability to determine carbonation. This suggests permeability alone is not a sufficient indicator for carbonation.

The most likely reason for the weak correlation between permeability and carbonation coefficient is the variance in concrete chemistry. Carbonation is a function of the concrete chemistry and the

exposure condition (for example, humidity, temperature). Thus, the slope of the regression line may change according to the relative humidity, and amount and binder type used.

Further investigation was done to determine whether a correlation exists between carbonation coefficeint and permeability with concrete mixes of the same binder type regardless of the replacement level. The reasoning behind this investigation was that it decreases the variance in the chemistry as only one binder type is investigated. It was thus expected that the correlation between permeability and carbonation would be improved.

Figures 4-29 to 4-36 show the carbonation coefficient-permeability correlations for FA, BS, LS and CS. With the exception of CS, the graphs reflect a stronger correlation than was the case when all the concrete mixes were included. This phenomenon was particularly noticeable in the FA and L correlations as the values resemble a near straight line, indicating a strong linear relationship. This observation was in agreement with the linear correlation values (R^2) achieved, which were a maximum of 0,80 and 0,93 for FA and L respectively.

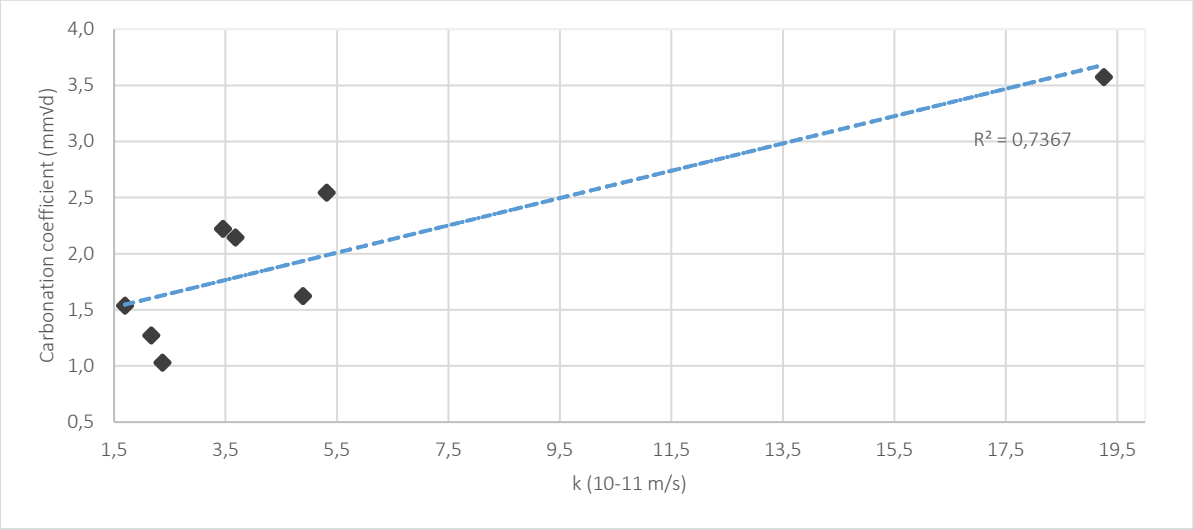

Figure 4-29: Correlation between carbonation coefficient and k-permeability for FA mixes

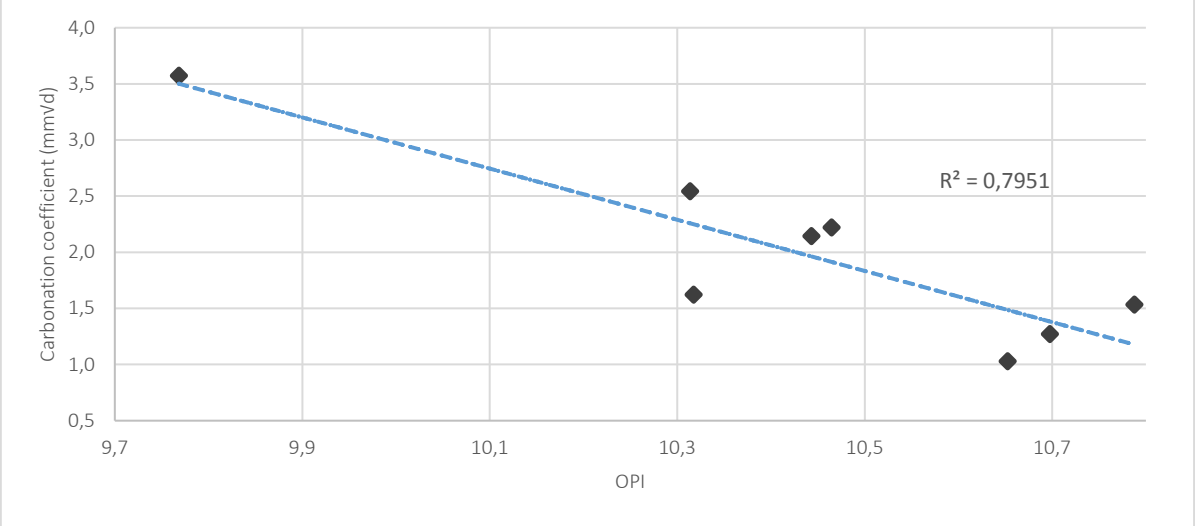

Figure 4-30: Correlation between carbonation coefficient and OPI for FA mixes

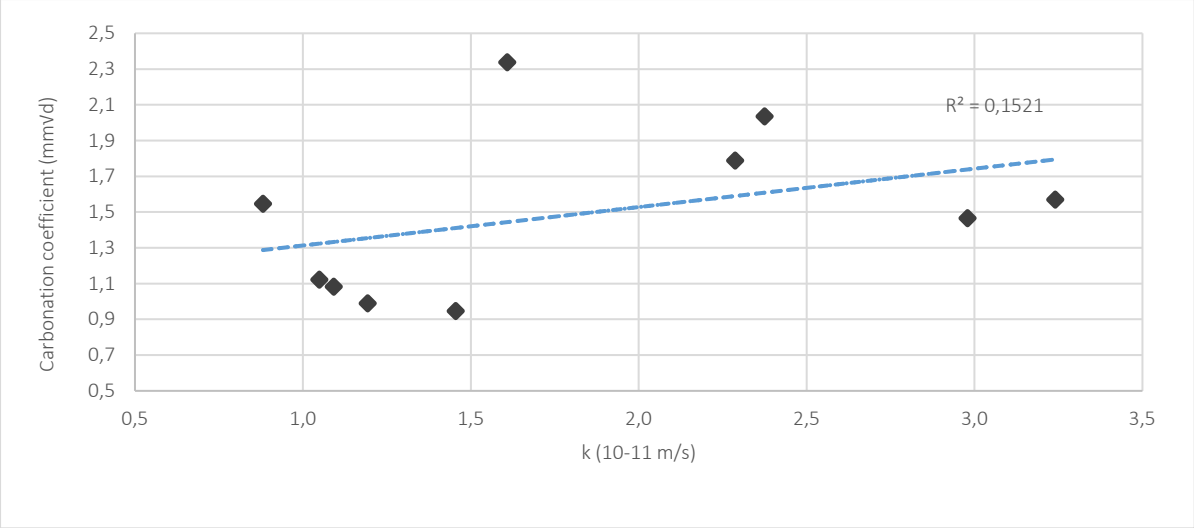

Figure 4-31: Correlation between carbonation coefficient and k-permeability for BS mixes

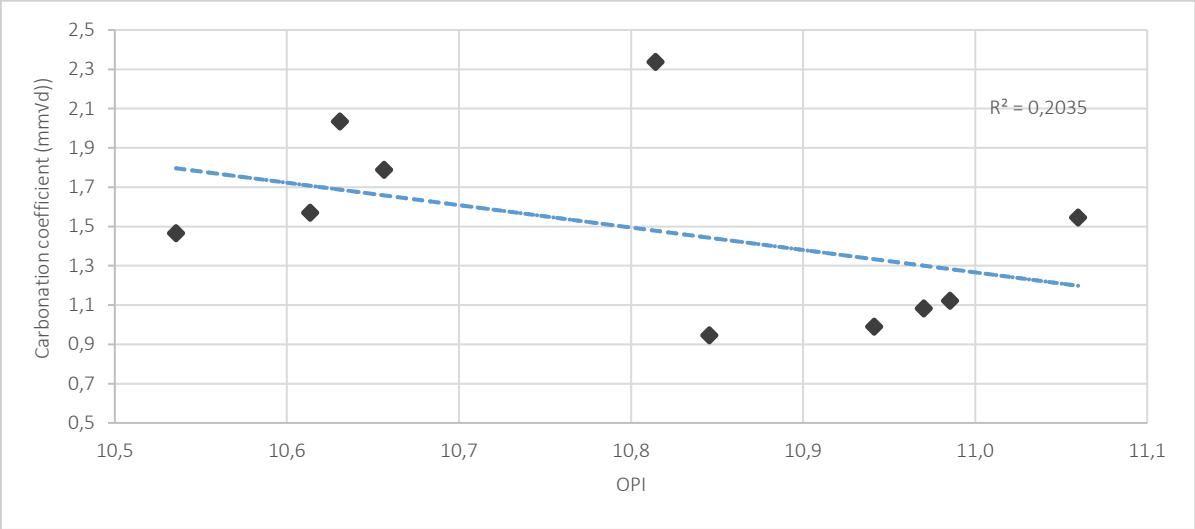

Figure 4-32: Correlation between carbonation coefficient and OPI for BS mixes

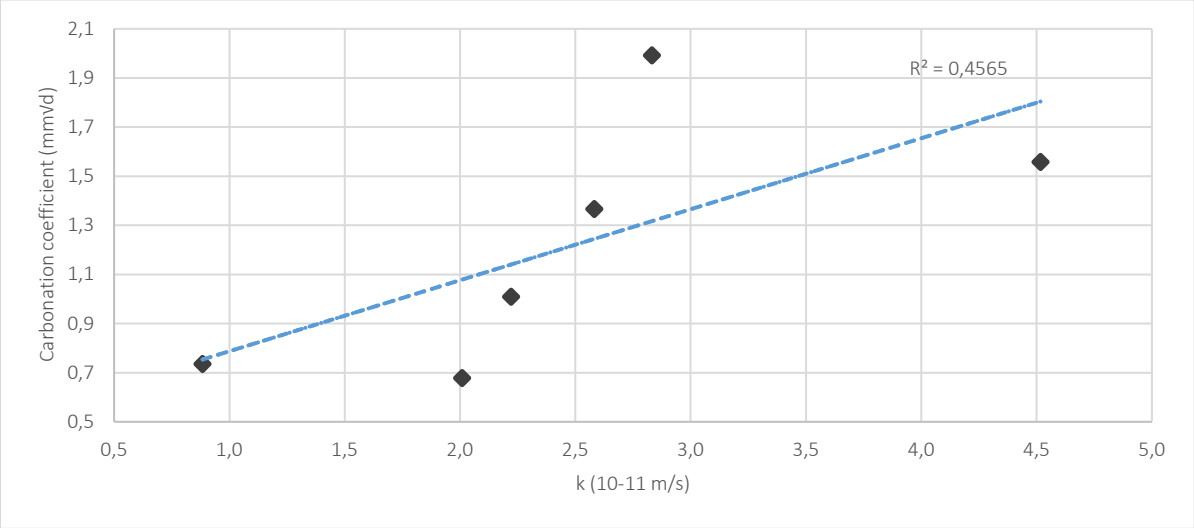

Figure 4-33: Correlation between carbonation coefficient and k-permeability for CS mixes

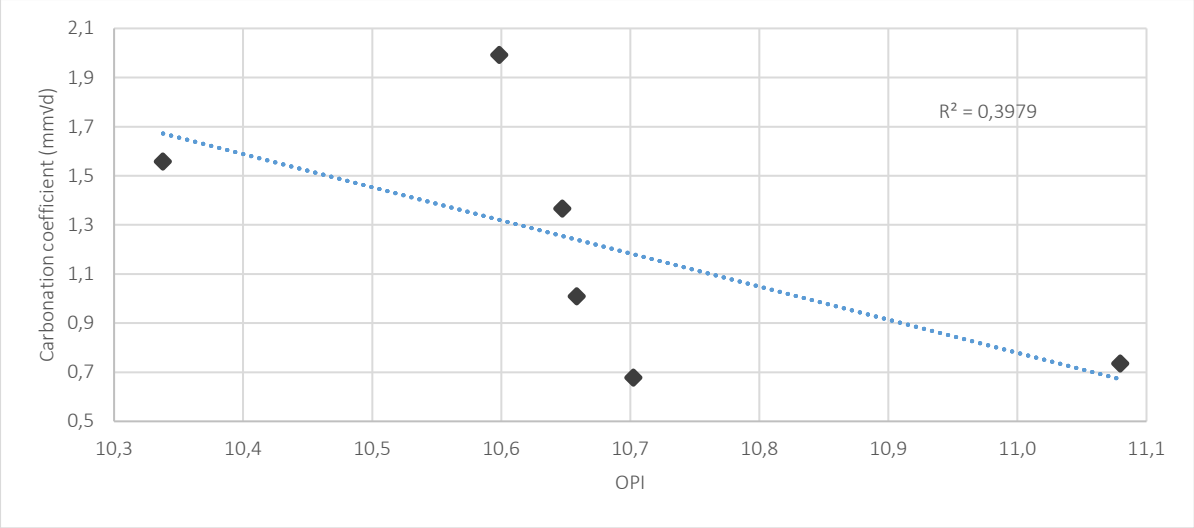

Figure 4-34: Correlation between carbonation coefficient and OPI for mixes

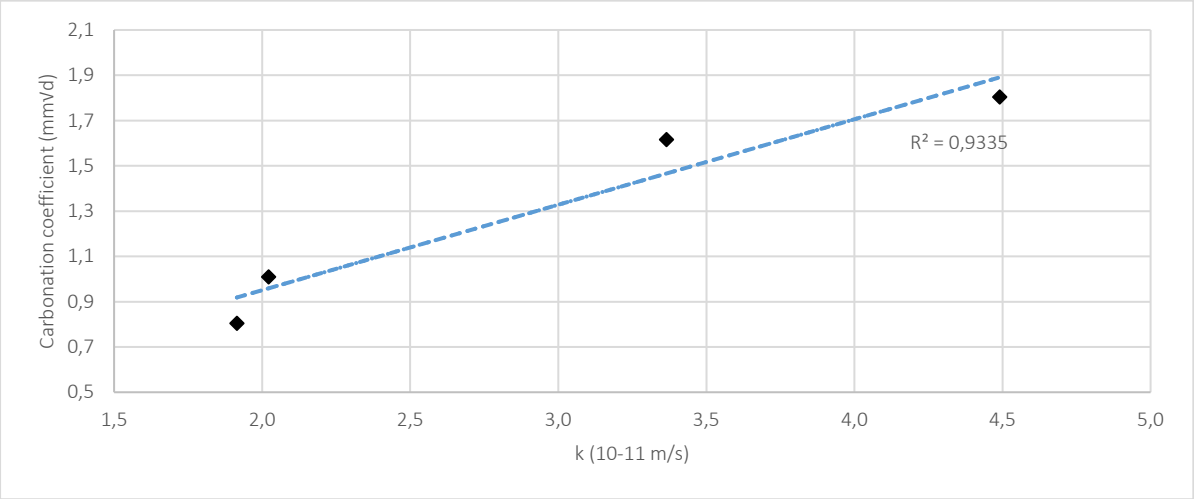

Figure 4-35: Correlation between carbonation coefficient and k-permeability for L mixes

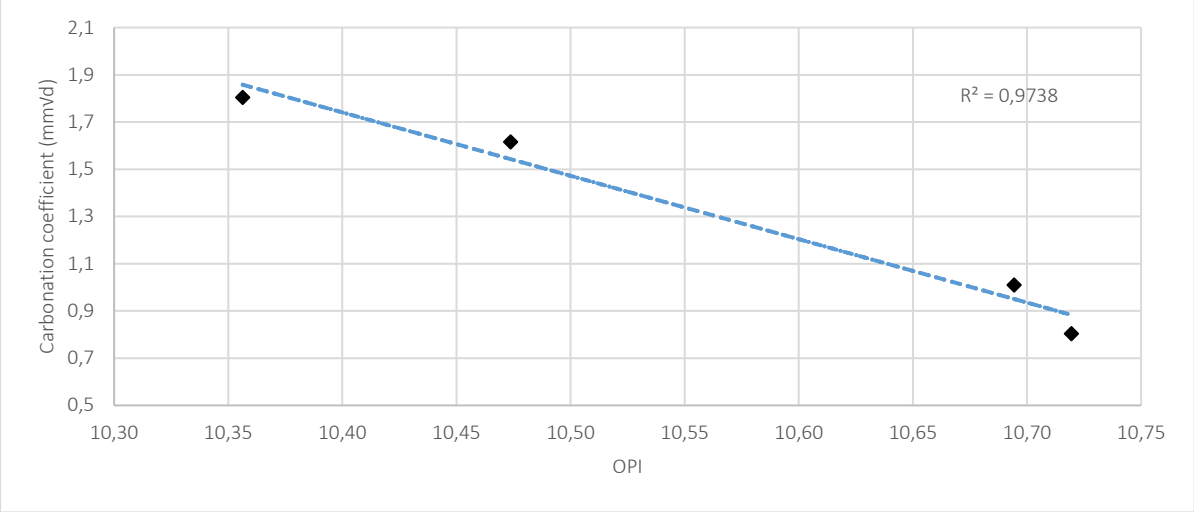

Figure 4-36: Correlation between carbonation coefficient and OPI for L mixes

The increase in strength of the correlation suggests that reasonable correlations may be made between permeability and carbonation coefficient for mixes with the same binder type regardless of

replacement level in comparison to all the mixes. However, more testing on a greater sample size would be required to confirm this. It is also noteworthy to reflect upon the fact that this correlation might not hold for specimens of a different curing regime.

In conclusion, the correlation with the carbonation coefficient cannot be solely reliant on one factor such as the oxygen permeability. Other factors must be considered, such as the cement chemistry or the amount of carbonatable material and exposure. Therefore, prediction model for a specific binder combination would not be necessarily applicable to another binder combination. In this study it was observed that there was an improvement in correlation when a singular binder type (regardless of the replacement level) is investigated to a point where it provides a reasonable correlation.

4.5 Summary of results

Generally, The OPI results in this study reached values greater than 10. In certain cases, particular mixes exceeded an OPI value of 11. To put this into perspective, OPI values typically range from 8 to 11, with an OPI of 11 indicating a permeability that is 3 orders of magnitude lower, compared to an OPI of 8. In addition, as stated in Section 2.3.1.1, OPI values greater than 10 represent relatively impermeable concrete and hence a durability class of excellent. For this reason, all obtained OPI values are considered high, indicating concrete of excellent quality and very low permeability. Some of the OPI results, shown in Table 4-19 were compared to the findings from other researchers who used the same binder replacement levels and performed the same curing regime. The findings from the latter generally showed a similar trend when producing concretes with low permeabilities as most of the results are greater than 10.

Due to the very low permeabilities exhibited in the mixes, it was difficult to visually distinguish the difference in the performance by mere observation as the range in performance was relatively small. It emerged that there are times when even statistical analysis may be deemed inadequate as the two statistical analysis results would contrast each other.

The control mixes already had very low permeability results. Thus, the addition of a mineral admixture is suspected not to significantly change the permeability further. It is therefore assumed that the addition of mineral admixtures has a minimal effect on permeability. It should be noted that this is deemed the case for a moist curing duration of 28 days. The prediction is that shorter moist curing durations will produce higher permeabilities and consequently, larger ranges in OPI results.

Table 4-19: Permeability results for concrete mixes of different w/b ratios

Mix	w/b ratio	OPI Obtained			
		Present Results	Salvoldi (2010)	Angelucci (2012)	Mukkadam (2014)
CEM I	0,5	10,70	10,11	10,41	10,4
30 FA	0,5	10,70	10,20	10,32	10,8
50 BS	0,5	10,99	10,30	9,97	10,12
B-M	0,5	10,93			10,14
CEM I	0,65	10,46			10,18
30 FA	0,65	10,44			10,38
50 BS	0,65	10,63			9,83
B-M	0,65	10,68			9,56

The discussion focuses on the frequency with which statistical insignificance was observed. This frequency finds support in the statement that the inclusion of mineral admixtures has minimal influence on permeability performance, and that possibly this is also attributable to the high dispersion of the results. Although oxygen permeability is generally considered to be high in variance, some mixes were particularly high in variance, thus increasing the probability of the acceptance of the null hypothesis which indicates no statistical significance. However, what has to be taken into account is that the OPI mean results are based on only four specimens. As the sample size increases, it is expected that the variance will decrease. Therefore, increasing the quantity of specimens tested may lead to a refinement of the analysis.

In general, the results show that as expected, the carbonation depth was directly proportional to the replacement level percentage due to the dilution effect. It was interesting to note that the statistical significance among the mixes decreases with a decrease in w/b ratio. Decreasing the w /b ratio thus leads to an improvement in the concrete pore structure as well as in the concentration of CH. Hence the rate of progression in the carbonation front slows down significantly, minimising the gap between carbonation depths and replacements.

Finally, reasonable correlations between the carbonation coefficient and permeability of all the mixes were found. However, the scatter of the results was quite dispersed, indicating that permeability is not the sole factor affecting carbonation. The investigation between carbonation and a single binder type, regardless of replacement level, generally showed a significant increase in correlation strength.

5 Conclusions and recommendations

5.1 Introduction

Reinforcement corrosion is a pervasive concern in the construction industry. One of the main causes of reinforcement corrosion is the concrete deterioration mechanism known as carbonation. In South Africa, the Durability Index (DI) approach can be used to estimate carbonation-induced corrosion, using the oxygen permeability index (OPI) as an input parameter for carbonation deterioration in the appropriate service life model. Over the years, the DI approach has undergone steady development. Simultaneously, concrete has undergone a significant evolution as concrete itself is becoming more sophisticated and complex through the inclusion of mineral admixtures which can improve its general properties. Even so, the DI approach may require further development to become more applicable for these modern concretes containing different mineral admixture types at various replacement levels and combinations. Given these developments and their challenges, the main objectives evaluated in this study were to:

- Assess the performance of binary and ternary mixes containing different mineral admixtures at varying cement replacement percentages, with regard to oxygen permeability and carbonation; and
- investigate the correlation between the oxygen permeability and carbonation depths for modern concretes using the appropriate carbonation prediction models.

This chapter summarises the main findings and discussion in Chapter 4. It begins with Section 5.2, which includes a summary of the influence of binary and ternary mixes on the gas permeability performance. This is followed by Section 5.3 which captures the findings observed in the binary and ternary mixes' influence on carbonation. Thereafter, the correlation between carbonation depth and oxygen permeability are discussed in Section 5.4. Additional findings, which are classified as observations that were not directly linked to the objectives of this study are shown in Section 5.5. Lastly, conclusions and recommendations based on the results are provided in Sections 5.6 and 5.7 respectively.

5.2 Influence of binary and ternary mixes on the permeability performance

Due to the generally low permeabilities exhibited in the concrete mixes that were investigated, it was difficult to distinguish the difference in the permeability performance by mere observation as the results lay in a relatively small range. The OPI values obtained in this study generally reached values greater than 10. In certain cases, mixes exceeded an OPI value of 11. OPI values greater than 10 represent relatively impermeable concrete and hence a durability class range of excellent was given as mentioned in Section 2.3.1.1. For this reason, it is deduced that the OPI values obtained in this study lied in a small range.

Statistically insignificant differences in results were often observed for the concrete mixes. This could be attributed to the low permeability exhibited in all the mixes. The control concrete mixes (CEM I) already exhibited very low permeability values. Therefore, it is suggested that the addition of mineral admixtures had minimal effect on the permeability performance for samples that underwent 28-day wet curing. It is predicted that a shorter curing regime would probably produce higher permeabilities and consequently a higher range of OPI values. The statistical insignificance could also

be attributed to the high dispersion of results. Although oxygen permeability is generally considered to be high in variance, the variance in some mixes was particularly high.

Generally, the addition of fly ash (FA) to the concrete mixes showed no discernible improvement in permeability for both w/b ratios, up to a replacement level of 40%. This finding was also supported by the statistical analysis. It was deduced that the magnitude of the positive effects on the permeability attributed to the fine filler and pozzolanic effect of FA were approximately equal to the negative effect caused by the dilution effect until a replacement level of 40%. Hence, no significant change was observed in permeability with the inclusion of FA. An increase in permeability was observed for a FA replacement level of 50% in comparison to the control especially for the 50 FA concrete mix with a w/b ratio of 0,65. This phenomenon is due to the dilution effect becoming the most dominant attribute contributing to the permeability performance subsequently increasing the permeability.

Observations of the addition of blast-furnace slag (BS) to the concrete mixes displayed a decrease in permeability for both w/b ratios up to BS replacement level of 60%. However, it was argued that a few permeability values among the BS mixes could be insignificant to the concrete mix due to the overlapping of the error bars. The statistical analysis results showed that the inclusion of BS was statistically insignificant in comparison to the control mix up to replacement levels of 30% and 50% for a w/b ratio 0,5 and 0,65 respectively. It is suspected that both the chemical and physical properties contributed positively to the permeability performance and were more dominant despite the negative contribution of the dilution effect.

The inclusion of Corex slag (CS) showed no clear trend up to a replacement level of 60% for both w/b ratios by comparing the results to the control mixes and it was thought that anomalies exist. In addition, it was observed that, generally CS had no significant influence on the permeability. It was predicted that an observed decreasing trend of permeability should have been observed for CS similar to the BS results.

No notable change in concrete permeability was observed for the addition of limestone (L) up to a replacement level of 20% for both w/b ratios as the error bars overlapped. Statistical analysis results supported this observation as the results showed no significant change in permeability in comparison with the respective control mixes or among the L mixes. It appeared that limestone's two contrasting attributes affecting permeability – the fine filler and dilution effect – counteracted each other and consequently, caused insignificant influence on permeability with respect to the increase in L replacement level.

A minor decrease in permeability with the inclusion of a replacement level of 5% silica fume (SF) in comparison to CEM I for both w/b ratios was observed and said to be statistically insignificant based on the analytical approach followed. SF is considered to be a highly reactive pozzolan and an effective fine filler, which positively affects the permeability performance. Despite these beneficial factors, results showed that a 5% SF replacement level was not adequate to make a statistically significant difference to the control mixes.

Regarding the ternary mixes, SF CS (containing 5% SF and 25% CS) had the best permeability performance followed by SF FA (containing 5% SF and 25% FA), and thereafter SF BS (containing 5% SF and 25% BS). However, statistically no significance was observed among the ternary mixes for both w/b ratios. Additionally, results from statistical analysis showed that the ternary mixes (excluding the

SF BS mix) were statistically significant in comparison to the control mix. Based on the results it appears that the transition from binary to ternary mixes for the same replacement level can potentially achieve a slight improvement in the concrete's permeability.

For a comparison between different mineral admixtures at the same replacement levels, the results obtained with mixes containing slags had the greatest positive effect on the permeability performance, followed by mixes containing FA then L. Despite permeability superiority of the slag mixes, the statistical analysis showed that this superiority was not entirely statistically significant. When comparing BS to the FA mixes, BS permeability performance was significant (apart from 40 FA) for the w/b ratio of 0,65; whereas, for the w/b ratio of 0,50, the comparison is only significant after a replacement level of 40%. No clear trend could be seen for comparison between CS and FA on a statistical level. Despite L being an inert filler, the statistical analysis results showed that in certain cases mixes were insignificant when compared to L. Most notably is that for both w/b ratios, differences in results obtained with L and FA were considered statistically insignificant.

For the commercial mixes, there was a minor decrease in permeability of CEM II A-L 52,5N (A-L) in comparison to the control mix for both w/b ratios. The statistical analysis results translated this minor decrease as no statistical significance difference. This indicates that the addition of limestone had an insignificant effect on the permeability performance.; and that its slight improvement was attributable to the nucleation and fine filler effect.

A decrease in permeability was observed when comparing CEM II B-M (L-S) 42,5N (referred to as B-M) mixes to the control for both w/b ratios. Conflicting statistical analysis results between the CEM I and B-M concrete mixes for the w/b ratio of 0,5 were observed. However, it was concluded that the permeability results of B-M was statistically significant to CEM I as the result provided by the t-test was more clearly valid. B-M consists nominally of 8% L and 25% CS, and factors affecting the permeability performance are derived from the synergistic combination of both binders such as the fine filler and pozzolanic effect.

5.3 Influence of binary and ternary mixes of the carbonation performance

Predominantly, the results showed that as expected, the carbonation depth was directly proportional to the increase in Portland cement (PC) replacement level percentage. Increasing the replacement level increases the magnitude of the dilution effect, therefore decreasing the amount of calcium hydroxide (CH) in the concrete. CH can be considered as a sacrificial layer opposing the migration of the carbonation front. Therefore, decreasing the concentration of CH increases the concretes vulnerability to carbonation. Binders possessing pozzolanic attributes (e.g. slag, fly ash and silica fume) could also have contributed to the carbonation depth as these consume CH to produce additional cementitious-like compounds. However, an additional chemical analysis is required to determine the significance of the pozzolanic reaction.

A clear increase in carbonation depth with the increase in FA up to a replacement level of 50% for both w/b ratios was detected. The statistical analysis supported this observation as its results showed that the carbonation depths among the FA mixes and the control mix (CEM I) were all statistically significant. This trend is mainly attributable to the dilution effect. Moreover, the pozzolanic nature may have influenced the carbonation progression due to its consumption of CH.

For the BS mixes, a general increase in carbonation depth with the increase in BS up to a replacement level of 60% for both w/b ratios was detected. Clearly, the trend of increasing

carbonation depth with the increase in BS was attributable to mainly the dilution and the pozzolanic effect to some degree. Interestingly, the decrease in w/b ratio leads to more concrete mixes being statically insignificant to one other. Lowering the w/b ratio increases the concentration of the sacrificial CH layer so that the progression of the carbonation front will be slower. Additionally, the permeability of the concrete will be improved. Similarly, results showed a general increase in carbonation depth with the increase in CS up to a replacement level of 60% for both w/b ratios. As such, this trend was mainly attributed to the dilution and the pozzolanic effect to a certain degree. As in the case of the BS carbonation results, the insignificance between some of the CS mixes, may be attributed to the change in w/b ratio.

There was a clear increase in carbonation depth with an increase in L up to a replacement level of 20% for both w/b ratios. The increasing trend in carbonation depth with the introduction of L is mainly attributable to the dilution effect. Unlike the other mineral admixtures used in this study, no chemical effects contributed to the dilution of CH as L is considered chemically inert in concrete.

SF mixes showed a slight increase in carbonation depth in comparison to the control mix, as expected. However, with a statistical approach the comparison was considered insignificant. It is suspected that the physical (fine filler effect) and chemical (pozzolanic effect) characteristics of SF might also have played a role in the insignificance thus improving the carbonation resistance by refining the concretes pore structure.

Regarding the ternary mixes, results showed a general decrease in carbonation depth in the transition from a binary to a ternary mix. The decrease in carbonation depth could be attributed to the inclusion of SF. SF is an effective fine filler and has a highly reactive nature, which contributes to refining the concrete pore structure, subsequently increasing the carbonation resistance. Note that the replacement level for the binary and ternary mixes were the same. The ascending order of the ternary mixes in terms of carbonation resistance ran as follows: SF FA, SF BS and then SF CS. However, the cause of this phenomenon is not evident and necessitates additional testing before conclusions can be drawn. In the comparison between different binders at the same replacement levels, the latent hydraulic binders demonstrated a dominating carbonation resistance (CS and then BS) amongst the binders, followed by FA and then L. However, the cause of this phenomenon is not evident. Additional testing is therefore required.

Finally, for the commercial mixes, an increase in carbonation depth could be seen between A-L and the control mix (CEM I). As with L, this phenomenon was attributed to the dilution effect. However, no statistical significance was observed for the mixes with the w/b ratio of 0,5. This could be attributed to the increase in CH concentration as a consequence of a decrease in the w/b ratio as well as the decrease in permeability. A similar result was observed when investigating the B-M mixes.

5.4 Investigation into the correlation between OPI and carbonation coefficient

Analytical observation of the permeability-carbonation coefficient graphs showed correlations. The direction of the trend showed a positive and negative association when the carbonation coefficient was plotted against k-permeability and OPI respectively. This suggests that with a decrease in permeability, higher resistance to carbonation may be expected. Additionally, it indicates that the permeability results may provide a reasonable measure for carbonation performance in modern concretes despite the two variables being derived from two different transport mechanisms. However, further investigation is needed to support this statement.

It was also observed that the scatter of the values was quite dispersed where results lie far from the regression line. Possible reasons for the weak trend in correlation could be due to the variance in concrete chemistry. Carbonation is a function of the concrete chemistry and the exposure condition (such as humidity and temperature). Hence the slopes of the regression lines for the respective concrete types may change according to the relative humidity, amount and type of mineral admixture used. Further investigation was pursued to determine whether a correlation exists between the carbonation coefficient and permeability with concrete mixes of the same binder type regardless of the replacement level. The graphs showed that a stronger correlation could be seen compared to when all the concrete mixes were included, with the exception of CS.

5.5 Additional findings

Additional findings observed in this research are detailed in this section. These findings are not directly related to the main objectives of this study. These include the influence of binary and ternary mixes containing different mineral admixture types at varying replacement levels on the permeability and carbonation performance. Additionally, the correlation between permeability and the carbonation coefficient.

It was clearly evident that the w/b ratio has a marked influence on the compressive strength of concrete. The results showed that an increase in binder replacement resulted in a decrease in compressive strength. This trend can be attributed to the dilution effect resulting in a lower degree of the hydration reaction especially at early ages subsequently decreasing the amount of calcium silica hydrate (CSH), a hydration product mainly contributing to the concrete strength.

In general, the results obtained from the OPI test showed that all the concretes made in this study were of high quality, exhibiting low permeabilities. A comparison with the findings of other researchers in the UCT laboratory who have made similar mixes with the same 28-day curing regime showed similar permeability performance. Thus, this leads to the conclusion that the oxygen permeability results of such magnitude are achievable for concrete mixes wet cured for 28-days under controlled conditions.

As expected the w/b ratio was found to be inversely proportional to the concrete's permeability; increasing the w/b ratio thus increases the permeability. This is due to the lower degree of hydration as well as an extension of the initial spacing between cement particles. Consequently, it can lead to increasing the size and connectivity of the pores within the hardened concrete.

The results also showed that the w/b ratio was inversely proportional to the carbonation depth, as expected. The amount of CH is a function of the w/b ratio property of the concrete. Therefore, altering the w/b ratio influences the rate of the carbonation front. Additionally, as noted previously, the w/b ratio influences the concrete's permeability. Permeability affects the progression of the carbonation front as this concrete property determines the ease with which the CO_2 can migrate within the interconnected pores of the concrete.

5.6 Conclusions

The following conclusions were drawn from the experimental investigation performed in this work:

- Generally, the increase in binder replacement level resulted in the decrease in 28-day compressive strength. This trend can be attributed to the dilution effect resulting in a lower degree of the hydration reaction decreasing the amount of calcium silica hydrate (CSH), a hydration product mainly contributing to the concrete strength.
- Generally, the results obtained from the OPI test after a 28-day wet curing showed that all concretes were of high quality with low permeabilities obtaining OPI values of greater than 10 regardless of the mix proportion.
- Generally, the inclusion of the mineral admixtures FA, BS, CS and L had a minimal effect on the permeability performance in comparison to the control mix, CEM I. The control concrete mixes already exhibited very low permeability values. Therefore, it is suggested that the addition of mineral admixtures had minimal effect on the permeability performance.
- For the transition between binary and ternary mixes performed in the study, the addition of SF, whilst maintaining a constant cement replacement level, resulted in the decrease in carbonation performance but not statistically.
- The w/b ratio was inversely proportional to the carbonation resistance due to decrease in CH and improvement of the pore structure. Additionally, the w/b ratio was inversely proportional to the permeability to the refinement of the pore structure.
- Generally, the increase in replacement level results in the increase in carbonation depth. This phenomenon was mainly attributed to the dilution effect decreasing the CH content in the concrete. Pozzolanic reactions could also be a factor but its significance is uncertain.
- Correlation between carbonation coefficient and permeability could be seen when all the mixes in the study were used, and the correlation was stronger when only concrete mixes of the same binder type, regardless of the replacement level, were used.

5.7 Recommendations

Based on the study conducted, the following recommendations for further research are proposed towards a better understanding of the permeability, carbonation and the correlation of the two for modern concretes:

5.7.1 Varying exposure conditions

Carbonation is dependent on the exposure condition. This study limited the accelerated carbonation testing to one exposure condition which was done in accordance with the fib Service life Model. Additional exposure conditions on carbonation specimens should be conducted, involving different humidity levels and exposure to a wetting and drying cycle to consider areas with seasonal rain.

5.7.2 Correlation between the oxygen permeability and the diffusion coefficient

Only the linear correlation between oxygen permeability and the carbonation coefficient was investigated in this study, which was considered the basis of South Africa's carbonation model. The correlation investigated by Salvoldi (2010) showed the power relationship between diffusion and permeability, but only for conventional concretes. This should therefore be investigated for modern concretes.

5.7.3 Verification with long term data

Due to the limited period allowed for this study, long term performance testing was not conducted. Verification of the permeability-carbonation correlation with long-term (greater than 6 months) site and controlled exposure data is an important step in improving the carbonation depth predictions of the model.

5.7.4 Chemical analysis

It remains necessary that some detailed results be obtained on the chemical properties of the mineral admixtures used in the research. This would shed light on which mineral admixture property is considered dominant in permeability or carbonation depth at a particular curing age. An example of the chemical analysis is the investigation of the degree of the pozzolanic reactions in the binders.

5.7.5 Ternary mixes

There is a growing interest in the use of ternary mixes due to the limitations of binary mixes, as in certain cases use of a single mineral admixture can improve one performance attribute of concrete, but at the cost of another. Only three ternary combinations were investigated in this study, but additional ternary combinations could be tested with different replacement levels and types.

5.7.6 Additional Curing Regimes

This study entailed limited seven-day and twenty-eight-day curing durations for the permeability and carbonation respectively. It is recommended that curing regimes of different duration be explored, especially for those that produce concrete of lower permeabilities.

References

ACI Committee 201, 2003. *Guide to durable concrete (ACI 201.2R-01).* Farmington Hills: American Concrete Institute.

ACMP, 2007. *Achieving a sustainable Southern African cement industry,* Pretoria: Association of Cementitious Material Producers (ACMP).

Addis, B. & Goodman, J., 2009. Concrete mix design. In: G. Owens, ed. *Fulton's concrete technology.* 9th ed. Midrand: Cement and Concrete Institute, pp. 219-228.

Aitcl̈n, P.-C., 2000. Cements of yesterday and today Concrete of tomorrow. *Cement and Concrete Research,* 30(9), pp. 1349-1359.

Aïtcin, P.-C., 2008. *Binders for Durable and Sustainable Concrete.* 1st ed. Oxon: Taylor & Francis.

Akram, M. R. & Raza, S., 2015. Effect of Micro Silica and GGBS on Compressive Strength and Permeability of Impervious Concrete as a Cement Replacement. *European Academic Research,* 3(7).

Alexander, M. & Beushausen, H., 2009. Concrete Repair. In: G. Owens, ed. *Fulton's Concrete Technology.* 9th ed. Midrand: Cement and Concrete Institute, pp. 393-409.

Alexander, M. G., 2017. *Durability Index Testing Procedure Manual,* Cape Town: University of Cape Town.

Alexander, M. G. & Heiyantuduwa, R., 2009. Studies on prediction models for concrete durability. *Concrete Repair, Rehabilitation and Retrofittng II.*

Alexander, M. G., Jaufeerally, H. & Mackechnie, J. R., 2003. *Structural and durability properties of concrete made with Corex slag,* Cape Town: Department of Civil Engineering (UCT).

Alexander, M. G. & Magee, B. J., 1999. Durability performance of concrete containing condensed silica fume. *Cement and Concrete Research,* Issue 29, pp. 917-922.

Angelucci, M., 2012. *The Influence of Mix Design Parameters and Compressive Strength on Durability Indices,* Cape Town: University of Cape Town.

ASTM, 2017. *Standard Specification for Fly Ash and Raw or Calcined Natural Pozzolan for Use in Concrete (ASTM C618-17a),* West Conshohocken: ASTM international.

Ballim, Y., Beushausen, H. & Alexander, M., 2009. Durability of concrete. In: G. Owens, ed. *Fulton's concrete technology.* Midrand: Cement and Concrete Institute, pp. 155-188.

Ballim, Y., Mackechnie, J. & Alexander, M., 1999. Guide to the use of durability indexes for achieving durability in concrete structures. *Research Monograph.*

Bertolini, L. et al., 2013. *Corrosion of Steel in Conrete - Prevention, Diagnosis, Repair.* Second ed. Germany: Wiley-VCH.

Beushausen, H. & Alexander, M. G., 2008. The South African durability index tests in an international comparison. *Journal of the South African Institution of Civil Engineering,* 50(1), pp. 25-31.

Bjegovic, D. et al., 2016. *Test Methods for Concrete Durability Indicators,* Cape Town: Springer.

Boshoff, W. P., 2015. CONCRETE : FRIEND OR FOE ?.

Broomfield, J., 2008. *Corrosion of Steel in Concrete: UNderstanding, INvestigation and Repair.* 2nd ed. Oxford: Taylor and Francis.

Chang, C.-F. & Chen, J.-W., 2006. The Experimental Investigation of Concrete Carbonation Depth. *Cement and Concrete Research,* 9(36), pp. 1760-1767.

Cyr, m., Lawrence, P. & Ringot, E., 2006. Efficiency of mineral admixtures in mortars: Quantification of the physical and chemical effects of fine admixtures in relation with compressive strength. *Cement and Concrete Research,* Issue 36, pp. 264-277.

De La RILEM Recommendations, 1988. CPC-18 Measurement of hardened concrete carbonation depth. *Material Structures,* Issue 21, pp. 453-455.

Ekolu, O. S., 2016. Towards Practical Carbonation Prediction and Modelling for Service Life Design of Reinforced Concrete Structures. IOP Conference Series: Materials Science and Engineering. *Materials Sciene and Engineering,* 96(1).

Elshafie, S., Boulbibane, M. & Whittleston, G., 2016. Influence of Mineral Admixtures on the Mechanical Properties of Fresh and Hardened Concrete. *Construction Science,* 19(1), pp. 4-12.

Emeritus, T., 1998. *Cement chemistry.* 2nd ed. London: Thomas Telford.

EN British Standard, 2002. *EN 206-1: Specification, performance, production and conformity,* s.l.: Eurocode.

Federation International du Beton, 2007. *fib Bulletin 34: Model code for Service Life Design,* s.l.: s.n.

Fernändez Luco, L. & Torrent, R., 2007. *Report 40: Non-Destructive Evaluation of the Penetrability and Thickness of the Concrete Cover,* France: RILEM Publications S.A.R.L.

Frenzer, G. & Torrent, R., 1995. A Method for the Rapid Determination of the Coefficient or Permeability of the "covercrete". *International Symposium Non-Destructive Testing in Civil Engineering,* pp. 985-992.

Golden, G., 2015. *The Effect of Cyclic Wetting and Drying on the Corrosion Rate of Steel in Reinforced Concrete,* Cape Town: University of Cape Town.

Grieve, G., 2009. Cementitious materials. In: G. Owens, ed. *Fulton's concrete technology.* 9th ed. Midrand: Cement and Concrete Institute, pp. 1-6.

Hewlett, P., 1998. *Lea's Chemistry of Cement and Concrete.* 1st ed. Burlington: Elsevier.

Houst, Y. F. & Wittmann, f. H., 2002. Depth Profiles of Carbonates Formed During Natural Carbonation. *Cement and Concrete Research.*

Hunkeler, F., 2005. *Corrosion in reinforced concrete structures.* England: Woodhead Publishing limited.

Jaufeerally, H., 2001. *Performance and Properties of Structural Concrete made with Corex Slag,* Cape Town: University of Cape Town.

Jin, R. & Chen, Q., 2013. An Investigation of Current Status of “Green” Concrete in the Construction Industry. *49th ASC Annual International Conference Proceedings.*

Jumate, E. & Manea, D. L., 2011. X-ray diffraction study of hydration proceses in the Porland Cement. *Civil Engineering Installations.*

Kellerman, J., 2009. Manufacture and handling of concrete. In: G. Owens, ed. *Fulton's Concrete Technology.* Midrand: Cement and Concrete Institute , pp. 229-250.

Kellerman, J. & Croswell, S., 2009. Properties of fresh concrete. In: G. Owens, ed. *Fulton's concrete technology.* Midrand: Cement and Concrete Institute.

Khan, M. I. & Lynsdale, C. J., 2012. Strength, permeability, and carbonation of high-performance concrete. *Cement and Concrete Research,* Volume 32, pp. 123-131.

Kollek, J. J., 1989. The determination of the permeability of concrete to oxygen by the Cembureau method -a recommendation. *Materials and Structures,* Volume 22.

Kropp, J. & Hilsdorf, H. K., 1995. *Peformance Criteria for Concrete Durability,* London: RILEM.

Lobo, C., Lemay, L. & Obla, K., 2005. Performance-Based Specifications for Concrete. *Indian Concrete Journal,* 79(12).

Lothenbach, B., Scivener, K. & Hooton, R. D., 2011. Supplementary cementitious materials. *Cement and Concrete Research,* Volume 41.

Lo, Y. & Lee, H. M., 2002. Curing effects on carbonation of concrete using a phenolphthalein indicator and Fourier-transform infrared spectroscopy. *Building and Environment,* Volume 37.

Mackechnie, J. R. & Alexander, M. G., 2002. Durability Predictions Using Early-Age Durability Index Testing. *Proc. Ninth Durability and Building Materials Conference, Australian Corrosion Association,* Volume 11.

Mackechnie, J. R., Alexander, M. G. & Ballim, Y., 2001. Use of durability indexes to achieve durable cover concrete in reinforced concrete structures. *Materials Science of Concrete,* Volume VI, pp. 483-511.

Markeset, G. & Myrdal, R., 2008. *Modelling of reinforcement corrosion in concrete- state of the art,* s.l.: Blindern: SINTEF Building and Infrastructure, Concrete Innovation Center.

Mays, G., 1992. *Durability of Concrete Structures.* 1st ed. London: E & FN Spon.

Moosberg-Butnes, H., Lagerblad, B. & Forssberg, E., 2004. The function of fillers in concrete. *Materials and Structures,* Volume 37, pp. 74-81.

Muigai, R. & Alexander, M. G., 2010. *Contribution of the Durability Index Approach towards Sustainable Concrete Structures,* Cape Town: University of Cape Town.

Mukadam, Z., 2014. *Critical Review of the South African Concrete Durability Index Tests,* Cape Town: Univeristy of Cape Town.

Neville, A., 2011. *Properties of Concrete.* 5th ed. England: Pearson.

Newman, J. & Choo, B. S., 2003. *Advanced Concrete technology - Constituent Materials.* 1st ed. London: Elsevier.

Newman, J. & Choo, B. S., 2003. *Advanced Concrete Technology: Testing and Quality.* 1st ed. Oxford: Butterworth-Heinemann.

Nganga, G., 2012. *Practical Implementation of the Durability Index-Based Performance Approach,* Cape Town: University of Cape Town.

Nilsson, L.-O. & Luping, T., 1995. Relations between Different Transport Parameters. In: *Performance Criteria for Concrete Durability.* London: E and FN Spon.

Ohanyere, C. I., 2013. *The South African Cement Industry: A Review of its Energy Efficiency and Environmental Performance Since 1980,* Cape Town: University of Cape Town.

Pacheco-Torgal, F., Jalali, S., Labrincha, J. & John, V. M., 2013. *Eco-efficient concrete.* First ed. Cambridge: Woodhead Publishing Limited.

Papadakis, V., 2000. *Effect of supplementary cementing materials on concrete resistance against carbonation and chloride ingress,* s.l.: Cement and Concrete Research.

Papadakis, V. G., Vayenas, C. G. & Fardis, M. N., 1991b. Physical and chemical characteristics affecting the durability of concrete. *ACI Mater J.*

Papadakis, V., Vayenas, C. & Fardis, M., 1991a. Fundamental modeling and experimental investigation of concrete carbonation. *ACI Materials Journal,* 88(4), pp. 363-373.

Parrot, L. J., 1988. Moisture profiles in drying concrete. *Advances in Cement Research,* 1(3).

Powers, T. C., Copeland, L. E., Hayes, J. C. & Mann, H. M., 1954. Permeability of Portland Cement Paste. *Proceedings of ACI,* Volume 51, pp. 285-298.

Powers, T. C., Copeland, L. E. & Mann, H. M., 1959. Capillary Continuity or Dscontinuity in Cement Pastes. *Journal of Portland Cement Association Research and Development Laboratories No. 110.*

Raupach, M. & Büttner, T., 2014. *Concrete Repair to EN 1504: Diagnosis, Design, Principle and Practice.* First ed. London: Taylor and Francis Group.

Richardson, M., 2002. *Fundamentals of durable reinforced concrete.* 1st ed. London: Spon Press.

Roberge, P. P., 2008. *Corrosion Engineering: Principles and Practice.* 1st ed. USA: McGraw-Hill Companies.

Saetta, A., Schrefler, B. & Vitaliani, B., 1993. The carbonation of concrete and the mechanism of moisture, heat and carbon dioxide flow through porous materials. Cement. *Cement and Concrete Research,* 23(4), pp. 761-772.

Salvoldi, B. G., 2010. *Modeling the Carbonation of Concrete using early age oxygen permeability index tests,* Cape Town: University of Cape Town.

Salvoldi, B. G., Beushausen, H. & Alexander, M. G., 2015. Oxygen permeability of concrete and its relation to carbonation. *Construction and Building Materials,* Volume 85, pp. 30-37.

Siddique, R. & Khan, M. I., 2011. *Supplementary Cementing Materials.* 1st ed. Berlin: Springer.

Simons, B., 2004. Concrete performance specifications: New Mexico Experience. *Concrete International,* 26(4), pp. 68-71.

South African National Standard (SANS), 2015. *Civil engineering test methods Part CO3-1: Concrete durability index testing - Preparation of test specimens (SANS 3001-CO3:2015),* Pretoria: SABS Standards Division.

South African National Standard (SANS), 2015. *Civil Engineering Test Methods Parts CO3-1: Concrete durability index testng - preparation of test specimens (SANS 3001-CO3-2015),* Pretoria: SABS Standards Division.

South African National Standard (SANS), 2017. *Civil engineering test methods Part CO3-1: Concrete durability index testing – Preparation of test specimens (SANS 3001-CO3:2017).,* Pretoria: SABS Standards Division.

South African National Standards (SANS), 2006. *Concrete tests — Compressive strength of hardened concrete (SANS 5863),* Pretoria: SABS Standards Division.

South African National Standards (SANS), 2015. *Civil engineering test methods Part CO3-2: Concrete durability index testing - Oxygen permeability test (SANS 3001-CO2:2015),* Pretoria: SABS Standards Division.

South African National Standards, 2006. *Concrete tests — Consistence of freshly mixed concrete - slump test (SANS 5862-1),* Pretoria: SABS Standards Division.

South African National Standards, 2006. *Concrete tests Part 3: Making and curing of test specimens (SANS 5861-3),* Midrand: SABS Standards Division.

South African National Standards, 2006. *SANS 5845: Bulk densitites and voids content of aggregates,* Pretoria: SABS Standards Division.

Stanish, K., Alexander, M. G. & Ballim, Y., 2006. Assessing the repeatability and reproducibility values of South African durability index tests. *journal of the Sourth African Institution of Civil Engineering,* 48(2), pp. 10-17.

Stanish, K., Ballim, Y. & Alexander, M. G., 2008. A framework for use of durability indexes in performance- based design and specifications for reinforced concrete structures. *Materials and Structures,* Volume 41, pp. 921-936.

Stutzman, P. E., 2000. Scanning Electron Microscopy in Concrete Petrography. *Materials Science of Concrete.*

Thomas, M., 2013. *Supplementary Cementing Materials in Concrete.* 1st ed. Washington: CRC Press.

Töpfer, M., 2017. *Quality Assurance Concept for the Durability of Concretes with Reduced CO2-Burden,* Germany: Leibniz Universität Hannover.

Tuutti, K., 1982. Corrosion of Steel in Concrete. *CBI Research.*

Villain, G., Thiery, M. & Platret, G., 2007. Measurement methods of carbonation profiles in concrete:. *Cement and Concrete Research,* Volume 37, pp. 1182-1192.

Villian, G., Thiery, M. & Platret, G., 2007. Investigation of the carbonation front shape on cementitious materials: Effects of the chemical kinetics. *Cement and Concrete Research,* Volume 37, pp. 1047-1058.

Walpole, R. E., Myers, R. H., Myers, S. L. & Ye, K., 2012. *Probability and Statistics for Engineers and Scientists.* 9th ed. Prentice Hall: s.n.

Wickens, K., 2013. *The use of construction and demoltion waster in concrete in Cape Town,* Cape Town: University of Cape Town .

Yam, W. K., 2004. *Carbonation of Concrete Bridge Structures in Three South African Localities,* Cape Town: University of Cape Town.

Zulu, S. & Allopi, D., 2015. OPTIMISING THE USAGE OF FLY ASH IN CONCRETE IN THE CONSTRUCTION OF ROADWORKS. *34th South African Transport Conference (SATC 2015).*

Appendices

Appendix A: detailed concrete mix design

Relevant information regarding the materials used in this research, trial mixes and the detailed mix concrete mix designs are provided in the following paragraphs

A1: Philippi dune sand

- Relative density of 2.67
- Fineness modulus of 1,94

Table A1: Sieve analysis Philippi dune sand

Sieve size	Mass retained	% Mass retained	Cumulative % mass retained	Cumulative % mass passing
mm	g	%	%	%
4,75	0	0	0	100
2,36	0	0	0	100
1,18	10	1	1	99
0,6	165	16,42	17,4	82,6
0,3	595	59,2	76,6	23,4
0,15	225	22,39	99	1
0,075	5	0,5	99,5	0,5
Pan	5	0,5	100	0
			Total (g)	1005

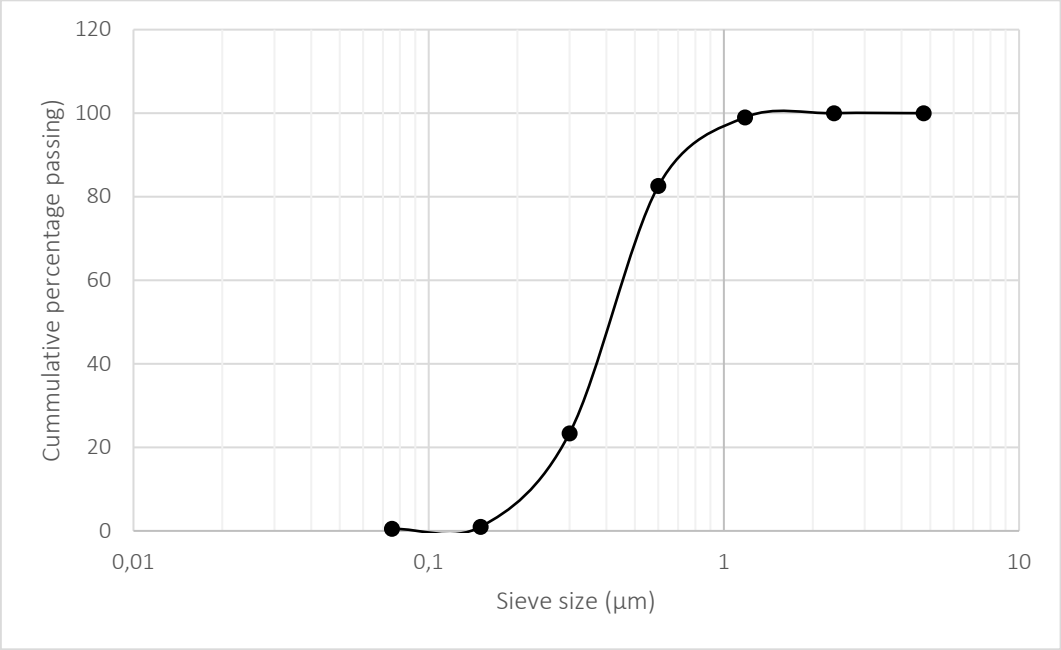

Figure A3: Particle size distribution of Philippi dune sand

A2: greywacke fine aggregate

- Relative density of 2.72
- Fineness modulus of 3,35

Table A2: Sieve analysis of Greywacke fine aggregate

Sieve size	Mass retained	% Mass retained	Cumulative % mass retained	Cumulative % mass passing
mm	g	%	%	%
4,75	8	98,0	1,0	99,0
2,36	243	24,5	25,5	74,5
1,18	318	31,4	56,9	43,1
0,6	171	17,6	74,5	25,5
0,3	117	10,8	85,3	14,7
0,15	62	6,9	92,2	7,8
0,075	43	4,9	96,1	3,9
Pan	31	3,9	100,0	0,0
			Total (g)	993

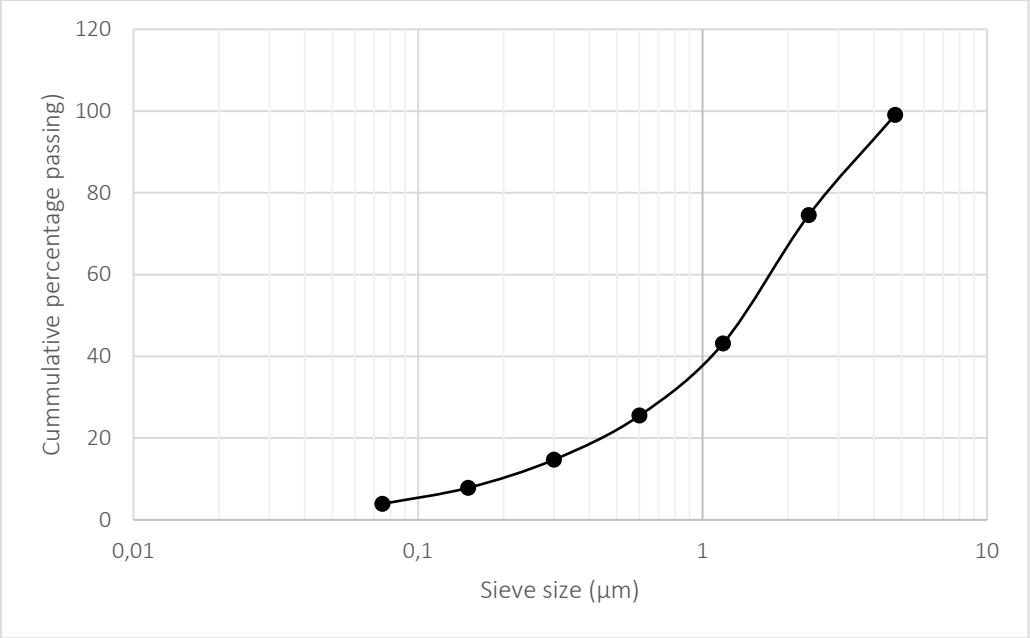

Figure A4: Particle size distribution of greywacke crusher sand

A3: superplasticiser (SP), Chryso Premia 310 (from Chryso SAF (Pty) Ltd)

- Relative density of 1.05 (kg/m^3)

A4: Binder Types

Table A3: Binder detailed information

Type	Source	Relative Density (R.D)
CEM I 52,5N	PPC Ltd	3,4
CEM II A/L 52,5N	PPC Ltd	3,4
CEM II B-S (L-M) 42,5N	PPC Ltd	3,15
Fly Ash (Durapozz)	Ash Resources	2,3
Blastfurnanace slag	PPC Ltd	2,9
Corex slag	PPC Ltd	2,9
Kulubrite 10 Limestone	Idwala Industrial holdings	2,7

A5: Mix design

The C&CI method was followed to determine the mix design for the long-term testing specimens, which is described below.

Water content

The water content was chosen based on the quality of sand used, coarse aggregate size (19 mm) and slump range. The use of a blend of crusher sand and Philippi dune sand, made for a sand of excellent quality, with a fineness modulus of 2.69 which offered a wide particle distribution as well as a good workability. Furthermore, an aggregate size was 19 mm was chosen and the chosen slump was 75 ±25 mm. The water content as suggested by Table 11.2: Addis & Goodman (2009) to be 180 l/m^3.

Binder content

Section 3.2.3 mentions that the chosen water to binder ratios (w/b) were 0,50 and 0,65. Using the w/b ratio and the chosen the water content, the total mass of binder (M_b) (in kilograms per metre cubed) was calculated as follows:

$$M_b = \frac{\text{water content}}{\frac{\text{water}}{\text{binder}}\text{ratio}}$$

Coarse aggregate content

Greywacke (GW) 19 mm was used for this study. The mass of stone per cubic metre (M_{ca}) of was calculated as follows:

$$M_{ca} = CBD \times (K - 0.1FM)$$

The 'K' value was assumed to be 1 (Table 11,4; Addis & Goodman, 2009), which was based on the aggregate size and slump range. The effective fineness modulus of the sand blend was determined to be 2.69. The Compacted bulk density (CBD) was calculated in accordance to SANS 5845 (2006) and results are shown in Table B4. The container used for this test had internal volume of 14,32 L.

Table A4: CBD results

Sample	Mass of aggregate + Container (kg)	Mass of aggregate (kg)	CBD
1	37,9	21,56	1506
2	37,9	21,54	1504
3	38,1	21,74	1518
		Average	1509

Fine aggregate content

The mass of fine aggregate was then calculated based on the remaining volume required to achieve a mix volume of 1 cubic metre. Note as 50/50 blended sand was used and thus the calculated value needed to be halved to determine the value for each sand type.

$$M_{sand}=RD_{sand}\times 1000\times\left(1-\frac{M_{cement}}{RD_{cement}\times 1000}-\frac{M_{binder}}{RD_{binder}\times 100}-\frac{M_{stone}}{RD_{stone}\times 1000}-\frac{M_{water}}{1\times 1000}\right)$$

Trial mixes

This section shows the various trial mixes and alterations that were performed on selected mixes to ensure that the concrete mixes were adequate for casting. A trail (ten-litre) mix was tested using a slump test ten-litre mix were its slump value as well as its consistency and cohesiveness as determined. Mixes CEM I (w/b ratio of 0,50), 50 FA and 60 BS (w/b ratio of 0,65) were chosen as they were suspected to cause the most difficulty. After three iterations, trial mix 3 was used as the basis to design the other concrete mixes used in the study.

Table A5: Trial concrete mix design

Trial mix	1			2			3		
Type	CEM I	50 FA	60 BS	CEM I	50 FA	60 BS	CEM I	50 FA	60 BS
w/b	0,5	0,65	0,65	0,5	0,65	0,65	0,5	0,65	0,65
	kg/m³			kg/m³			kg/m³		
CEM I	360	138	111	340	131	104	340	131	104
Water	180	180	180	170	170	170	170	170	170
FA		138			131			131	
BS			166			157			157
Stone	1117	1124	1117	1117	1124	1117	1050	1056	1050
Sand	406	406	426	418	419	447	452	421	479
Density (kg/m³)	2469	2392	2426	2463	2394	2442	2464	2411	2440
Slump	80	-	80	-	85	-	85	85	65
SP	2,5	0	0	-	0	-	10	0	5
Comment	Failed			-	Too much stone	-			

Appendix B: detailed compressive strength test results

Table B1: 28-day compressive strength results for a w/b ratio of 0,50

Type	Cube no.	Saturated Density	Mean Sat. Density	Failure Load	Comp. Strength	Mean Comp. Strength	S.D
		kg/m^3	kg/m^3	kN	MPa	MPa	%
CEM I	1	2420		548	54,8		
	2	2386	2406	588	58,8	55,9	2.57
	3	2412		540	54,0		
20 FA	1	2450		524	52,40		
	2	2426	2446	522	52,20	51,30	1,75
	3	2460		493	49,30		
30 FA	1	2445		452	45,20		
	2	2445	2429	448	44,80	45,10	0,26
	3	2397		453	45,30		
40 FA	1	2446		384	38,40		
	2	2440	2439	392	39,20	39,30	0,95
	3	2431		403	40,30		
50 FA	1	2420		292	29,20		
	2	2386	2046	287	28,70	28,73	0,45
	3	2412		283	28,30		
20 BS	1	2401		548	54,26		
	2	2431	2419	576	57,03	55,53	1,40
	3	2425		553	55,30		
30 BS	1	2381		514	50,89		
	2	2435	2424	512	51,20	51,90	1,48
	3	2455		536	53,60		
40 BS	1	2378		477	47,70		
	2	2435	2409	496	49,60	48,47	1,00
	3	2415		481	48,10		
50 BS	1	2403		444	44,40		
	2	2436	2422	434	43,40	44,63	1,37
	3	2427		461	46,10		
60 BS	1	2425		412	41,20		
	2	2395	2422	411	41,10	41,43	0,49
	3	2445		420	42,00		
20 CS	1	2415		602	60,20		
	2	2441	2427	631	62,48	62,83	2,82
	3	2425		658	65,80		
40 CS	1	2435		598	59,80		
	2	2439	2420	590	59,60	59,50	0,36
	3	2386		597	59,11		
60 CS	1	2422		520	50,98		
	2	2422	2427	537	52,65	52,02	0,91
	3	2437		540	52,43		
10 L	1	2421		553	54,75		
	2	2436	2437	619	61,29	59,64	4,30
	3	2455		635	62,87		

Table B1 continued

Type	Cube no.	Saturated Density	Mean Sat. Density	Failure Load	Comp. Strength	Mean Comp. Strength	S.D
		kg/m^3	kg/m^3	kN	MPa	MPa	%
20 L	1	2387		510	50,00		
	2	2415	2404	524	52,40	51,57	1,36
	3	2410		523	52,30		
A-L	1	2440		577	57,70		
	2	2470	2430	560	56,00	57,17	1,02
	3	2381		584	57,82		
B-M	1	2485		530	53,00		
	2	2445	2458	505	50,50	52,23	1,50
	3	2445		532	53,20		
SF 5	1	2410		501	50,10		
	2	2390	2407	500	50,00	50,37	0,55
	3	2420		510	51,00		
SF FA	1	2406		528	52,28		
	2	2395	2389	512	51,20	52,02	0,72
	3	2366		531	52,57		
SF BS	1	2401		574	56,83		
	2	2435	2407	573	57,30	57,31	0,48
	3	2385		578	57,80		
SF CS	1	2401		630	62,38		
	2	2402	2395	619	60,69	63,36	3,29
	3	2381		677	67,03		

Table B2: 28-day compressive strength results for a w/b ratio of 0,65

Type	Cube no.	Saturated Density	Mean Sat. Density	Failure Load	Comp. Strength	Mean Comp. Strength	S.D
		kg/m^3	kg/m^3	kN	MPa	MPa	%
CEM I	1	2435		449	44,90		
	2	2455	2460	420	42,00	43,43	1,45
	3	2490		434	43,40		
20 FA	1	2441		366	36,24		
	2	2441	2446	367	35,98	35,54	1,00
	3	2455		344	34,40		
30 FA	1	2500		308	30,80		
	2	2446	2459	317	31,08	30,43	0,90
	3	2431		297	29,41		
40 FA	1	2410		244	24,40		
	2	2445	2428	241	24,10	25,09	1,46
	3	2429		265	26,77		
50 FA	1	2420		200	20,00		
	2	2420	2447	180	18,10	19,27	1,02
	3	2500		197	19,70		
20 BS	1	2426		405	40,50		
	2	2431	2419	415	41,50	41,13	0,55
	3	2401		414	41,40		
30 BS	1	2446		401	40,10		
	2	2431	2436	401	40,10	40,40	0,52
	3	2430		410	41,00		
40 BS	1	2397		362	36,20		
	2	2425	2403	370	37,00	37,13	1,01
	3	2386		382	38,20		
50 BS	1	2425		321	32,10		
	2	2421	2408	343	34,30	33,80	1,51
	3	2376		350	35,00		
60 BS	1	2410		268	26,80		
	2	2390	2400	279	27,90	26,97	0,86
	3	2400		262	26,20		
20 CS	1	2421		477	47,70		
	2	2446	2334	460	46,00	47,03	0,91
	3	2436		474	47,40		
40 CS	1	2460		402	40,20		
	2	2431	2440	432	43,20	41,80	1,51
	3	2430		420	42,00		
60 CS	1	2401		362	36,20		
	2	2407	2396	372	37,20	36,77	0,51
	3	2380		369	36,90		
10 L	1	2430		405	40,50		
	2	2381	2412	389	38,90	39,80	0,82
	3	2425		400	40,00		

Table B2 continued

Type	Cube no.	Saturated Density	Mean Sat. Density	Failure Load	Comp. Strength	Mean Comp. Strength	S.D
		kg/m^3	kg/m^3	kN	MPa	MPa	%
20 L	1	2385		318	31,80		
	2	2396	2396	319	31,90	32,37	0,90
	3	2406		334	33,40		
A-L	1	2436		420	42,00		
	2	2411	2421	431	43,10	42,33	0,67
	3	2416		419	41,90		
B-M	1	2425		370	37,00		
	2	2415	2432	368	36,80	37,53	1,10
	3	2455		388	38,80		
SF 5	1	2410		449	44,90		
	2	2370	2383	431	43,10	44,43	1,17
	3	2370		453	45,30		
SF FA	1	2410		320	32,00		
	2	2410	2400	339	33,90	32,77	1,00
	3	2380		324	32,40		
SF BS	1	2365		406	40,60		
	2	2415	2395	380	38,00	39,53	1,36
	3	2405		400	40,00		
SF CS	1	2388		442	44,20		
	2	2405	2403	464	46,40	45,67	1,27
	3	2415		464	46,40		

Appendix C: oxygen permeability index (OPI) results

Table C1: k-permeability results

Type	w/b	k-permeability (E-11)				Average	S.D	CoV
		1	2	3	4	(m/s) (E-11)	%	%
CEM I	0,50	1,5	2,4	1,5	3,1	2,1	0,8	37
	0,65	4,2	3,6	2,6	3,6	3,5	0,7	19
20 FA	0,50	1,6	3,8	1,8	2,3	2,4	1,0	43
	0,65	6,1	5,4	3,9	4,2	4,9	1,0	21
30 FA	0,50	3,7	2,0	1,7	1,3	2,2	1,0	48
	0,65	4,7	3,8	3,4	2,7	3,7	0,9	23
40 FA	0,50	2,1	2,1	1,5	1,1	1,7	0,5	30
	0,65	7,4	3,5	2,9	7,5	5,3	2,5	47
50 FA	0,50	3,0	3,3	3,4	4,1	3,5	0,5	14
	0,65	21,7	8,2	79,9*	27,9	19,3	10,1	52
20 BS	0,50	1,3	1,5	1,1	1,9	1,5	0,3	23
	0,65	2,8	3,9	3,0	2,2	3,0	0,7	24
30 BS	0,50	1,7	0,9	0,9	1,4	1,2	0,4	33
	0,65	2,3	2,4	5,0	1,3	3,2	1,6	49
40 BS	0,50	0,9	0,8	1,3	1,3	1,1	0,2	22
	0,65	3,2	1,5	2,1	2,4	2,3	0,7	31
50 BS	0,50	1,0	1,1	0,8	1,3	1,0	0,2	19
	0,65	2,3	3,1	1,9	2,2	2,4	0,5	21
60 BS	0,50	1,0	0,9	0,7	0,9	0,9	0,1	17
	0,65	2,3	1,8	1,1	1,3	1,6	0,6	35
20 CS	0,50	2,3	1,6	3,0	1,4	2,0	0,7	36
	0,65	1,6	3,5	2,2	2,0	2,6	0,8	32
40 CS	0,50	1,4	0,9	0,6	0,7	0,9	0,4	42
	0,65	5,0	5,3	3,6	4,7	4,5	0,7	17
60 CS	0,50	2,5	9,5*	1,8	2,4	2,2	0,4	18
	0,65	4,8	2,2	1,5	14,7*	2,8	1,7	61
10 L	0,50	1,7	2,0	1,8	2,1	1,9	0,2	10
	0,65	3,4	3,7	3,1	3,3	3,4	0,2	7
20 L	0,50	2,1	2,0	2,0	2,0	2,0	0,1	3
	0,65	3,3	5,7	4,2	4,8	4,5	1,0	23
A-L	0,50	2,0	1,3	1,9	1,8	1,8	0,3	19
	0,65	4,2	2,4	2,4	3,4	3,1	0,9	19
B-M	0,50	1,0	1,5	1,0	1,3	1,2	0,2	20
	0,65	2,7	1,8	2,0	1,9	2,1	0,4	20
SF 5	0,50	1,4	1,7	1,6	2,3	1,9	0,4	21
	0,65	4,0	3,2	3,5	2,7	3,4	0,5	16
SF FA	0,50	1,3	1,1	1,1	1,2	1,2	0,1	5
	0,65	2,2	2,6	2,4	2,5	2,4	0,2	3
SF BS	0,50	0,8	2,3	1,6	0,7	1,4	0,7	54
	0,65	2,6	1,5	2,3	3,5	2,5	0,8	40
SF CS	0,50	1,0	0,9	1,2	0,8	1,0	0,2	17
	0,65	1,9	2,7	1,6	1,8	2,0	0,5	30

*result not used in the calculation

Table C2: OPI results

Type	w/b	OPI (Log scale)				Average	S.D	CoV
		1	2	3	4			%
CEM I	0,50	10,8	10,6	10,8	10,5	10,7	0,16	1,50
	0,65	10,4	10,4	10,6	10,4	10,5	0,09	0,84
20 FA	0,50	10,8	10,4	10,8	10,6	10,7	0,17	1,60
	0,65	10,2	10,3	10,4	10,4	10,3	0,09	0,88
30 FA	0,50	10,4	10,7	10,8	10,9	10,7	0,19	1,79
	0,65	10,3	10,4	10,5	10,6	10,4	0,10	0,98
40 FA	0,50	10,7	10,7	10,8	11,0	10,8	0,14	1,32
	0,65	10,1	10,5	10,5	10,1	10,3	0,22	2,11
50 FA	0,50	10,5	10,5	10,5	10,4	10,5	0,06	0,56
	0,65	9,7	10,1	9,1*	9,6	9,6	0,41	4,24
20 BS	0,50	10,9	10,8	11,0	10,7	10,8	0,10	0,90
	0,65	10,5	10,4	10,5	10,7	10,5	0,11	1,00
30 BS	0,50	10,8	11,1	11,1	10,9	10,9	0,14	1,31
	0,65	10,6	10,6	10,3	10,9	10,6	0,24	2,31
40 BS	0,50	11,0	11,1	10,9	10,9	11,0	0,10	0,90
	0,65	10,5	10,8	10,7	10,6	10,7	0,14	1,29
50 BS	0,50	11,0	11,0	11,1	10,9	11,0	0,09	0,79
	0,65	10,6	10,5	10,7	10,7	10,6	0,08	0,80
60 BS	0,50	11,0	11,0	11,2	11,0	11,1	0,08	0,71
	0,65	10,6	10,7	11,0	10,9	10,8	0,15	1,43
20 CS	0,50	10,6	10,8	10,5	10,8	10,7	0,15	1,39
	0,65	10,8	10,5	10,7	10,7	10,6	0,14	1,32
40 CS	0,50	10,9	11,1	11,2	11,2	11,1	0,17	1,53
	0,65	10,3	10,3	10,4	10,3	10,3	0,08	0,73
60 CS	0,50	10,6	10,0*	10,8	10,6	10,5	0,32	3,09
	0,65	10,3	10,7	10,8	9,8*	10,4	0,44	4,18
10 L	0,50	10,8	10,7	10,7	10,7	10,7	0,04	0,39
	0,65	10,5	10,4	10,5	10,5	10,5	0,03	0,29
20 L	0,50	10,7	10,7	10,7	10,7	10,7	0,01	0,11
	0,65	10,5	10,2	10,4	10,3	10,4	0,10	0,98
A-L	0,50	10,7	10,9	10,7	10,7	10,8	0,09	0,84
	0,65	10,4	10,6	10,6	10,5	10,5	0,12	1,15
B-M	0,50	11,0	10,8	11,0	10,9	10,9	0,09	0,79
	0,65	10,6	10,8	10,7	10,7	10,7	0,08	0,75
SF 5	0,50	10,9	10,8	10,8	10,6	10,8	0,09	0,85
	0,65	10,4	10,5	10,5	10,6	10,5	0,07	0,67
SF FA	0,50	10,9	10,9	10,9	10,9	10,9	0,02	0,18
	0,65	10,7	10,6	10,6	10,6	10,6	0,03	0,29
SF BS	0,50	11,1	10,6	10,8	11,1	10,9	0,24	2,17
	0,65	10,6	10,8	10,6	10,5	10,6	0,15	1,44
SF CS	0,50	11,0	11,1	10,9	11,1	11,0	0,07	0,67
	0,65	10,7	10,6	10,8	10,8	10,7	0,10	0,92

*result not used in the calculation

Appendix D: accelerated carbonation results

Table D1: 6 week accelerated carbonation results

Type	w/b	Carbonation Depth (mm)				Average	S.D
		1	2	3	4	(mm)	%
CEM I	0,50	3,9	3,4	4,9	4,7	4,2	0,7
	0,65	8,4	7,2	7,9	6,7	7,5	0,7
20 FA	0,50	6,4	6,9	5,9	8,4	6,9	1,0
	0,65	10,8	12,5	15,3	9,8	12,1	2,4
30 FA	0,50	10,8	8,6	11,4	8,6	9,8	1,4
	0,65	15,1	15,1	12,2	18,4	15,2	2,5
40 FA	0,50	11,2	12,8	12,5	11,3	12,0	0,8
	0,65	21,8	18,7	19,4	19,1	19,8	1,4
50 FA	0,50	17,1	16,5	17,3	17,8	17,2	0,5
	0,65	23,4	25,8	24,1	24,5	24,5	1,0
20 BS	0,50	5,7	6,7	6,4	5,7	6,1	0,5
	0,65	10,0	9,2	11,8	8,6	9,9	1,4
30 BS	0,50	7,4	6,5	6,3	8,0	7,1	0,8
	0,65	13,7	10,7	12,9	12,1	12,4	1,3
40 BS	0,50	6,9	8,4	8,6	8,3	8,0	0,8
	0,65	14,5	13,3	10,4	-	12,7	2,1
50 BS	0,50	5,4	7,9	8,7	7,8	7,4	1,4
	0,65	11,4	15,9	15,9	15,0	14,5	2,2
60 BS	0,50	11,0	9,9	10,2	11,5	10,6	0,7
	0,65	18,7	16,7	17,2	13,2	16,5	2,3
20 CS	0,50	6,9	3,4	3,9	3,0	4,3	1,8
	0,65	7,3	11,0	11,1	11,3	10,2	1,9
40 CS	0,50	6,3	5,5	4,1	3,9	4,9	1,1
	0,65	12,1	10,6	11,5	10,0	11,1	0,9
60 CS	0,50	8,5	6,2	6,8	6,1	6,9	1,1
	0,65	11,9	15,8	14,0	13,2	13,7	1,7
10 L	0,50	4,4	4,9	4,4	5,5	4,8	0,5
	0,65	9,7	11,0	10,8	11,2	10,7	0,7
20 L	0,50	7,8	7,4	6,5	5,9	6,9	0,9
	0,65	12,2	10,8	14,7	11,8	12,3	1,6
A-L	0,50	4,1	2,7	3,4	3,8	3,5	0,6
	0,65	9,2	7,9	7,9	10,2	8,8	1,1
B-M	0,50	4,1	4,9	4,0	4,4	4,3	0,4
	0,65	11,4	7,7	9,7	9,9	9,7	1,5
SF 5	0,50	4,3	4,1	3,8	3,6	4,0	0,3
	0,65	8,8	9,0	8,2	7,5	8,4	0,7
SF FA	0,50	7,1	7,6	7,4	6,9	7,3	0,3
	0,65	12,9	14,2	13,9	16,9	14,5	1,7
SF BS	0,50	7,2	7,1	6,5	6,4	6,8	0,4
	0,65	10,6	9,8	11,9	11,9	11,0	1,0
SF CS	0,50	6,6	5,6	5,4	6,2	6,0	0,5
	0,65	8,9	8,7	8,0	10,3	9,0	1,0

Table D2: 9 week accelerated carbonation results

Type	w/b	Carbonation Depth (mm)				Average	S.D
		1	2	3	4	(mm)	%
CEM I	0,50	6,4	6,7	4,1	6,5	5,9	1,22
	0,65	10,4	7,7	10,6	8,5	9,3	1,42
20 FA	0,50	9,2	7,1	7,1	9,0	8,1	1,16
	0,65	10,6	11,3	13,9	14,1	12,5	1,80
30 FA	0,50	10,5	8,3	10,9	10,6	10,1	1,22
	0,65	17,7	13,9	16,8	18,5	16,7	2,03
40 FA	0,50	11,8	13,3	11,7	12,6	12,3	0,75
	0,65	22,9	18,8	22,0	23,5	21,8	2,10
50 FA	0,50	20,5	19,6	21,2	19,9	20,3	0,68
	0,65	31,1	30,6	30,9	30,1	30,7	0,43
20 BS	0,50	7,8	6,3	8,7	4,9	6,9	1,66
	0,65	12,1	11,3	12,2	10,6	11,5	0,73
30 BS	0,50	9,1	6,6	9,3	9,4	8,6	1,35
	0,65	12,0	16,6	12,3	15,1	14,0	2,25
40 BS	0,50	8,8	7,8	8,5	9,7	8,7	0,76
	0,65	14,9	15,5	11,6	-	14,0	2,08
50 BS	0,50	7,0	7,4	10,2	7,9	8,1	1,44
	0,65	13,4	19,7	17,3	16,4	16,7	2,62
60 BS	0,50	12,0	13,3	13,2	12,0	12,6	0,71
	0,65	19,2	15,8	22,6	26,0	20,9	4,38
20 CS	0,50	3,7	5,4	4,3	3,4	4,2	0,90
	0,65	11,6	7,3	12,3	12,4	10,9	2,45
40 CS	0,50	6,1	5,6	5,5	7,0	6,1	0,68
	0,65	15,8	11,7	12,3	13,6	13,3	1,81
60 CS	0,50	11,7	9,6	6,4	7,8	8,9	2,29
	0,65	12,8	17,3	13,6	15,9	14,9	2,10
10 L	0,50	4,6	5,4	7,2	5,0	5,5	1,15
	0,65	13,3	12,5	11,2	13,7	12,7	1,13
20 L	0,50	9,7	6,9	6,7	8,1	7,8	1,37
	0,65	16,1	13,8	12,1	13,0	13,7	1,71
A-L	0,50	5,0	4,7	5,3	6,2	5,3	0,68
	0,65	8,5	8,6	10,8	9,1	9,2	1,08
B-M	0,50	5,2	5,8	6,6	4,6	5,5	0,87
	0,65	10,4	11,4	13,5	12,3	11,9	1,32
SF 5	0,50	7,6	5,9	6,6	4,5	6,2	1,31
	0,65	9,0	9,7	8,3	10,6	9,4	1,00
SF FA	0,50	8,1	8,6	8,6	8,4	8,5	0,25
	0,65	17,0	19,3	15,3	16,0	16,9	1,75
SF BS	0,50	9,2	9,8	6,1	5,2	7,6	2,25
	0,65	11,8	13,1	13,0	13,1	12,7	0,65
SF CS	0,50	7,5	7,6	7,8	5,9	7,2	0,86
	0,65	7,7	10,1	8,5	9,7	9,0	1,10

Table D3: 12 week accelerated carbonation results

Type	w/b	Carbonation Depth (mm)				Average	S.D
		1	2	3	4	mm	%
CEM I	0,50	6,7	6,2	6,5	6,6	6,5	0,18
	0,65	10,2	10,0	9,6	10,0	10,0	0,27
20 FA	0,50	8,4	10,0	8,2	11,1	9,4	1,36
	0,65	14,9	15,6	13,1	15,8	14,9	1,24
30 FA	0,50	12,0	11,9	10,3	12,4	11,7	0,92
	0,65	21,9	17,9	20,2	17,7	19,4	2,00
40 FA	0,50	13,2	14,7	14,2	14,2	14,1	0,65
	0,65	23,6	23,4	23,6	22,6	23,3	0,48
50 FA	0,50	20,4	19,4	20,4	21,1	20,3	0,71
	0,65	33,3	31,4	33,4	32,9	32,7	0,94
20 BS	0,50	8,4	8,1	9,0	6,7	8,0	0,94
	0,65	14,0	14,6	14,6	14,2	14,3	0,29
30 BS	0,50	8,3	10,1	10,8	7,0	9,1	1,75
	0,65	16,3	12,9	14,2	14,1	14,4	1,41
40 BS	0,50	10,5	10,4	9,5	9,3	9,9	0,62
	0,65	16,5	18,0	15,4	15,6	16,4	1,18
50 BS	0,50	10,5	11,2	11,6	7,9	10,3	1,68
	0,65	19,3	19,0	19,3	17,0	18,7	1,08
60 BS	0,50	15,7	14,1	13,6	13,3	14,2	1,06
	0,65	22,3	21,5	20,8	21,2	21,4	0,62
20 CS	0,50	7,1	6,4	5,8	5,6	6,2	0,69
	0,65	13,6	11,6	12,9	11,9	12,5	0,92
40 CS	0,50	6,3	7,6	7,6	5,5	6,7	1,05
	0,65	13,8	15,1	14,4	13,9	14,3	0,58
60 CS	0,50	10,1	8,3	8,7	8,7	9,0	0,77
	0,65	20,1	16,5	19,9	16,5	18,3	2,02
10 L	0,50	7,2	7,8	7,4	7,0	7,4	0,36
	0,65	14,4	15,1	15,2	14,5	14,8	0,39
20 L	0,50	8,4	10,2	10,1	8,3	9,3	1,07
	0,65	16,6	16,9	17,2	15,5	16,5	0,75
A-L	0,50	6,5	6,8	6,7	5,8	6,5	0,45
	0,65	10,7	10,8	10,7	10,7	10,7	0,02
B-M	0,50	6,3	6,8	6,0	6,3	6,4	0,33
	0,65	15,8	12,8	13,1	16,1	14,4	1,74
SF 5	0,50	6,2	7,9	7,4	7,2	7,2	0,70
	0,65	10,8	10,8	10,2	11,5	10,8	0,54
SF FA	0,50	10,4	10,6	10,0	9,6	10,2	0,44
	0,65	19,9	16,8	16,8	16,7	17,6	1,58
SF BS	0,50	6,9	10,2	10,4	8,5	9,0	1,63
	0,65	13,5	13,5	13,5	13,5	13,5	0,04
SF CS	0,50	8,4	8,9	8,3	9,3	8,7	0,46
	0,65	10,4	11,0	10,3	10,3	10,5	0,35

Appendix E: Statistical analysis worked examples

E1: T-test

The t-test was used to determine whether OPI results of two mixes were significant. Its results were used to verify the results obtained from the Rank-sum test. The t-test could be used as the results obtained from the OPI results are normally distributed. Below shows a worked example of the execution of the t-test of the significance between mixes of CEM I and 20 FA for a w/b ratio of 0,50. Their results are shown in Table X.X. The same procedure may be used for the accelerated carbonation results. The equations used for the t-test are shown below:

$$t=\frac{(\bar{x}_1-\bar{x}_2)}{\sigma_p\sqrt{\frac{1}{n_1}+\frac{1}{n_2}}}$$

$$\sigma_p^2=\frac{(n_1-1)\sigma_1^2+(n_2-1)\sigma_2^2}{n_1+n_2-2}$$

Where: $\bar{x}_1$; $\bar{x}_2$ = mean for sample 1 and sample 2 respectively

σ_p = Pooled standard deviation

σ_1 = sample 1 standard deviation

σ_2 = sample 2 standard deviation

n_1; n_2 = Size of sample 1 and sample 2 respectively

The null hypothesis, H_0, states that the means of the two samples are equivalent while the alternative hypothesis, H_1, the means of the two samples are not equivalent. For the t-test, the value of t is compared with a critical value t_{crit} obtained from Table X.X. If $|t| > t_{crit}$ then the null hypothesis is rejected. The critical region value is dependent on the degrees of freedom which is calculated as n_1+n_2-2.

Table E1: t_{crit} values (Walpole, et al., 2012)

Degrees of freedom	t_{crit}
4	2,776
5	2,571
6	2,447

Table E2: Statistical treatment of k-values for CEM I and 20 FA with w/b of 0,50 for the t-test

Specimen	CEM I	20 FA
1	10,83	10,81
2	10,62	10,42
3	10,83	10,75
4	10,51	10,63
Mean	10,7	10,65
S.D	0,16	0,171

Therefore, the calculation is as follows,

$$\sigma_p^2 = \frac{(n_1-1)\sigma_1^2+(n_2-1)\sigma_2^2}{n_1+n_2-2}$$

$$= \frac{(4-1)0.160^2+(n_2-1)0.171^2}{4+4-2}$$

$$= 0{,}02737$$

$$\sigma_p = 0{,}16544$$

$$t = \frac{(10{,}70-10{,}65)}{0{,}165\sqrt{\frac{1}{4}+\frac{1}{4}}}$$

$$|t| = 0{,}391<2{,}447$$

As $|t| < t_{crit}$, H_0 is accepted. Therefore, CEM I and 20 FA for the w/b ratio of 0,50 are equivalent.

E2: The rank-sum test

For the k-permeability tests, the rank-sum test (U) was used to determine the significance between the means as they are non-parametric as they are logarithmic distributed. A worked example on the same samples used in the previous section is used here.

Let n_1 and n_2 be the number of observations from the smaller and larger sample respectively. n_1 and n_2 are interchangeable for cases where sample sizes are equal. The specimens from both samples are combined and ranked in ascending order. The ranks of the determinations from each sample are summed and is denoted by w_1 and w_2 respectively.

w_1 = sum of ranks of sample 1 ; w_1 = sum of ranks of sample 2

$$u_1 = w_1 - \frac{n_1(n_1+1)}{2} \quad ; \quad u_2 = w_2 - \frac{n_2(n_2+1)}{2}$$

The null hypothesis, H_0, states that the means of the two samples are equivalent while the alternative hypothesis, H_1, the means of the two samples are not equivalent. For the rank-sum test, the value of the smaller u is compared with a critical value, U_{crit} obtained from Table X.X. If $U < U_{crit}$ then the null hypothesis is rejected.

Table E3: t_{crit} values (Walpole, et al., 2012)

U_{crit}	n_2	
		4
n_1	3	1
	4	1

Table E4: Statistical treatment of k-values for CEM I and 20 FA with w/b of 0,50 for the rank-sum test

Type	Specimen	k(m/s) (E-11)	Rank
CEM I	1	1,46	1
	2	2,42	6
	3	1,48	2
	4	3,07	7
20 FA	1	1,57	3
	2	3,79	8
	3	1,77	4
	4	2,34	5

Therefore, the calculation is as follows:

$$w_1 = 1+6+2+7=16 \quad ; \quad w_1 = 3+8+4+5=20$$

$$u_1 = w_1 - \frac{n_1(n_1+1)}{2} \quad ; \quad u_2 = w_1 - \frac{n_1(n_1+1)}{2}$$

$$= w_1 - \frac{n_1(n_1+1)}{2} \quad ; \quad = w_1 - \frac{n_1(n_1+1)}{2}$$

$$= 6 \quad ; \quad = 10$$

$U(10) > U_{crit.}(1)$, H_0 is accepted. Therefore, CEM I and 20 FA for the w/b ratio of 0,50 are equivalent

Appendix F: ethics form

Application for Approval of Ethics in Research (EIR) Projects
Faculty of Engineering and the Built Environment, University of Cape Town

APPLICATION FORM

Please Note:
Any person planning to undertake research in the Faculty of Engineering and the Built Environment (EBE) at the University of Cape Town is required to complete this form **before** collecting or analysing data.The objective of submitting this application *prior* to embarking on research is to ensure that the highest ethical standards in research, conducted under the auspices of the EBE Faculty, are met. Please ensure that you have read, and understood the **EBE Ethics in Research Handbook**(available from the UCT EBE, Research Ethics website) prior to completing this application form: http://www.ebe.uct.ac.za/usr/ebe/research/ethics.pdf

APPLICANT'S DETAILS		
Name of principal researcher, student or external applicant		Nabeel Omar
Department		Civil Engineering
Preferred email address of applicant:		Omnab005@myuct.ac.za
If a Student	Your Degree: e.g., MSc, PhD, etc.,	MSc Civil Engineering
	Name of Supervisor (if supervised):	Prof. Hans Beushausen
If this is a researchcontract, indicate the source of funding/sponsorship		
Project Title		Carbonation Predictions for Modern South African Concretes

I hereby undertake to carry out my research in such a way that:

- there is no apparent legal objection to the nature or the method of research, and
- the research will not compromise staff or students or the other responsibilities of the University;
- the stated objective will be achieved, and the findings will have a high degree of validity;
- limitations and alternative interpretations will be considered;
- the findings could be subject to peer review and publicly available; and
- I will comply with the conventions of copyright and avoid any practice that would constitute plagiarism.

SIGNED BY	Full name	Signature	Date
Principal Researcher/ Student/External applicant	Nabeel Omar		[illegible]

APPLICATION APPROVED BY	Full name	Signature	Date
Supervisor (where applicable)	Prof. Hans Beushausen		21/10/16
HOD (or delegated nominee) Final authority for all applicants who have answered NO to all questions in Section1; and for all Undergraduateresearch (Including Honours).	~~Prof. Neil Armitage~~ M Vandersluren		21/10/16
Chair : Faculty EIR Committee For applicants other than undergraduate students who have answered YES to any of the above questions.			

Page 1 of 1